AERODYNAMICAL INVESTIGATIONS

ON

REACTION TURBINE BLADES.

M. R. YOUSSEF, B.Sc., Ph.D., M.I. Mech.E.

.....

ProQuest LLC.
789 East Eisenhower Parkway
P.O. Box 1346
Ann Arbor, MI 48106 – 1346

AERODYNAMICAL INVESTIGATIONS

ON

REACTION TURBINE BLADES.

ABSTRACT.

So far no theory of the Reaction Turbine has as yet been investigated which is capable of clarifying fully the effect of such factors as the number of blades, the blade angle, the blade pitch and the breadth of the blade upon the action of these machines.

It is known that the "lift" of biplanes and triplanes per unit of wing surface is inferior to that of a monoplane, and that the degree of departure depends upon the gap-chord ratio.

Published data indicate that the lift increases with increasing gap, apparently towards some limiting value.

Regarding steam turbine wheels as rings of multiplanes, it may be asked "Is there any direct evidence that the torque on each blade is influenced by the presence of the other blades?"

Many experiments have been made to determine the optimum circumferential pitch for a given blade shape, but most of these have aimed simply at arriving empirically at the best efficiency, without inquiry into the factors involved.

The present investigations were carried

out on Model Reaction Blades reproduced several times the actual full size so that the Reynold's number is maintained at a value of interest in turbine design, but with comparatively low air speeds usual in WIND TUNNEL work, to examine the effects of the number of blades, the blade pitch and the blade angle.

INTRODUCTION.

Now that the science of practical hydrodynamics and aerodynamics is becoming more and more applied to turbines, pumps, fans, and compressors, it is of interest to inquire how far the knowledge of aerofoil mechanics is applicable to Reaction Steam Turbines.

In practical steam turbines, it is not yet possible to use aerofoil blades, that is, streamline contours of small curvature.

Almost all steam turbine blades have a much greater curvature than aerofoils, on account of the necessity for utilizing the entire head of steam in a practicable number of stages.

Looked at in a general way, an aeroplane and a steam turbine have very little in common.

Their functions are so different, and their performances are judged by such different

standards that the designer of one can hardly be expected to be an expert concerning the details of the other.

Certain analogies between them are, however, to be found, for both ultimately depend for their efficiencies upon the behaviour of a mass fluid moving rapidly over curved surfaces.

The wings of an aeroplane react in much the same way as the blades of a turbine on the fluid flowing past them and experience a pressure due to similar causes.

But like all analogies, this one must not be pushed too far.

There are fundamental differences as well as similarities between the conditions in the two cases.

The blade of a Reaction Turbine has a form clearly akin to that of the wing of an aeroplane, but its transverse curvature is greater, and it has to deal with the fluid in an expanding condition instead of at constant pressure, while, and perhaps more important from an aerodynamical point of view, the flow past the tip is not unrestricted as it is with an aeroplane wing.

EXPERIMENTS WITH MODELS.

The foundation of small scale research as now understood was laid in the latter half of the last century by the work of Darcy and Bazin in France, Osborne Reynolds and James Thomson in England and Engels in Germany.

The utility of model experiments had not been proved, and hydrodynamical theory, confined to the motion of a perfect fluid often gave misleading results and so made no appeal to the Engineer.

With the beginning of the present century came a new outlook.

It was realised that the flow phenomena in which engineers were interested could be simulated under appropriate conditions by means of model research, and that such model experiments gave results of great practical value.

A fresh impetus to the study of fluid motion was also given by the advent of the aeroplane.

A knowledge of the forces acting on the constituent parts of an aeroplane, and of the flow

past them, became a necessity if flight were to be achieved economically.

Power had to be expended not only to overcome the resistance to motion, but also to sustain the weight of the craft.

Aerodynamical Laboratories were installed in progressive countries for the purpose of a scientific study of the problems of flight, with a view to a practical solution.

The experience gained in hydraulic laboratories made it clear that experiments with models would yield valuable information.

Accordingly WIND TUNNELS were designed to obtain uniform streams of air in which the behaviour of models could be investigated.

The subject matter of this work has been obtained from experiments with Model (1) Reaction Blades made of Pine Wood and reproduced several times the original full size. Fig. I.

---

(1) It may be mentioned that the general subject of research in mechanical Engineering by Models was dealt with in a paper by F.D. Johanssen, Proc. I. Mech.E., 1929, p. 151.

The Reaction Blade Model Sections were made from yellow pine wood and were supplied with other parts of the apparatus used for the tests through the courtesy of Messrs. G. & J. Weir & Co. Ltd., Holm Foundry, Cathcart, Glasgow.

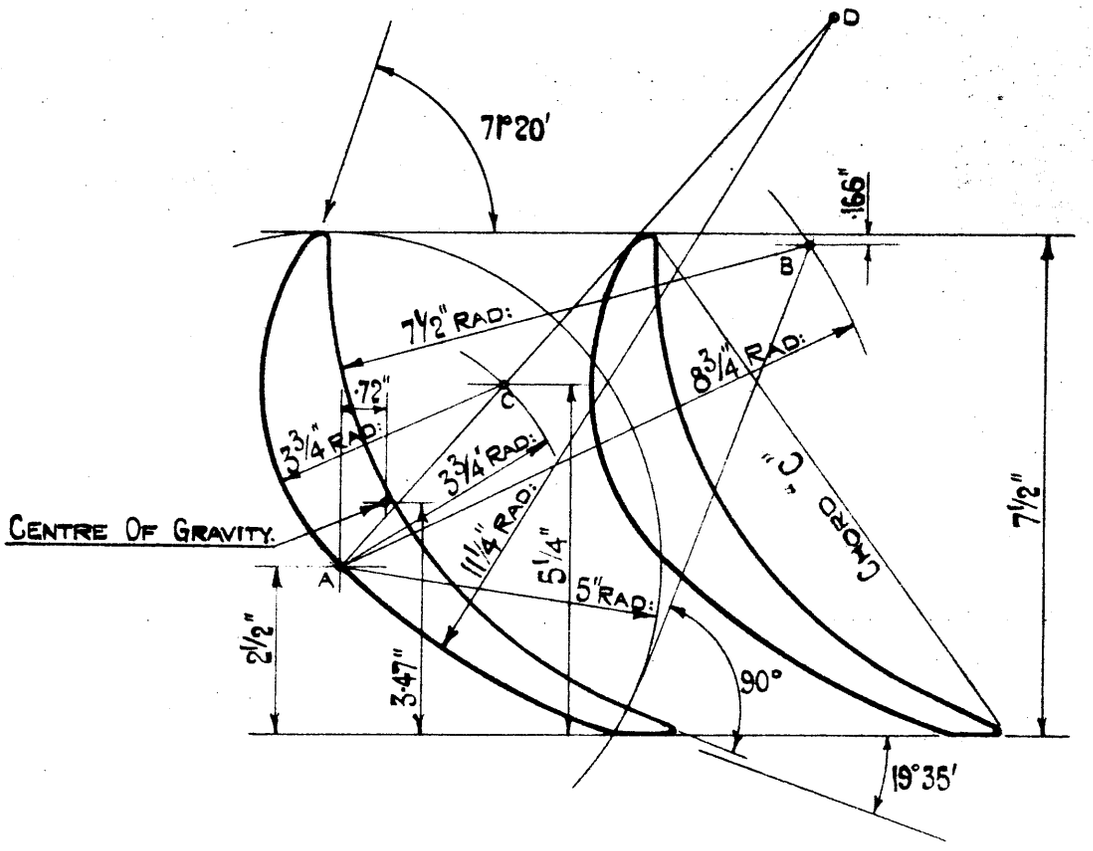

ENLARGED SECTION OF PARSONS' REACTION BLADE.

FIG I

The investigations were carried out on these models, in the Wind Tunnel at the Royal Technical College (by the kind permission of the Governors and the Professor of Civil and Mechanical Engineering of the College) to examine the aerodynamic characteristics of a series of blades and a solitary blade by;-

(a) Pressure Distribution Tests,

and (b) Aerodynamic Balance Tests.

THE WIND TUNNEL.

The Wind Tunnel is a five foot diameter open-jet closed circuit Wind Tunnel.

It has a speed range of zero to 100 M.P.H. and can set to run constantly at any speed within that range by means of an electrical pressure balance.

The maximum speed variation possible when the balance is in operation is $\pm \frac{1}{2}\%$.

There are slots round the bell mouth of the collector to prevent the stagnant air, picked up by the jet in crossing the gap, from being drawn into the air stream; immediately

downstream from the fan there are other slots, which are called the collector slots and bottom slots respectively.

TWO-DIMENSIONAL FLOW.

In practice, the direct effects of viscosity are confined to a thin boundary layer at the surface of a body and to the trailing wake. Outside these regions, the fluid behaves as if it had no viscosity, and there the methods of classical hydrodynamics can be used to account for flow phenomena.

Fig. (2) shows the arrangement of the Blades for Two-Dimensional Flow.

If a long cylindrical body is placed in a perfect fluid with its axis normal to the stream it can be made to experience a lift, if the flow selected is such that there is a circulation round the contour enclosing a section of the body.

Kutta and Joukowsky have shown that the strength of this circulation (and so of the lift) can be calculated, when the conformal transformation by means of which the section is derived from a circle is known, on the hypothesis that the streams above and below the body unite smoothly at the trailing edge.

This is satisfied when the body has a sharp trailing edge.

The theoretical lift is not quite realised in practice, because the theory ignores the presence of the trailing wake formed behind the body.

The resistence of a body in two dimensional flow is called the profile resistence.

The theory of a perfect fluid does not indicate the existence of this resistance, but its value can be predicted for a thin aerofoil at a small incidence to the general stream, and

at a high Reynold's number, for then the resistance arises almost entirely from surface friction, and is very closely the same as that experienced by a flat plate.

Lifting parts of modern aeroplanes - wings, elevators, ailerons etc. - are often designed on the Joukowsky hypothesis.

Two Dimensional Flow was secured in the present investigations by having the Model Reaction Blades placed between two large plates - Fig(2) - projecting through the jet for some distance above and below the stream and for a large distance up and down stream.

The jet is deflected downwards due to the reaction from the lift experienced on the blade.

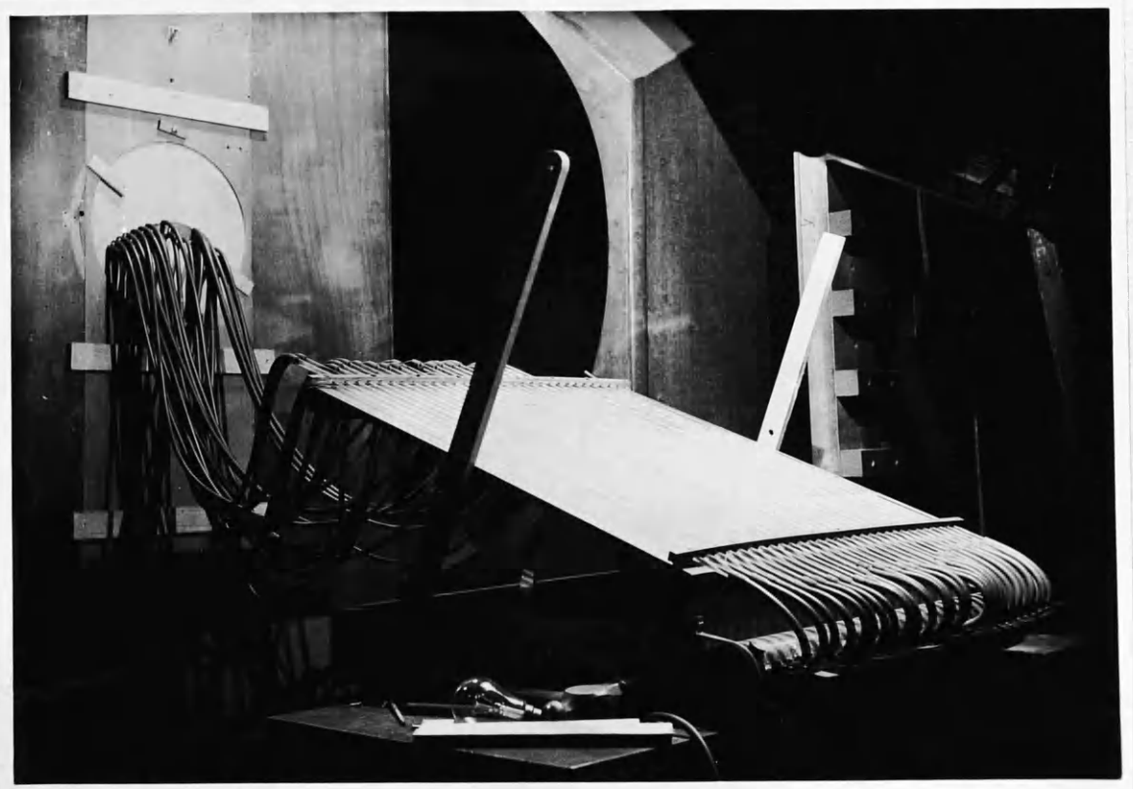

FIG 3

(a) PRESSURE DISTRIBUTION TESTS.

APPARATUS.

The essential apparatus consisted of the 5 foot diameter open jet wind tunnel at the Royal Technical College, two large side planes to maintain Two Dimensional Flow over the models and five models of a Reaction Blade produced five times the original full size.

An illustration of the experimental layout is given in Figs. (2), (3), (4) and (6).

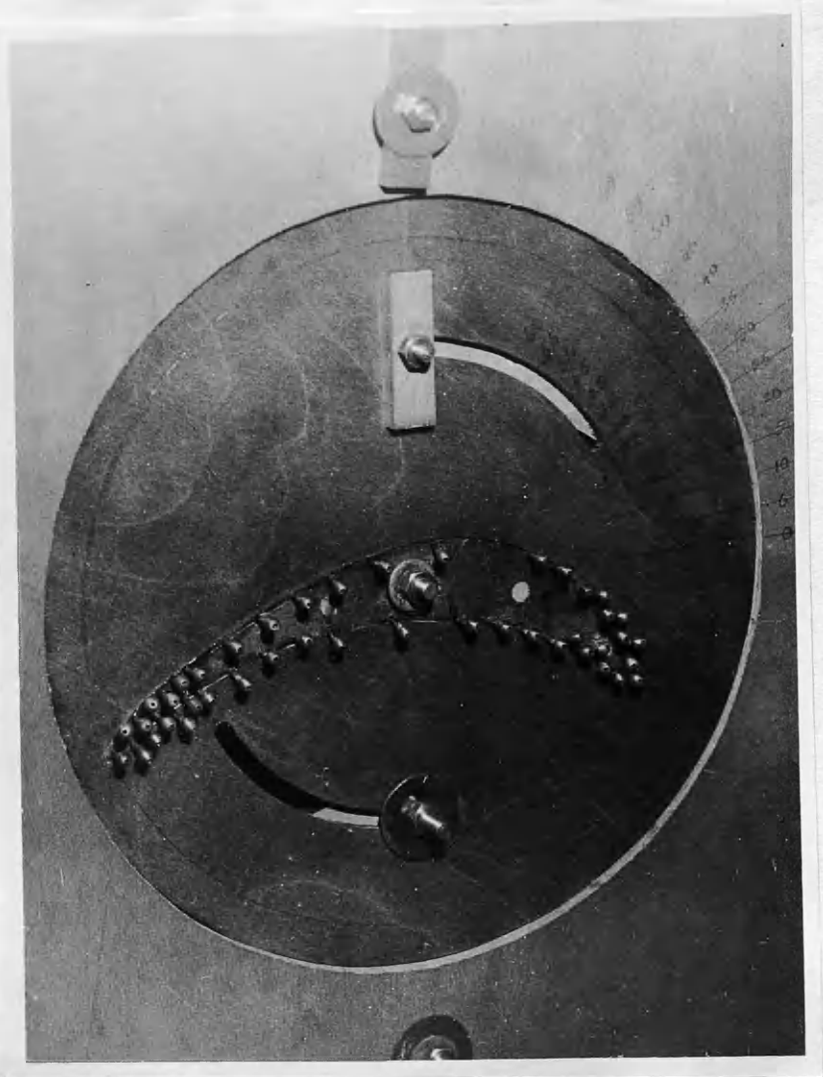

Fig. (4) shows the arrangement of the rotating disc housed in the side planes and carrying the pressure Blades.

The Blade model sections have a chord of 9.2 inches and a span of 24 inches.

One blade only, its section exactly the same as the rest, had small copper tubes $\frac{3}{32}$" O.D. embedded in its body, Fig. (4a) and were made flush with the surface.

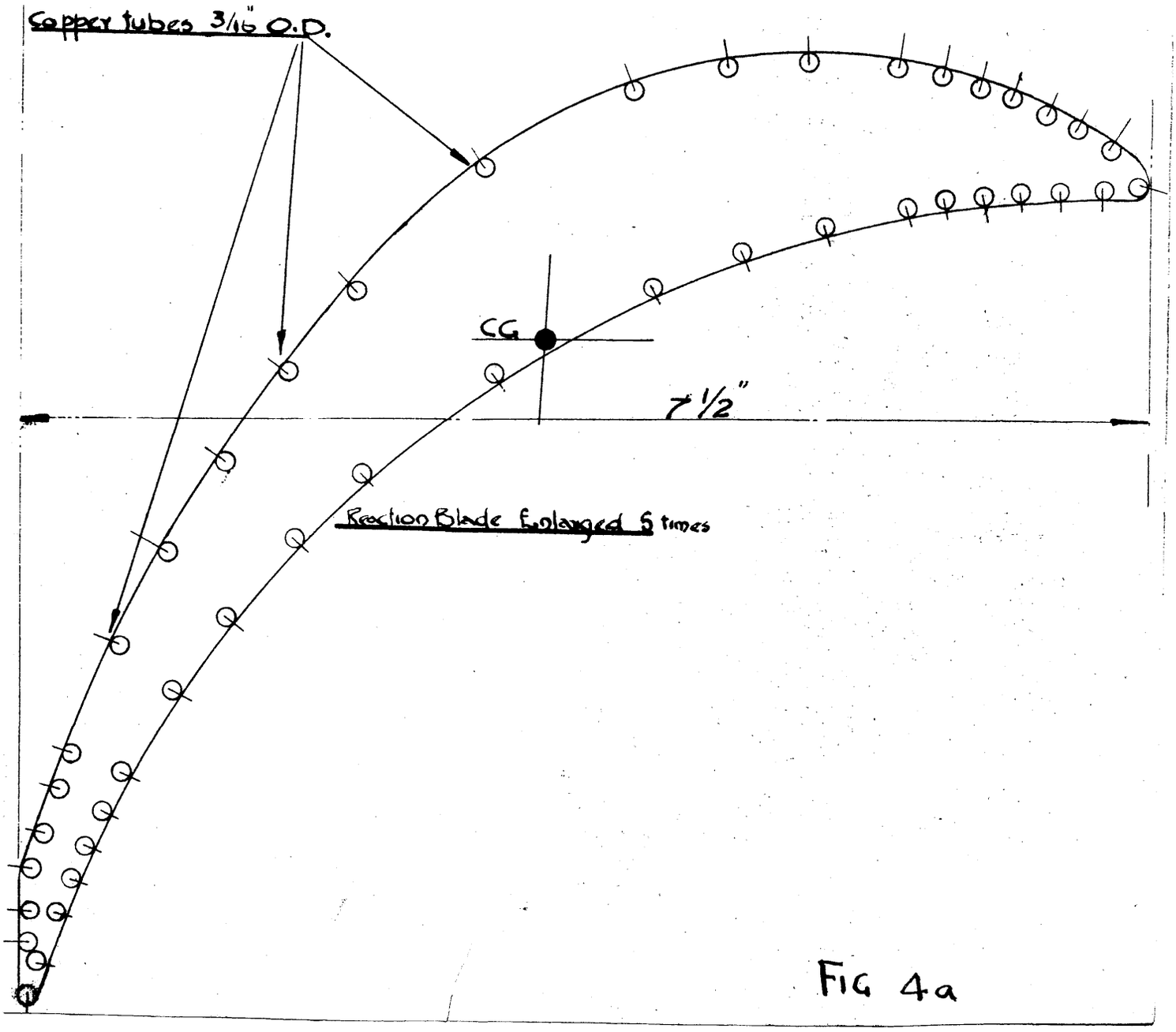

Fig 4a

The copper tubes on this pressure blade were soldered at one end and protruded at the other beyond the end of the vertical plane where they were connected to a photographic multi-tube manometer by high pressure rubber tubing, a $\frac{1}{32}$" inch diameter hole being drilled in each tube at mid span normal to the surface.

Four of the Blade Model Sections were placed between the two side planes by a long bolt fixing them to the two planes and allowing free movement unless locked with the side planes at any desired position.

The fifth or "pressure blade" was rigidly attached at each end to a circular housed in the planes themselves. These discs - Fig. (4) - were calibrated to give the desired angle of inclination of the blade.

A vertical slot was cut in the side planes to allow for the change of blade pitch without having to remove the blades for every varying pitch.

With this arrangement two dimensional flow was maintained over the model.

Adjustment of the angle of incidence was accomplished by rotating the circular disc attached to the pressure blade and then locking it in the desired inclination.

The other four blades were then rotated round their axis to the desired inclination and checking, by measuring the pitch between the blades both at the leading and trailing edges and then all five blades were locked in position.

The angles of incidence were also checked at each position by means of a Watkins Inclinometer.

All the tests were made with an air flow of ninety feet per second.

The range of incidence varied over a range from zero to fifty degrees.

These angles of incidence were all corrected to infinite aspect ratio by taking account of all the interference factors.

A multi-tubular manometer - Figs. (2) and (3) - consisting of thirty glass tubes arranged on an inclined board and adjustable to any desired angle. The lower ends of the tubes were connected to a common reservoir containing water which served as the manometer fluid.

The other ends of the glass tubes were connected to the copper tubes protruding from the pressure blade beyond the end of the plane by high pressure rubber tubing.

Twenty seven tubes were available for connection to the model, the three remaining ones being reserved for reference measurements.

Of these, one tube at each end registers the Static pressure, a line drawn between the liquid levels giving a datum line for pressure measurement.

The third was directly connected to the pitot tube in the wind tunnel and thus registered the dynamic head of the air jet.

The different pressures on the contour of the Model Blade were measured from the static datum line and were expressed as ratios of the dynamic pressure, the results being therefore independent of the manometer liquid.

To simplify pressure recording, photographic prints were taken.

These were obtained by slipping printing paper between the glass tubes and the board and exposing to the light of an arc lamp fitted with a parabolic reflector - Fig. (2).

A typical record taken by this means is shown in Fig. (5).

PITCH 5" ANGLE αe = 25°

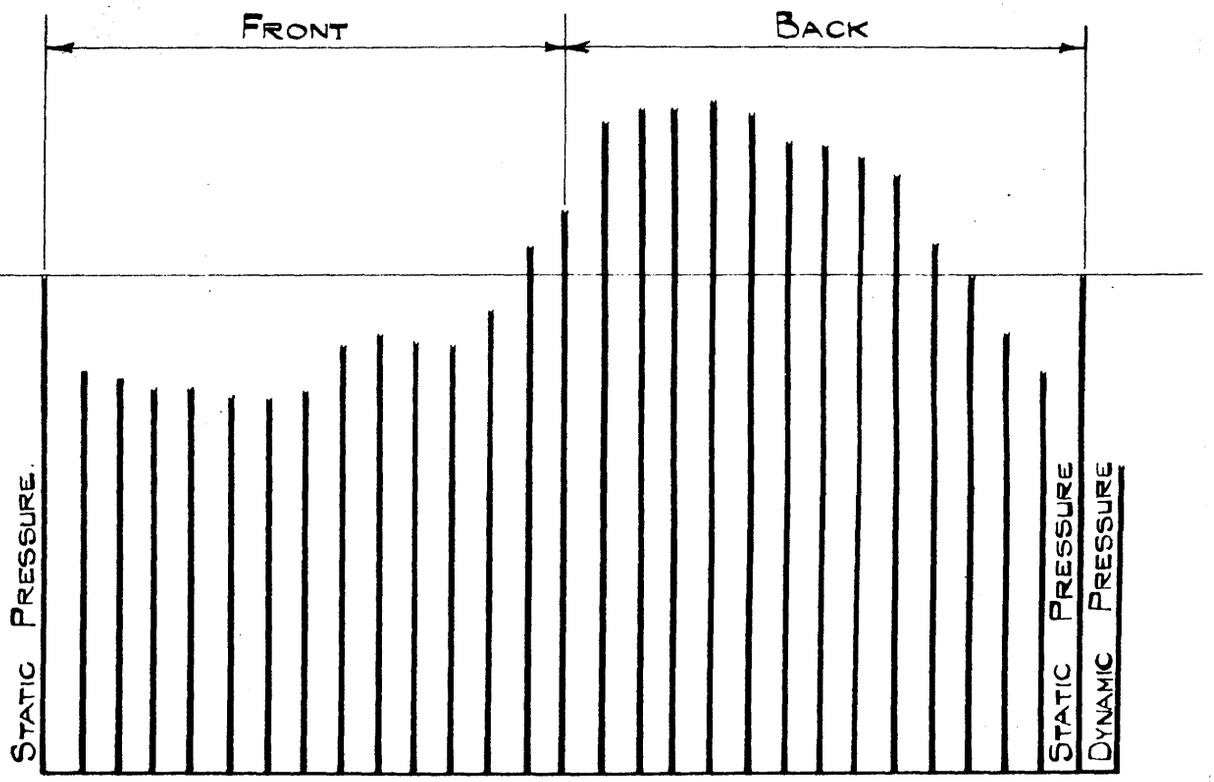

TYPICAL MANOMETER PRINT OF PRESSURE DISTRIBUTION ON THE BACK AND FRONT OF BLADE.

Fig. (5)

To ensure that no variation of pressure took place while printing, each tube was fitted with a cock for isolating the tube from the main reservoir.

This allowed the pressure distribution to be retained in the tubes while the print was being taken.

The cocks were connected in groups so that they could be closed almost simultaneously.

An air speed of ninety feet per second was maintained throughout all the tests.

The range of angles of incidence (or chord inclination) was varied from zero to Fifty degrees.

With the models set at the desired angle and at the pre-arranged blade pitch, a few minutes were allowed to lapse to ensure steady conditions.

The cocks were then closed and a photographic record taken.

These operations could be carried out very rapidly and allowed the pressure distributions to be explored over minute changes in the angles of incidence.

It also facilitated the checking of any unexpected results.

The "Pressure Blade" was placed at each of the positions A, B, C, D. & E alternately. It was, however, found that the manometer tubes registered the same pressures approximately for the blade in the three positions, B, C. & D. - Fig. (6).

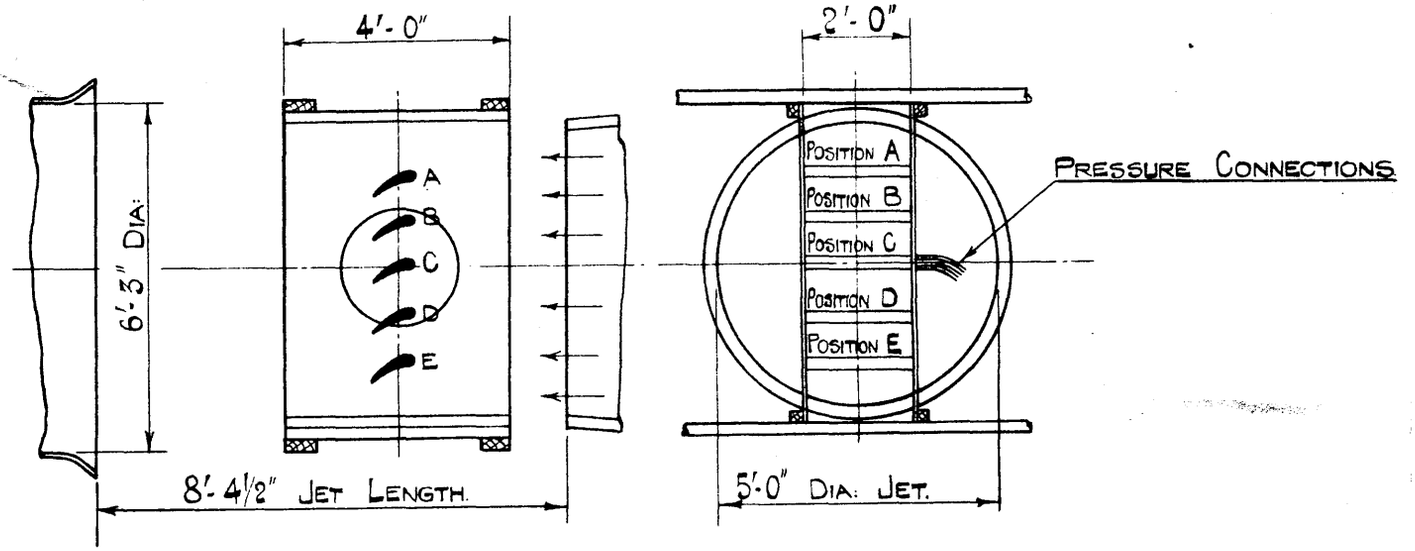

DETAILS OF APPARATUS SHOWING DIFFERENT BLADE POSITIONS

FIG. (6)

The plottings for the pressure distributions for these positions are given in Figs (≡) 8 - 12.

This is due to the fact that the flow above and below the blade in any of these three positions is guided by the two blades at the top and bottom of it, which are of equal section, the same material, and the same finish.

This procedure was only carried out for the 4" Blade Pitch, Figs. (8), (9), (10), (11), and (12).

It was therefore unnecessary to repeat the examination of the pressure distributions for the different Blade positions for every Blade Pitch, and so the Pressure Blade was kept in position C for all the following tests.

The Blade Pitch was then changed and pressure distribution records were again registered for the different chord inclinations of the blade.

Four different Blade Pitches were examined, i.e., 4", 5", 6", and 8".

The above tests constituted an examination of the aerodynamic characteristics of a blade which is a MEMBER of a series of blades of the same section.

The four blades at the positions A, B, D & E were then removed and tests were carried out for the solitary blade at the position C and under the same conditions of flow and inclinations as before.

The pressure distribution curves on a base of incidences is given in Figs. (28), (29), (30), (31), and (32).

WIND TUNNEL CORRECTIONS.

From the dimensions of the apparatus the correction formula was deduced as follows -

$$\alpha_\infty = \alpha_e - 5.55 C_L$$

where

α_∞ = True angle of incidence

α_e = Experimental angle of incidence

C_L = The Lift coefficient

$$= \frac{\text{Lift per inch}}{\rho \frac{V^2}{2} C}$$

C being the chord length in inches.

LIFT AND DRAG COEFFICIENTS.

As the flow is two dimensional we can consider unit axial length.

Taking an element of the surface δs Fig. (7), where the pressure is P, then the total force normal to δs is $P \delta s$

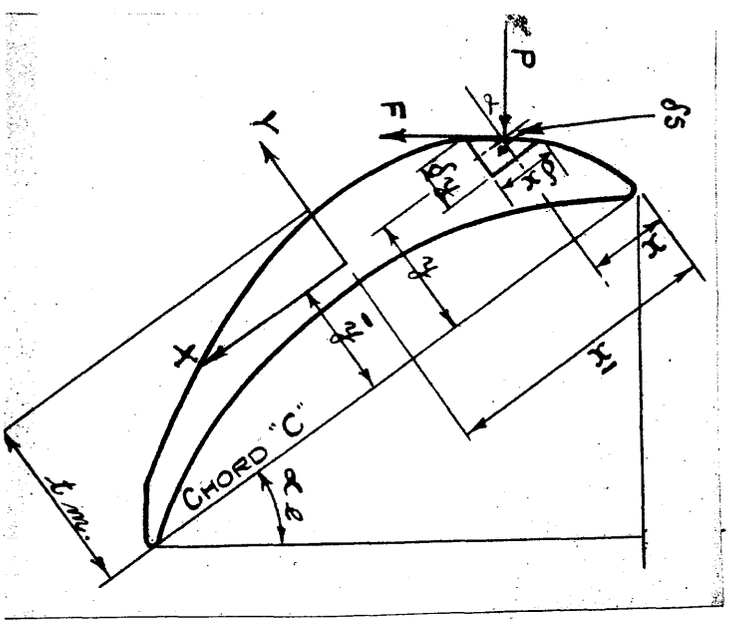

Fig. 7.

Resolving into force components normal and parallel to the chord we get

$$\delta Y = P \delta s \cos \alpha$$

$$= P \delta x$$

and $$\delta X = P \delta s \sin \alpha$$

$$= P \delta Y$$

Hence $$Y = \int_A P \, dx$$

and $$X = \int_A P \, dy$$

$P \delta x$ will be regarded as positive when upwards and $P \delta Y$ positive when to the left.

All the pressures are plotted in the dimensionless form $\frac{P}{\rho \frac{V^2}{2}}$ against the chord lengths.

This corrects for small errors of $\rho \frac{V^2}{2}$ in the individual readings.

Hence $$Y' = \frac{Y}{\rho \frac{V^2}{2} C} = \int_A \frac{P}{\rho \frac{V^2}{2}} \frac{dx}{C}$$

$$X' = \frac{X}{\rho \frac{V^2}{2} C} = \int_A \frac{P}{\rho \frac{V^2}{2}} \frac{dy}{C}$$

The values of Y' and X' are obtained from the appropriate diagrams by taking the areas and are given in the table of results.

If the aerofoil is set an at angle of incidence α_e to the nominal wind direction the nominal lift force is given by

$$L_e = Y \cos\alpha_e - X \sin\alpha_e$$

and

$$C_{Le} = \frac{L_e}{\rho \frac{V^2}{2} C}$$

$$= Y' \cos\alpha_e - X' \sin\alpha_e$$

There is a downward deflection of the jet due to the lift reaction and the actual angle of incidence α_∞ or the corrected chord inclination is given by;-

$$\alpha_\infty = \alpha_e - 5.55\, C_L \quad \text{(degrees)}$$

for the present experimental arrangement.

It will be noticed that to use this formula to obtain the correct wind direction we require to know $C_{L\infty}$

A satisfactory solution to the problem was arrived at by using the nominal angle of incidence α_e (the measured angle of incidence) to give a first approximation to the correct value of α_∞

Then a first approximation to C_{L_∞} was calculated and hence a second approximation to α_∞ obtained.

THE DRAG COEFFICIENT.

$$C_D = \frac{D}{\rho \frac{v^2}{2} C}$$

$$= Y' \sin \alpha + X' \cos \alpha$$

The coefficient, if derived from the pressure distribution curves, would only represent the drag due pressure and the drag due to skin friction would be neglected.

In evaluating the coefficients of drag by this method the diagrams of pressure ratio plotted on the aerofoil heights would naturally have a large effect on the final results.

Inspection of these curves shows that generally two main loops are formed, the difference in area of these loops represents the force acting on the aerofoil parallel to the chord.

Owing to the peculiar configuration of the diagrams, the curves are not accurately defined at all points by the number of pressure readings available.

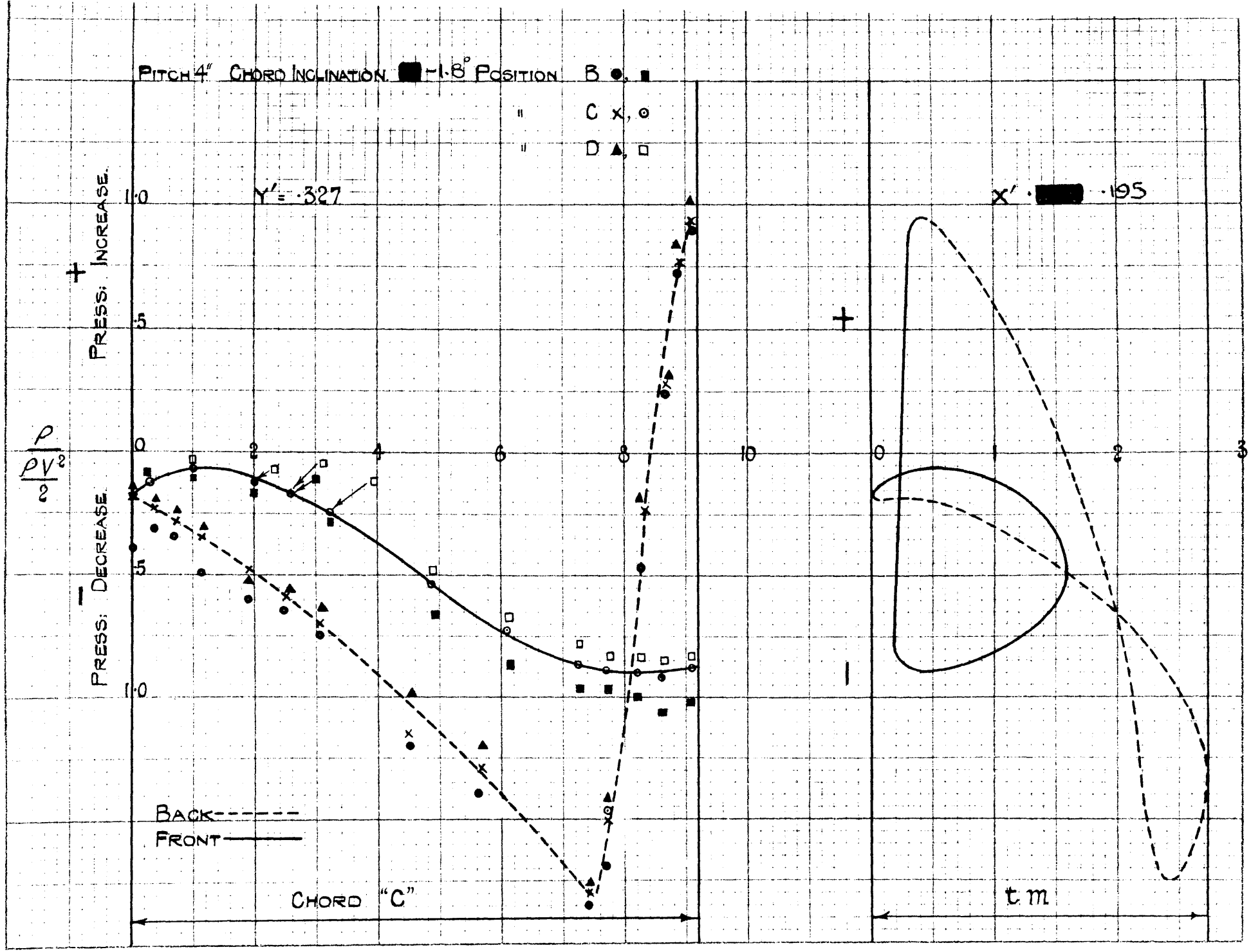
PITCH 4" CHORD INCLINATION [redacted] -1.8° POSITION B ●, ■
" C ×, ⊙
" D ▲, □
Y' = .327
X' · [redacted] ·195
+ PRESS: INCREASE.
- PRESS: DECREASE.
ρ / (ρV²/2)
1.0
.5
0
.5
1.0
0
2
4
6
8
10
0
1
2
3
BACK
FRONT
CHORD "C"
t.m

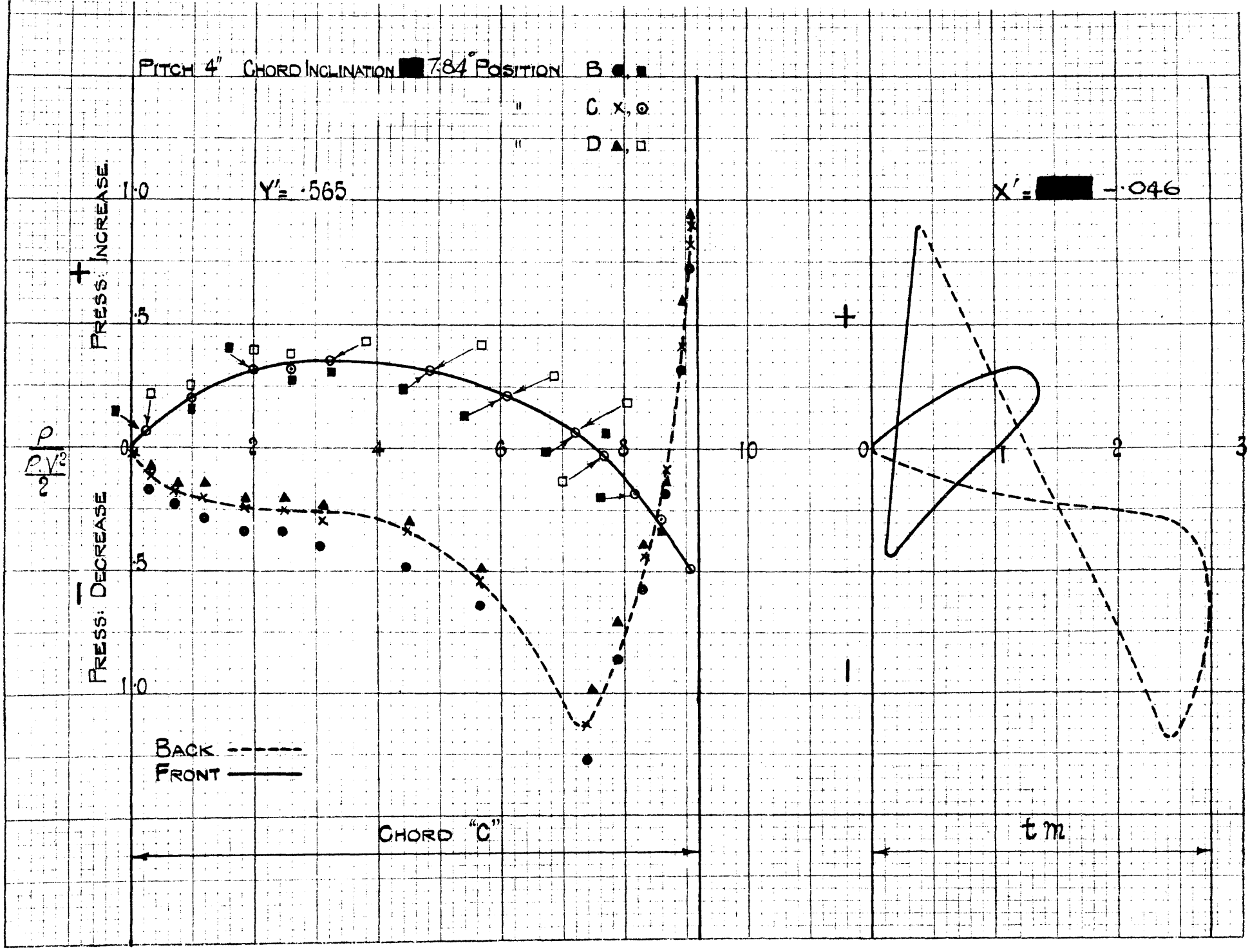
PITCH 4" CHORD INCLINATION [redacted] 7.84° POSITION B ●, ■
" C x, ⊙
" D ▲, □
Y'= ·565
X'= [redacted] -·046
+ PRESS: INCREASE.
- PRESS: DECREASE
ρ / ρV²/2
1·0
·5
0
2
4
6
8
10
·5
1·0
BACK
FRONT
CHORD "C"
+
0
1
2
3
1
t m

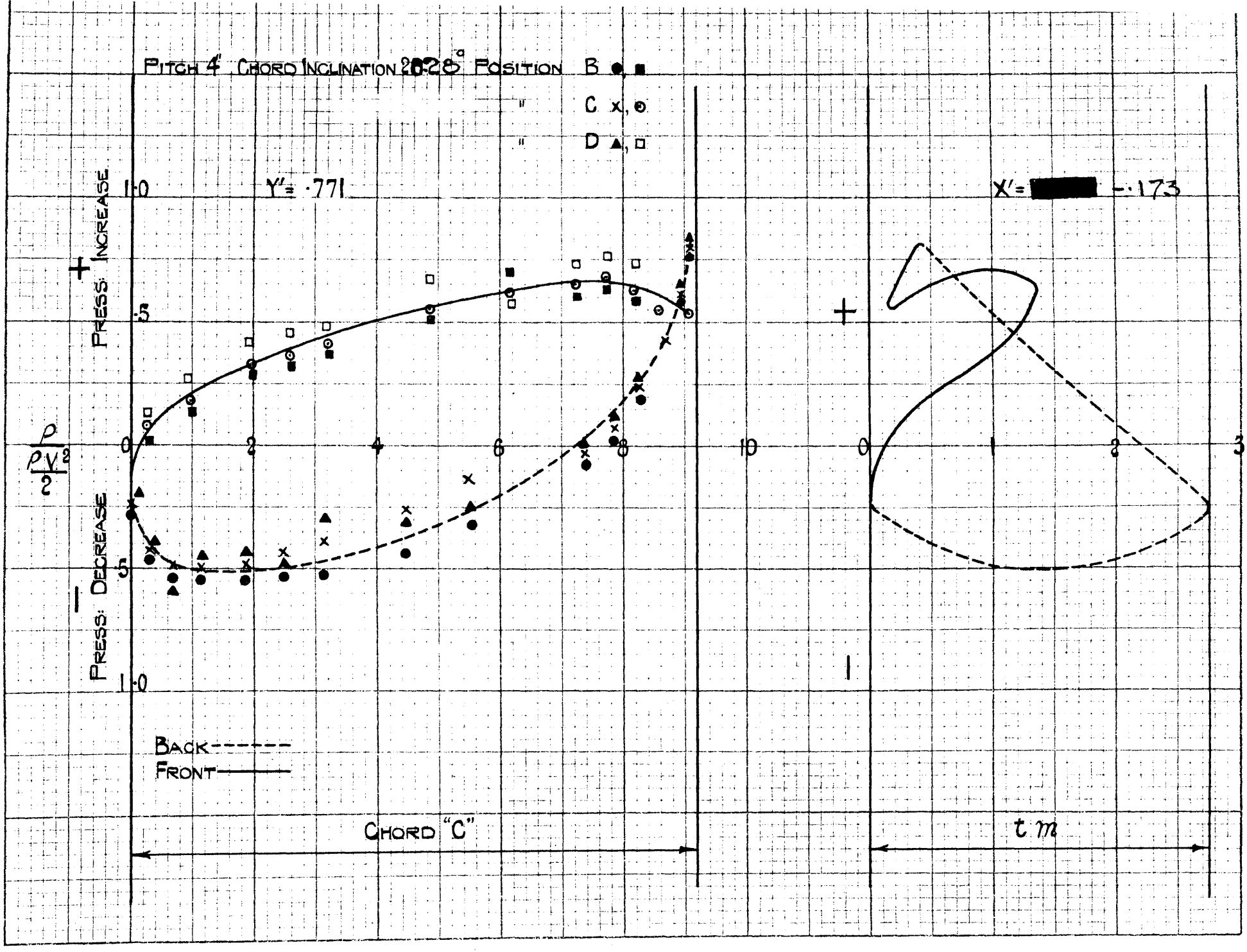
PITCH 4' CHORD INCLINATION 20.28° POSITION B ●, ■
" C x, ⊙
" D ▲, □
Y'' = .771
X' = [redacted] -.173
+ PRESS: INCREASE
− PRESS: DECREASE
$\frac{p}{\frac{\rho V^2}{2}}$
1.0
.5
0
.5
1.0
2
4
6
8
10
+
−
0
1
2
3
BACK ------
FRONT ——
CHORD "C"
t m

FIG 10

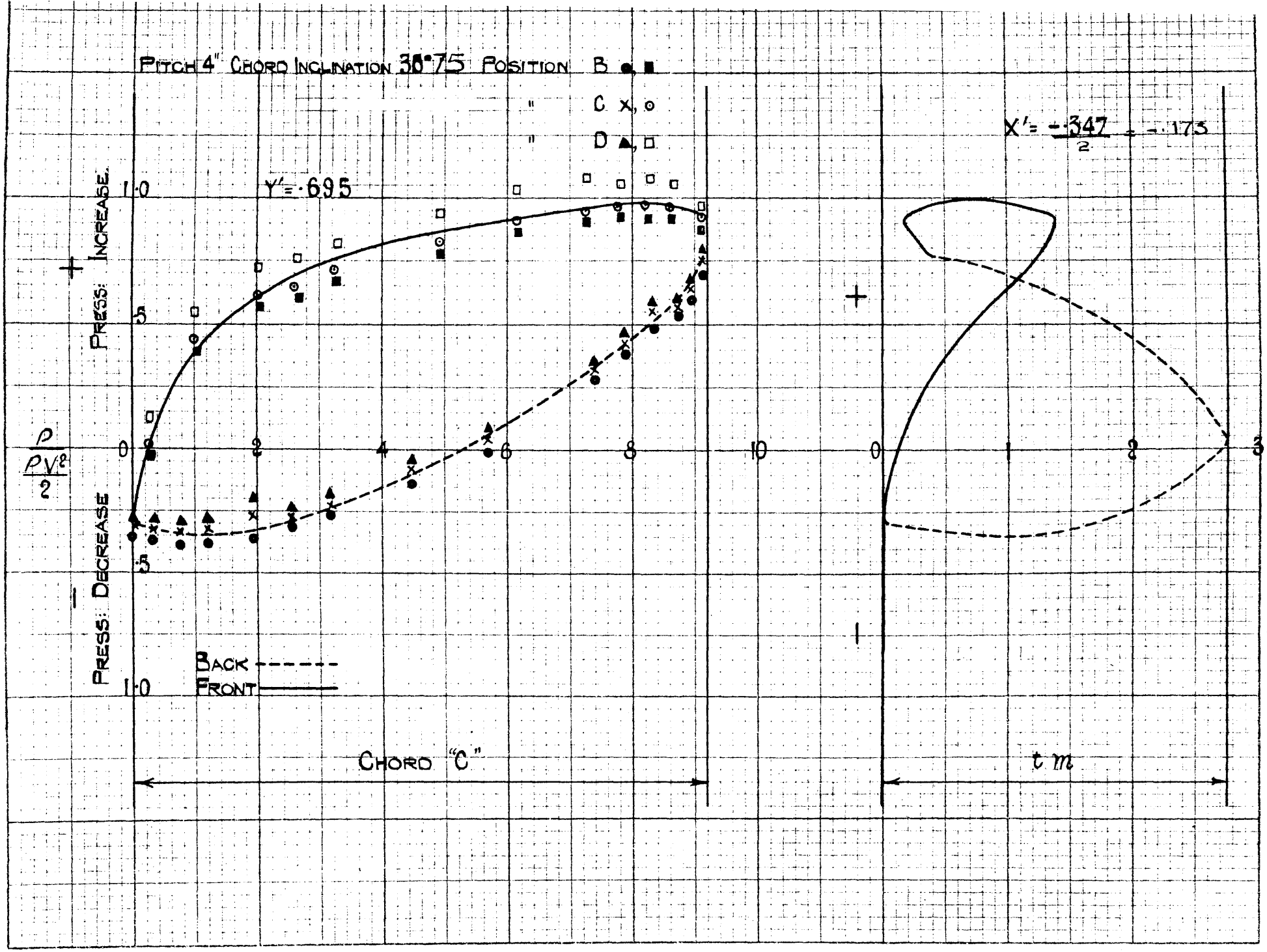
Pitch 4" Chord Inclination 38°75 Position B ●, ■
" C ×, ⊙
" D ▲, □
Y'=·695
X'= -·347/2 = -·173
Press: Increase
Press: Decrease
ρ / ρV²/2
1·0
·5
0
2
4
6
8
10
1
3
Back
Front
Chord "C"
t m

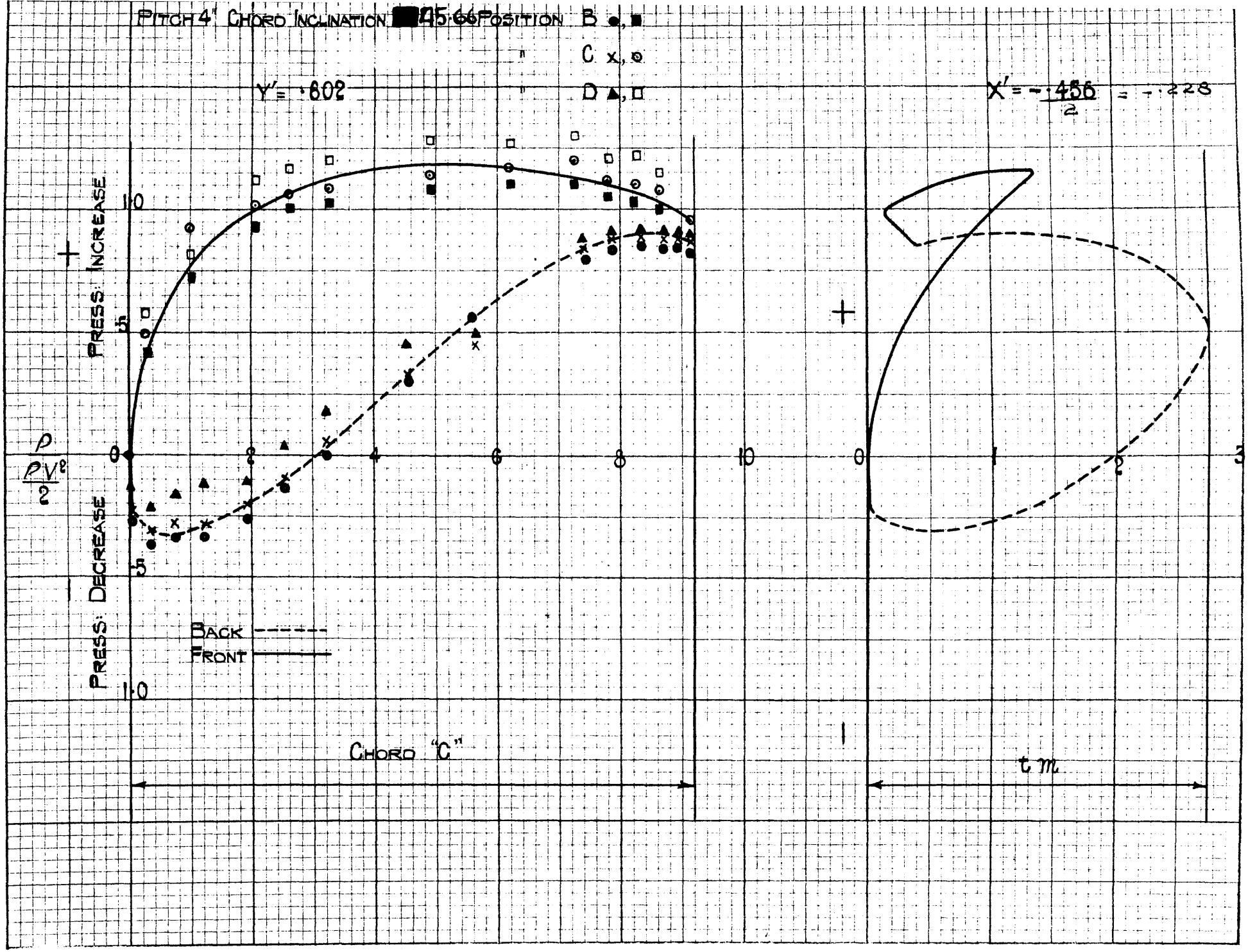
PITCH 4° CHORD INCLINATION [redacted]45·66 POSITION B ●, ■
C x, ⊙
D ▲, □
Y' = ·602
X' = -·456/2 = +·228
PRESS: INCREASE
PRESS: DECREASE
ρ/(ρV²/2)
BACK
FRONT
CHORD "C"
t m

FIG 12

A small difference in the area of each loop in any one diagram would have a relatively big effect on the difference of the two areas, and hence THE DRAG COEFFICIENT WHICH DEPENDS GREATLY ON THE DIFFERENCE OF THE TWO LOOPS WOULD BE CHANGED CONSIDERABLY.

Thus, the Drag Coefficients were calculated by weighing the forces on a floating blade by means of aerodynamic balances (given later).

THE PRESSURE DISTRIBUTION CURVES.

Pressure ratios were plotted in the dimensionless form $\frac{P}{\rho \frac{V^2}{2}}$ against the chord lengths Figs. 8 - 27 for a blade in a grate of a series of equal blades and Figs. 28 - 32 for a solitary blade.

Referring again to Fig. (7), the tangential force F, will have no component parallel to the span, as the flow is two dimensional.

P & F vary from point to point over the blade, leading to a variation of force from one element to another in both magnitude and direction.

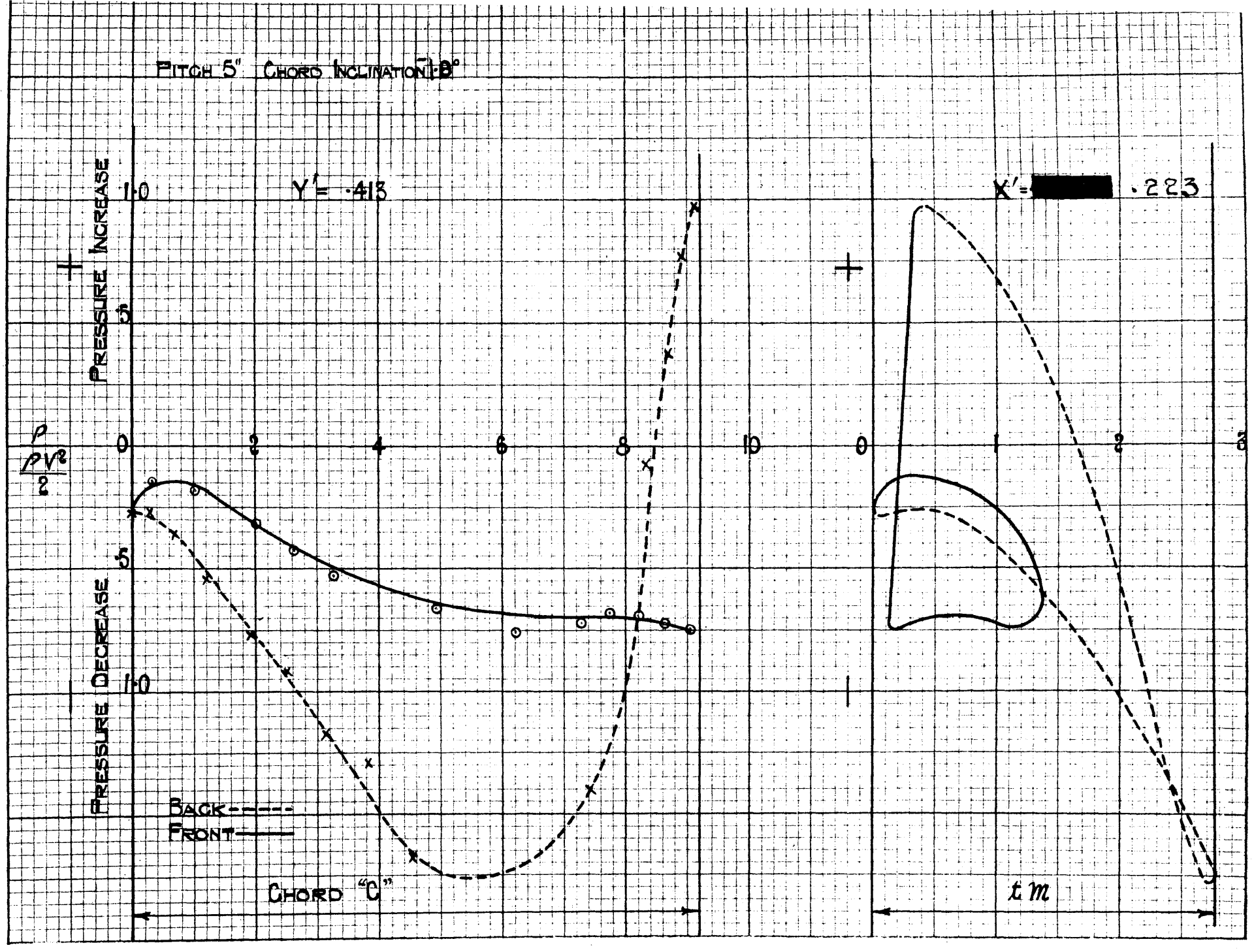
PITCH 5" CHORD INCLINATION -1.8°
Y' = .413
X' = .223
PRESSURE INCREASE
PRESSURE DECREASE
$\frac{p}{\frac{\rho V^2}{2}}$
1.0
.5
0
2
4
6
8
10
.5
1.0
BACK
FRONT
CHORD "C"
t m
0
1
2
3

FIG 13

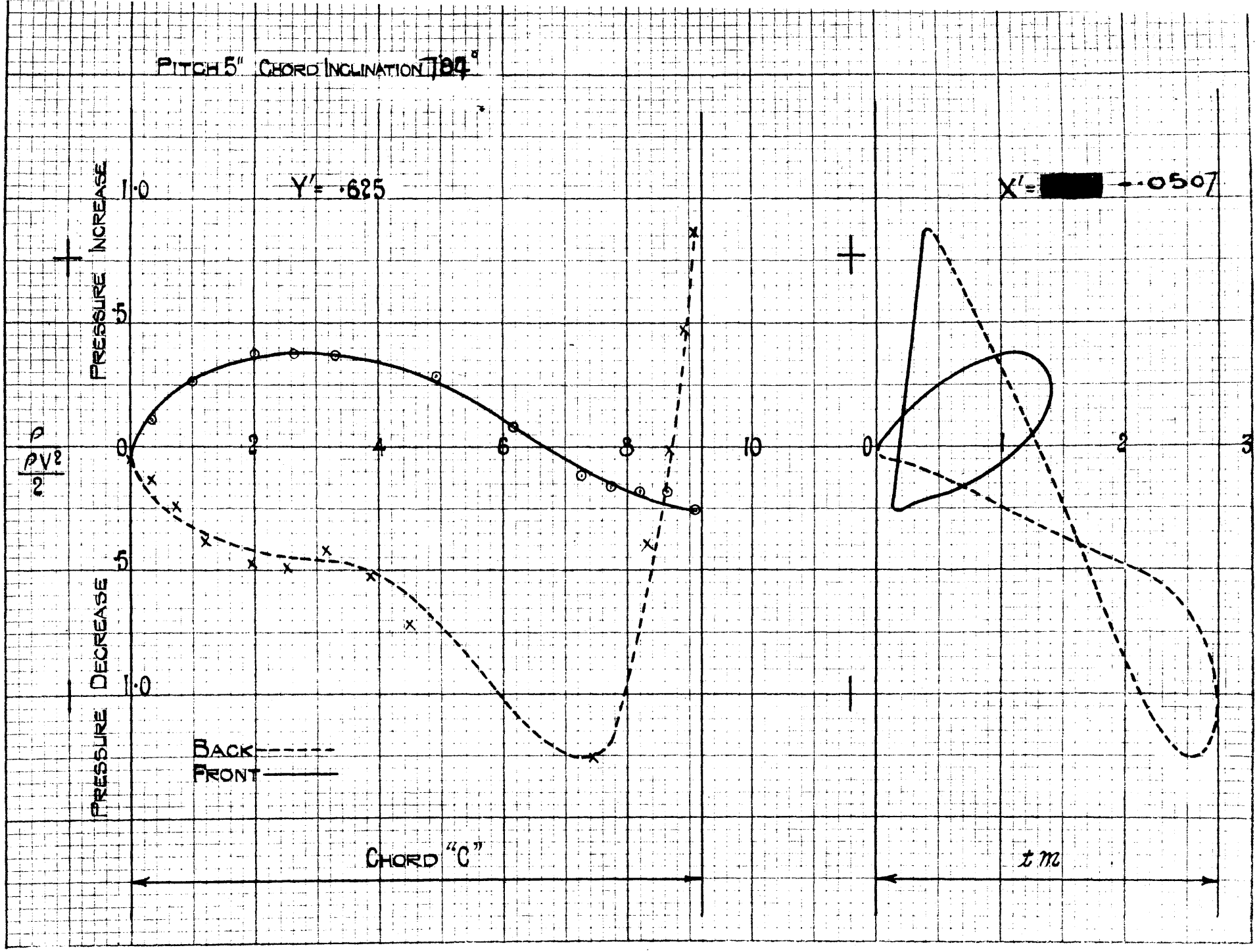
PITCH 5" CHORD INCLINATION 7.84°
Y' = .625
X' = [redacted] + .0507
PRESSURE INCREASE
PRESSURE DECREASE
$\frac{p}{\frac{\rho V^2}{2}}$
1.0
.5
0
2
4
6
8
10
.5
1.0
BACK
FRONT
CHORD "C"
0
1
2
3
t m

Fig. 14

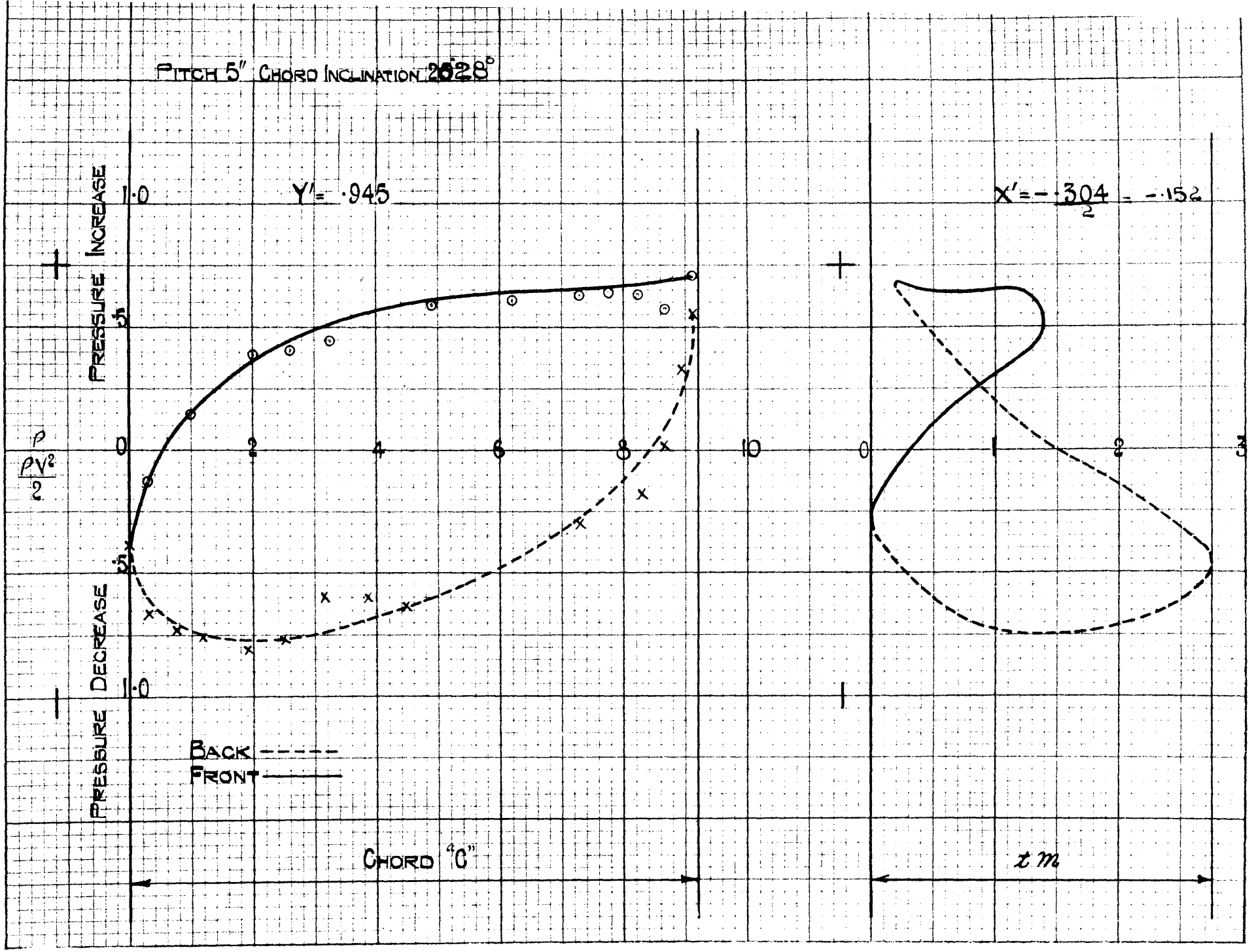
PITCH 5" CHORD INCLINATION 26°28'
Y'= ·945
X'= -·304/2 = -·152
PRESSURE INCREASE
PRESSURE DECREASE
ρ/(ρV²/2)
1·0
0
2
4
6
8
10
1·0
BACK
FRONT
CHORD "C"
x m

FIG 15

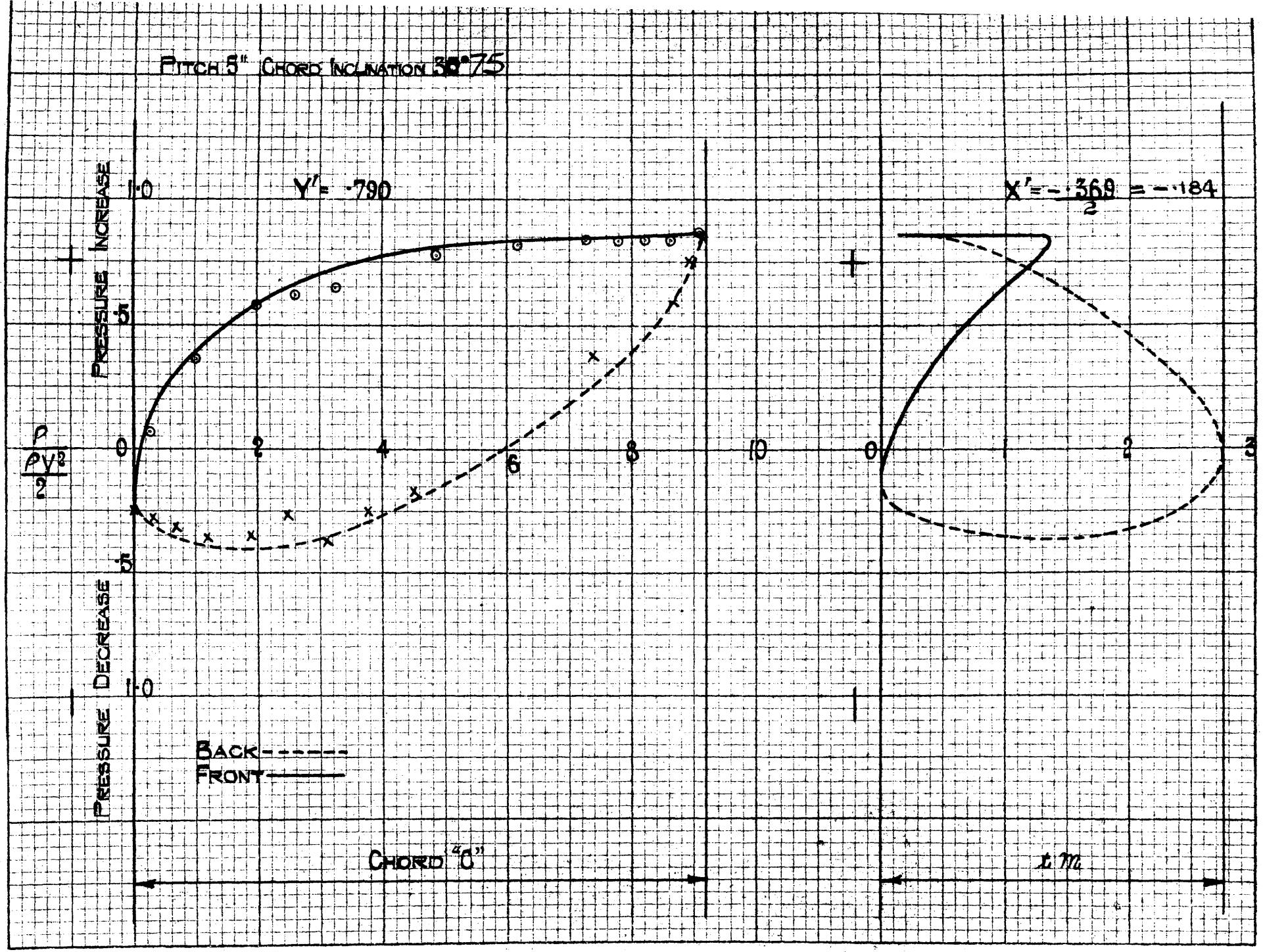
PITCH 5" CHORD INCLINATION 38°75
Y' = ·790
X' = -·369/2 = -·184
PRESSURE INCREASE
PRESSURE DECREASE
p / ρV²/2
1·0
0
2
4
6
8
10
1·0
BACK
FRONT
CHORD "C"
t m

FIG 16

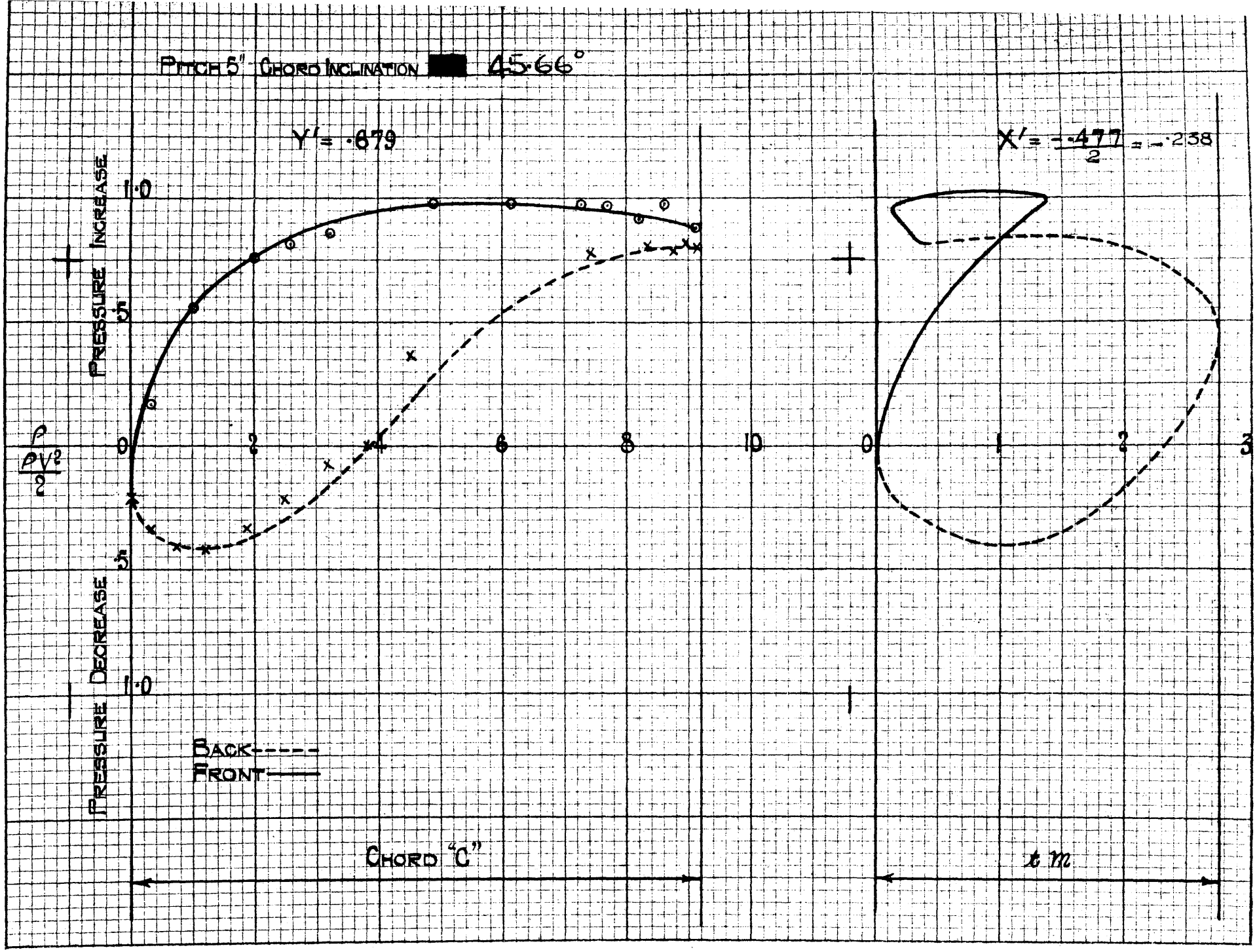
Pitch 5" Chord Inclination [redacted] 45·66°
Y' = ·679
X' = -·477/2 = -·238
Pressure Increase
Pressure Decrease
1·0
·5
0
·5
1·0
2
4
6
8
10
0
1
2
3
Back
Front
Chord "C"
t m

Fig. 17

The area enveloped by the curves which are obtained by joining the pressure ratios (registered by the pressure holes drilled in mid span of the copper tubes) on a base of chord lengths, Fig. (4a), and completed so as to represent the pressure round the whole contour of the blade, is proportional to that part of the lift which is due to P.

Projections from points on these curves to the left, Fig. 8 - 32, were then made along a line parallel to the line of action of P, and the pressure ratios set normally to this line and a closed curve was obtained by joining all the points and completing it, so as to include all positions round the contour. The net area enclosed by this curve on the right is proportional to the contribution to drag by P.

Integration of the areas enclosed by these curves allows the values of the forces normal and parallel to the chord to be calculated.

From the values of these forces, i.e., Y' and X', the first approximation to the lift coefficient is obtained.

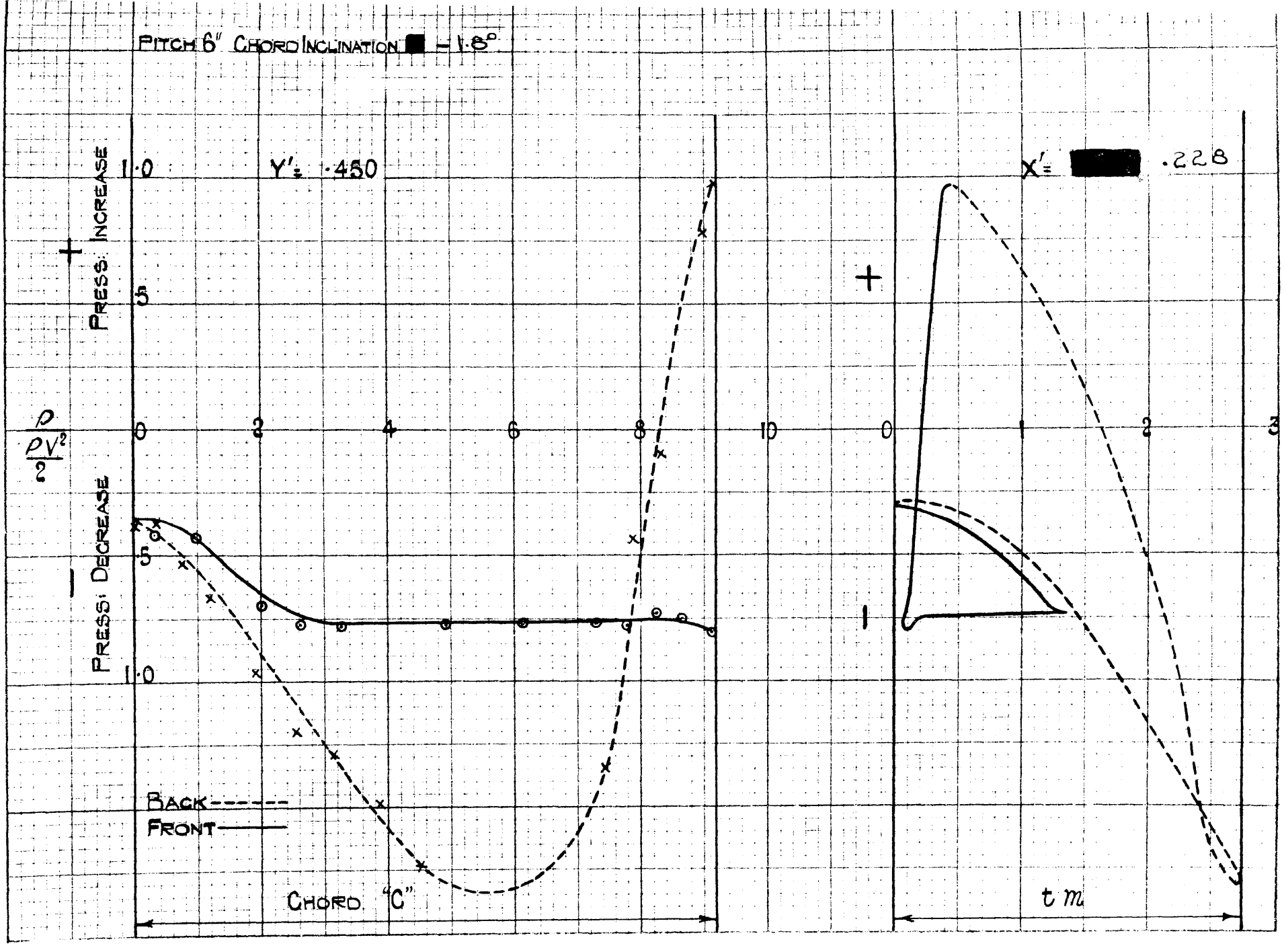
PITCH 6" CHORD INCLINATION [redacted] = 1·8°
Y' = ·450
X' = [redacted] ·228
PRESS: INCREASE
PRESS: DECREASE
+
−
$\frac{p}{\frac{\rho V^2}{2}}$
1·0
5
0
2
4
6
8
10
5
1·0
BACK ------
FRONT ——
CHORD "C"
0
1
2
3
t m

FIG 18

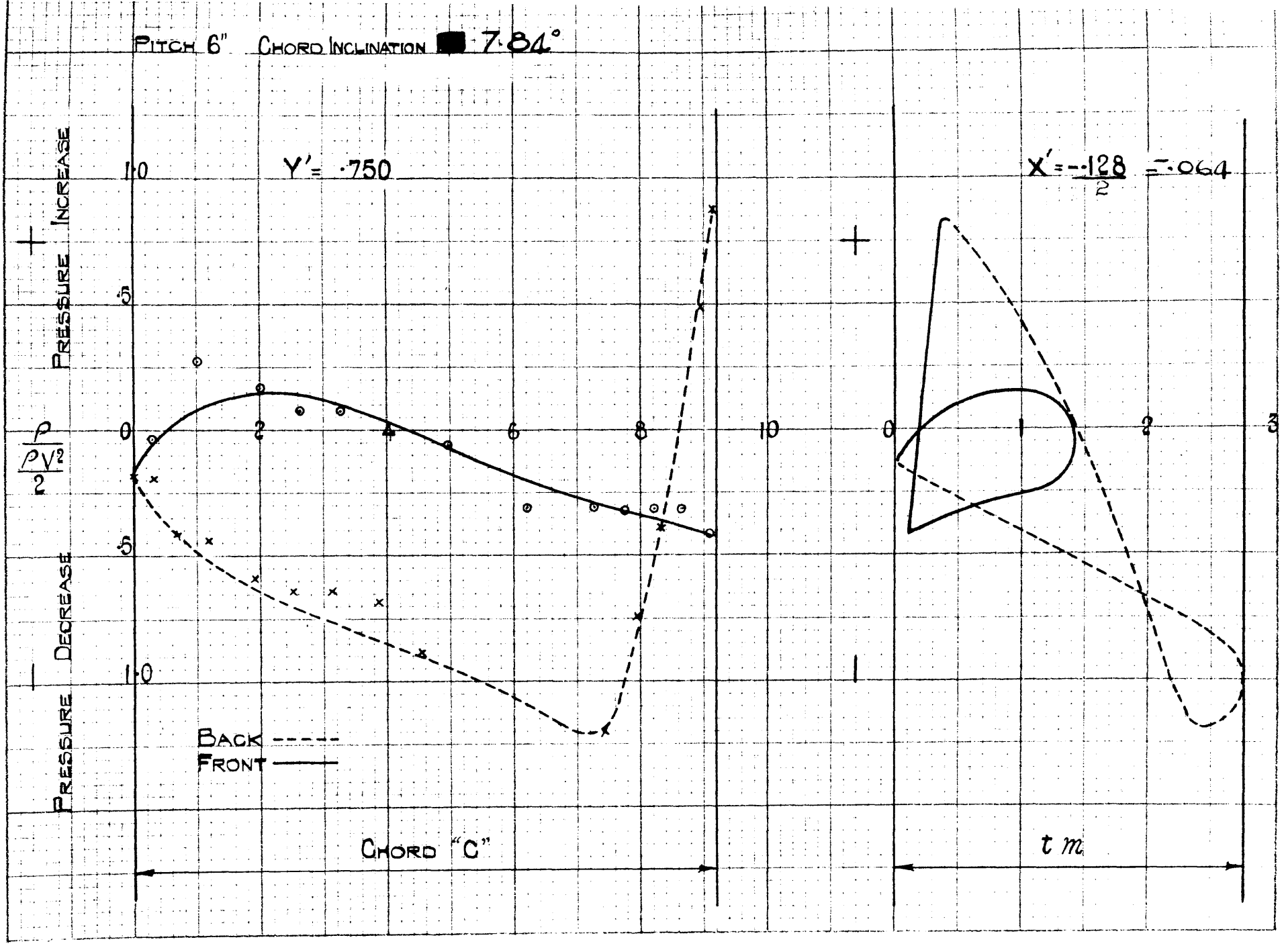
PITCH 6" CHORD INCLINATION ■ 7·84°
Y'= ·750
X'= -·128/2 = -·064
+ PRESSURE INCREASE
- PRESSURE DECREASE
ρ / (ρV²/2)
1·0
·5
0
·5
1·0
2
4
6
8
10
0
1
2
3
BACK -----
FRONT ——
CHORD "C"
t m

FIG 19

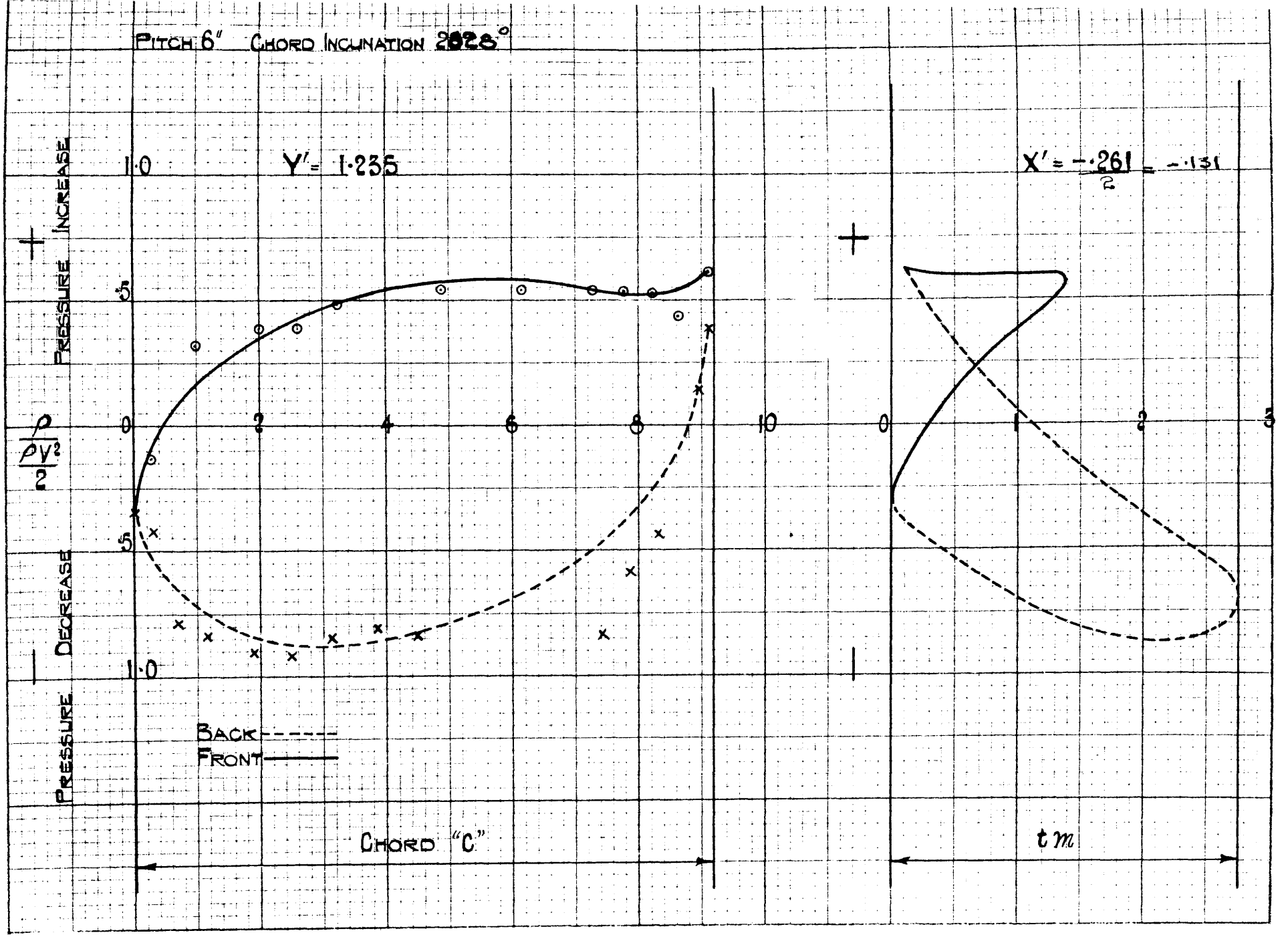
PITCH 6" CHORD INCLINATION 2828°
Y' = 1.235
X' = -.261/2 = -.131
+ PRESSURE INCREASE
- PRESSURE DECREASE
ρ / (ρV²/2)
1.0
.5
0
2
4
6
8
10
.5
1.0
BACK
FRONT
CHORD "C"
tm
0
1
2
3

FIG 20

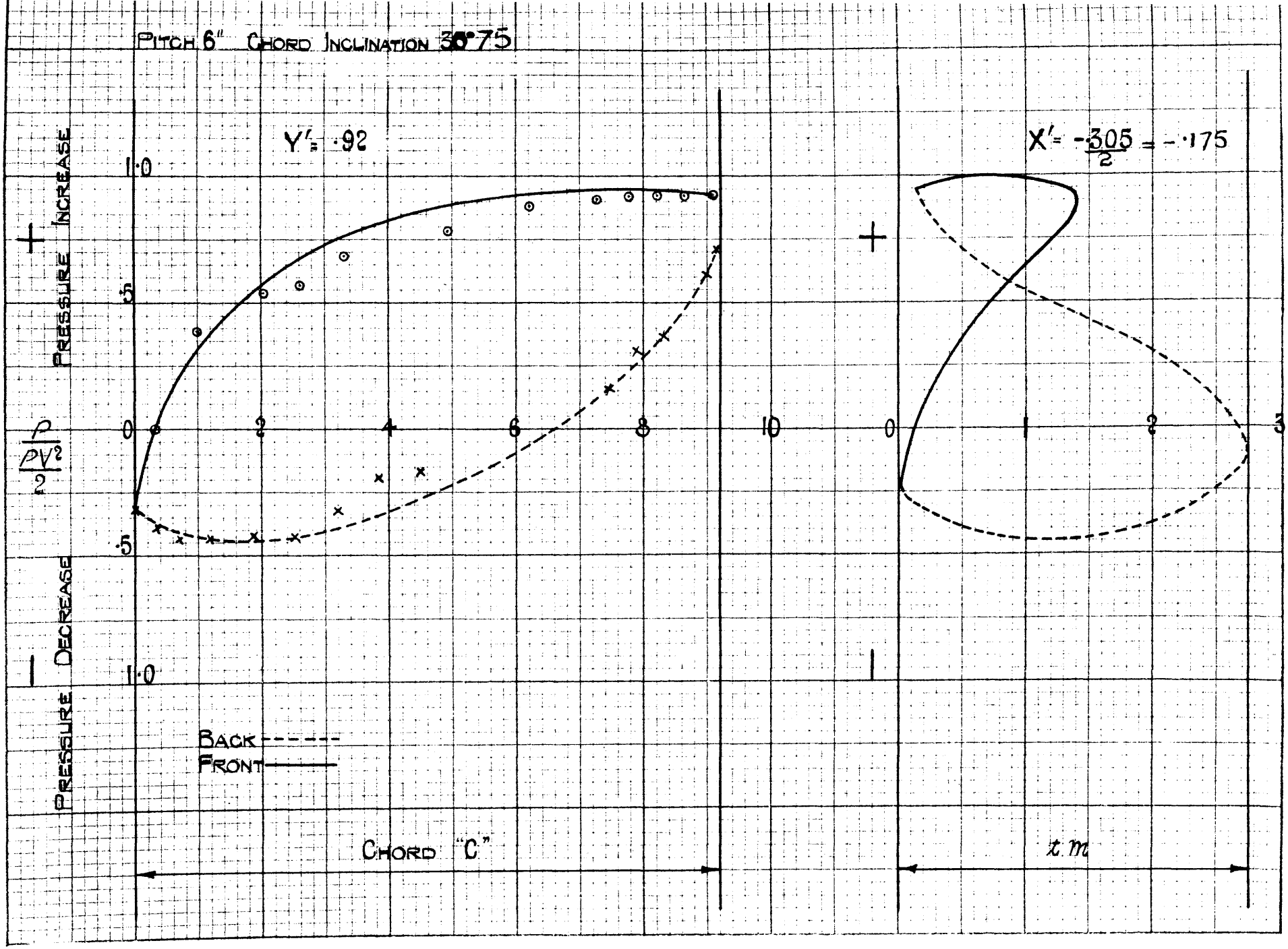
PITCH 6" CHORD INCLINATION 30°75'
Y'= ·92
X'= -·305/2 = -·175
PRESSURE INCREASE
PRESSURE DECREASE
+
−
ρ/(ρV²/2)
1·0
·5
0
2
4
6
8
10
1
3
BACK
FRONT
CHORD "C"
x.m

FIG. 21

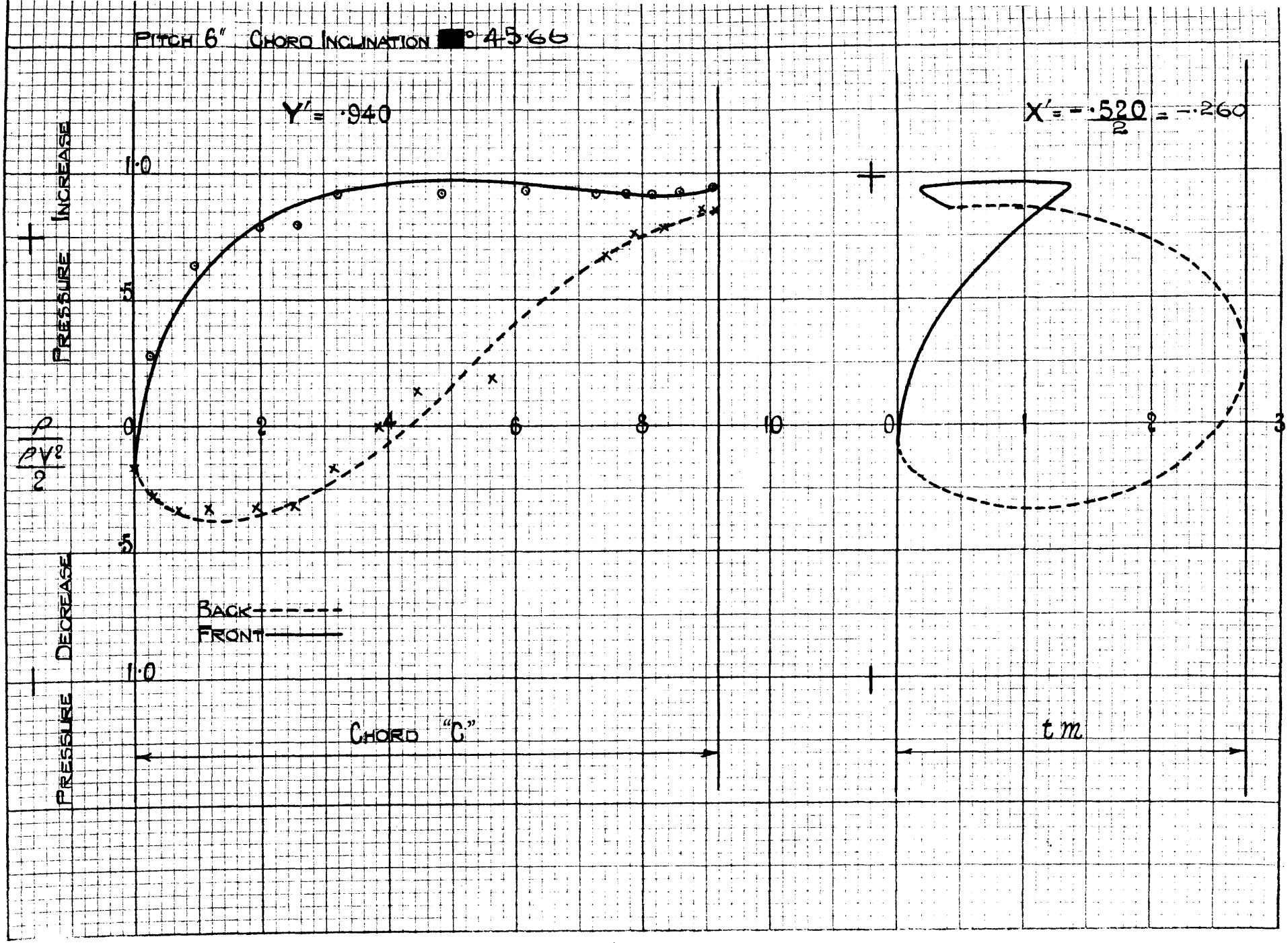
PITCH 6" CHORD INCLINATION [redacted]° 4566
Y' = ·940
X' = -·520/2 = -·260
+ PRESSURE INCREASE
- PRESSURE DECREASE
p / ρV²/2
1·0
·5
0
2
4
6
8
10
BACK
FRONT
CHORD "C"
+
-
0
1
2
3
tm

FIG 22

All the results were corrected to infinite aspect Ratio by taking account of the interference factors.

Figs. 8 - 27 give the Pressure Distribution diagrams fora blade which is a member of a series of equal blades, for varying Blade Pitches and over a wide range of chord inclinations (angles of incidence) which have been selected so that the various changes due to the varying angles of incidence may be studied.

The examination of these curves reveals the interesting fact that most of the lifting force at the back of the blade is due to negative pressure. This, however, is specially marked in the lower incidences.

It will also be noticed that the biggest force Y' is given when the blade chord is inclined at an angle of about 20°.

Incidentally at this chord inclination the blade is at its designed angle (the angle at which the blade is fixed on the rotor to give the maximum torque).

The pressure distribution at this particular incidence for any blade pitch is more uniform on both the upper and lower surfaces of the blade.

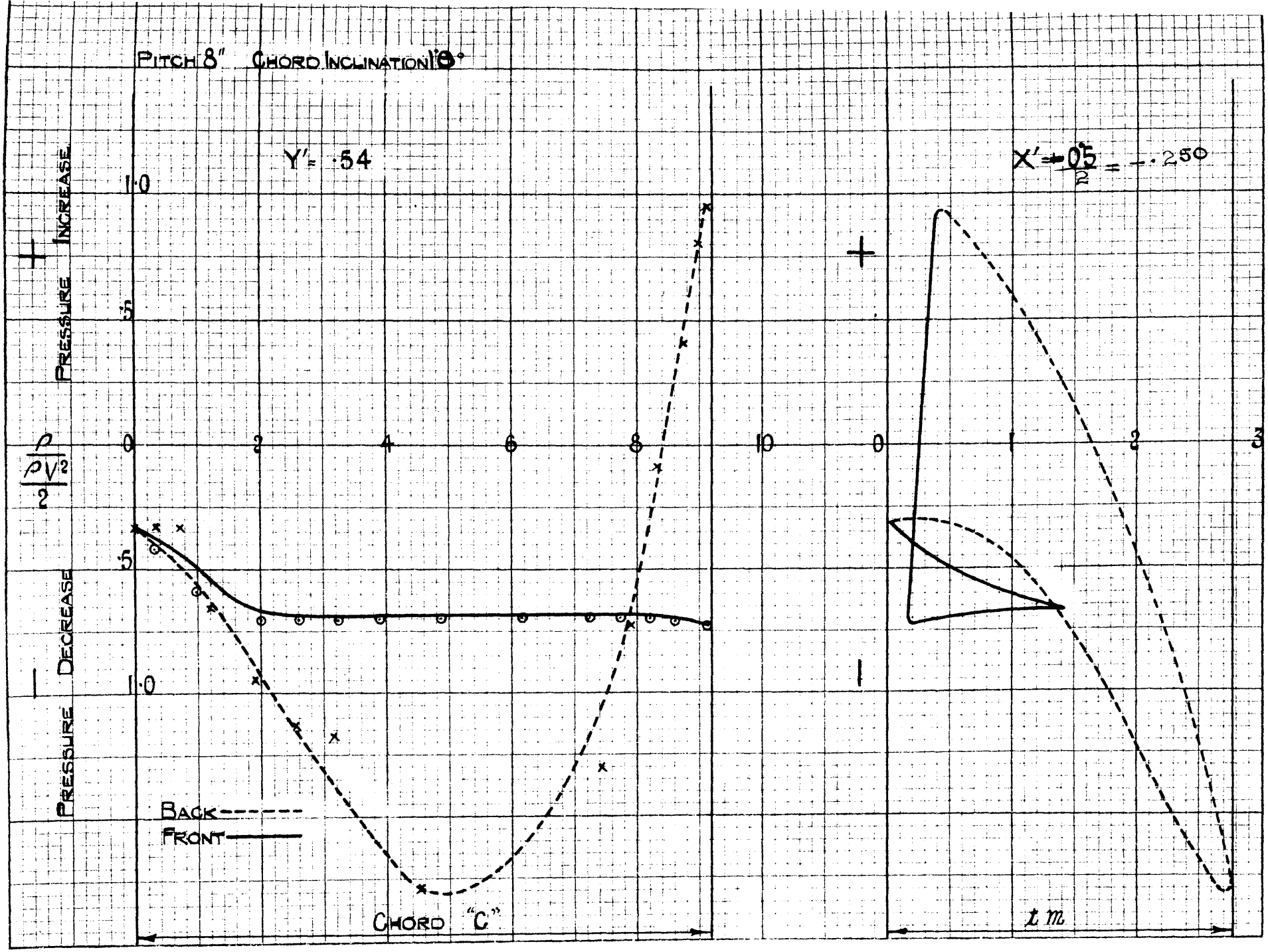
PITCH 8" CHORD INCLINATION 8°
Y' = .54
X' = .05/b = .250
+ PRESSURE INCREASE
- PRESSURE DECREASE
p / (ρV²/2)
1.0
.5
0
2
4
6
8
10
0
1
2
3
1.0
BACK
FRONT
CHORD "C"
t m

FIG 23

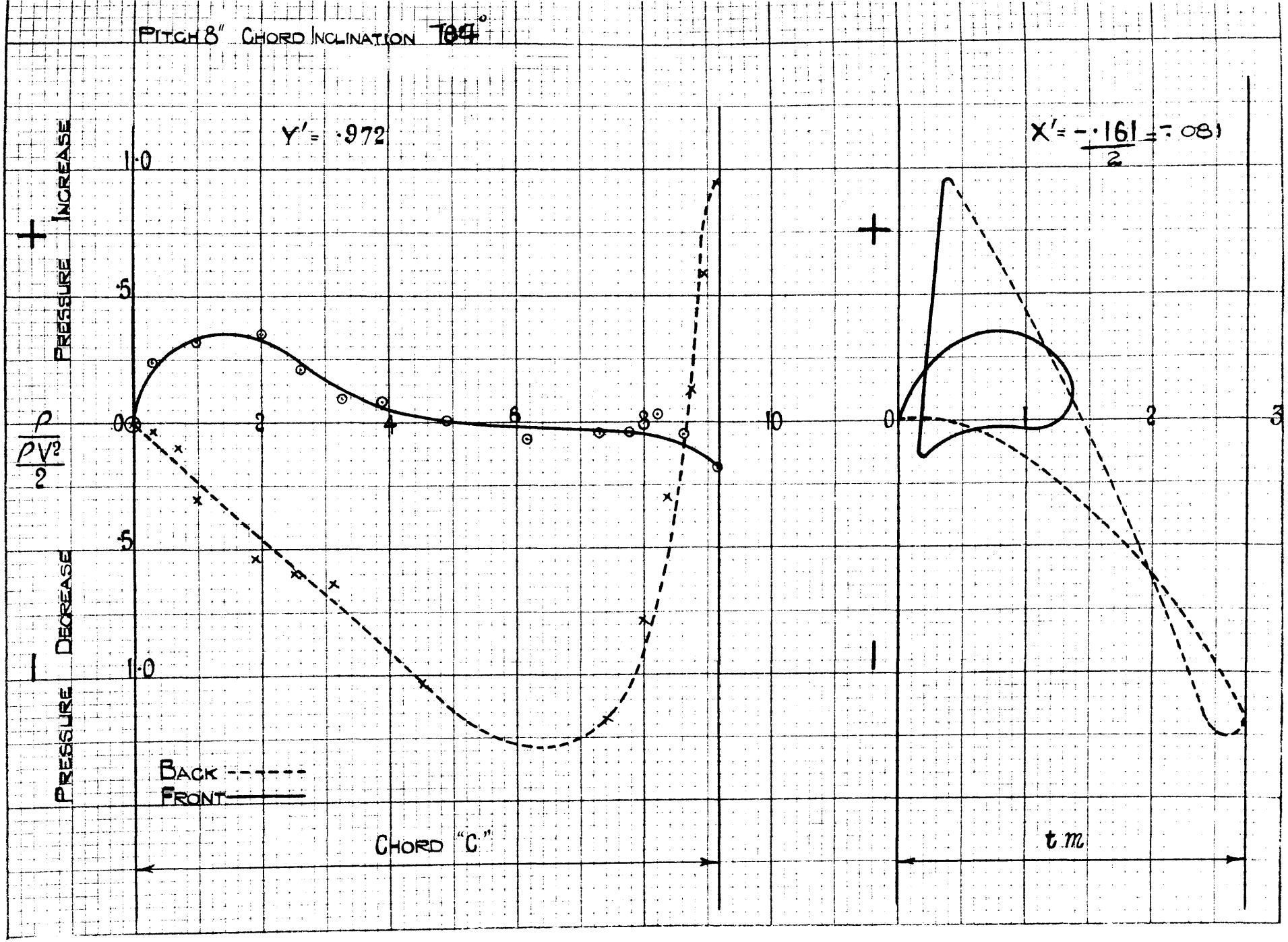
PITCH 8" CHORD INCLINATION 18½°
Y' = ·972
X' = -·161/2 = ·081
+ PRESSURE INCREASE
- PRESSURE DECREASE
ρ / (ρV²/2)
1·0
·5
0
2
4
6
8
10
·5
1·0
BACK
FRONT
CHORD "C"
+
0
1
2
3
1
t m

FIG 24

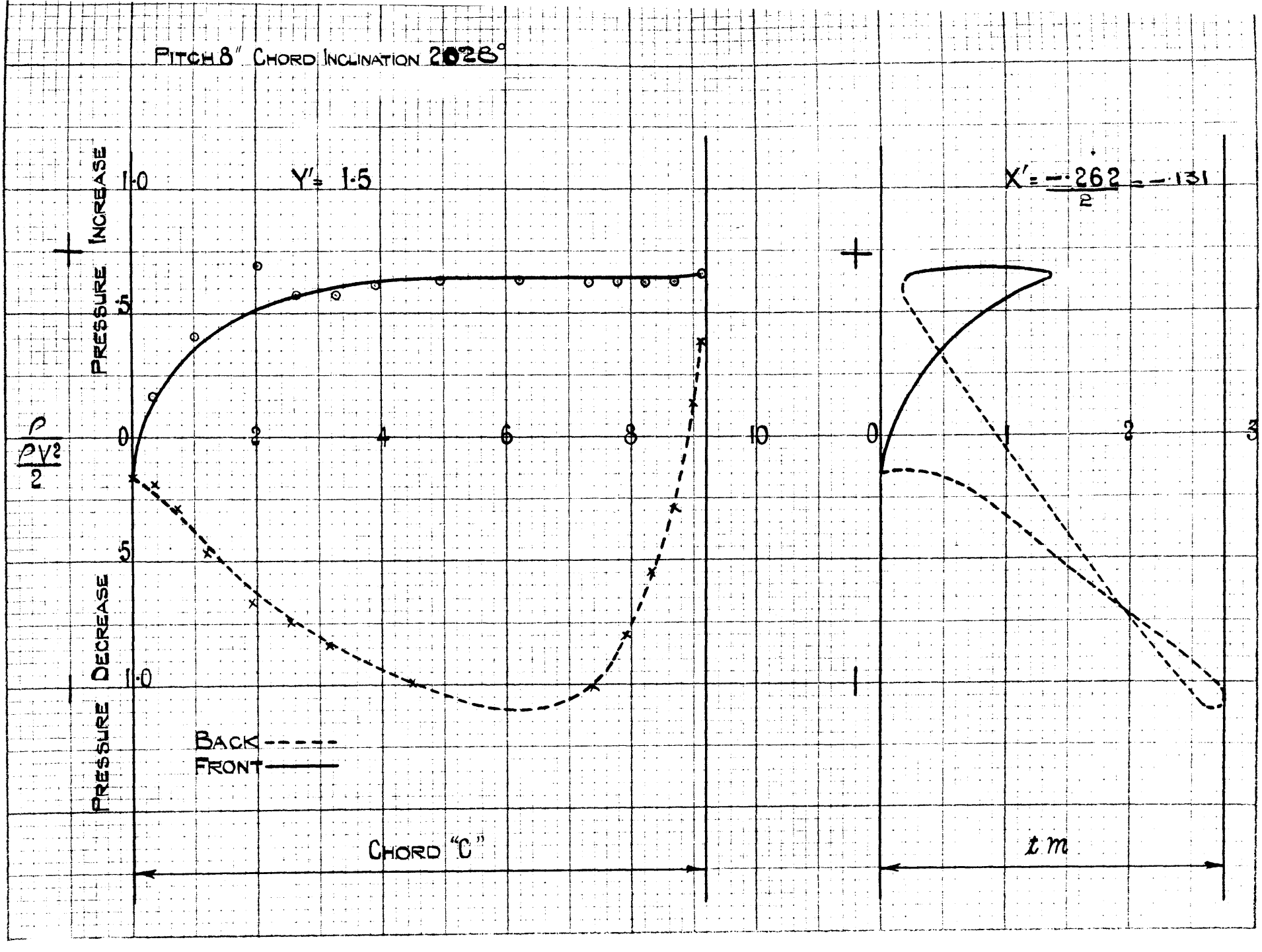
PITCH 8" CHORD INCLINATION 2028°
Y'= 1·5
X'= −·262 / 2 = −·131
PRESSURE INCREASE
PRESSURE DECREASE
1·0
1·0
0
2
4
6
8
10
0
1
2
3
ρ / (ρV²/2)
BACK
FRONT
CHORD "C"
t m

FIG 25

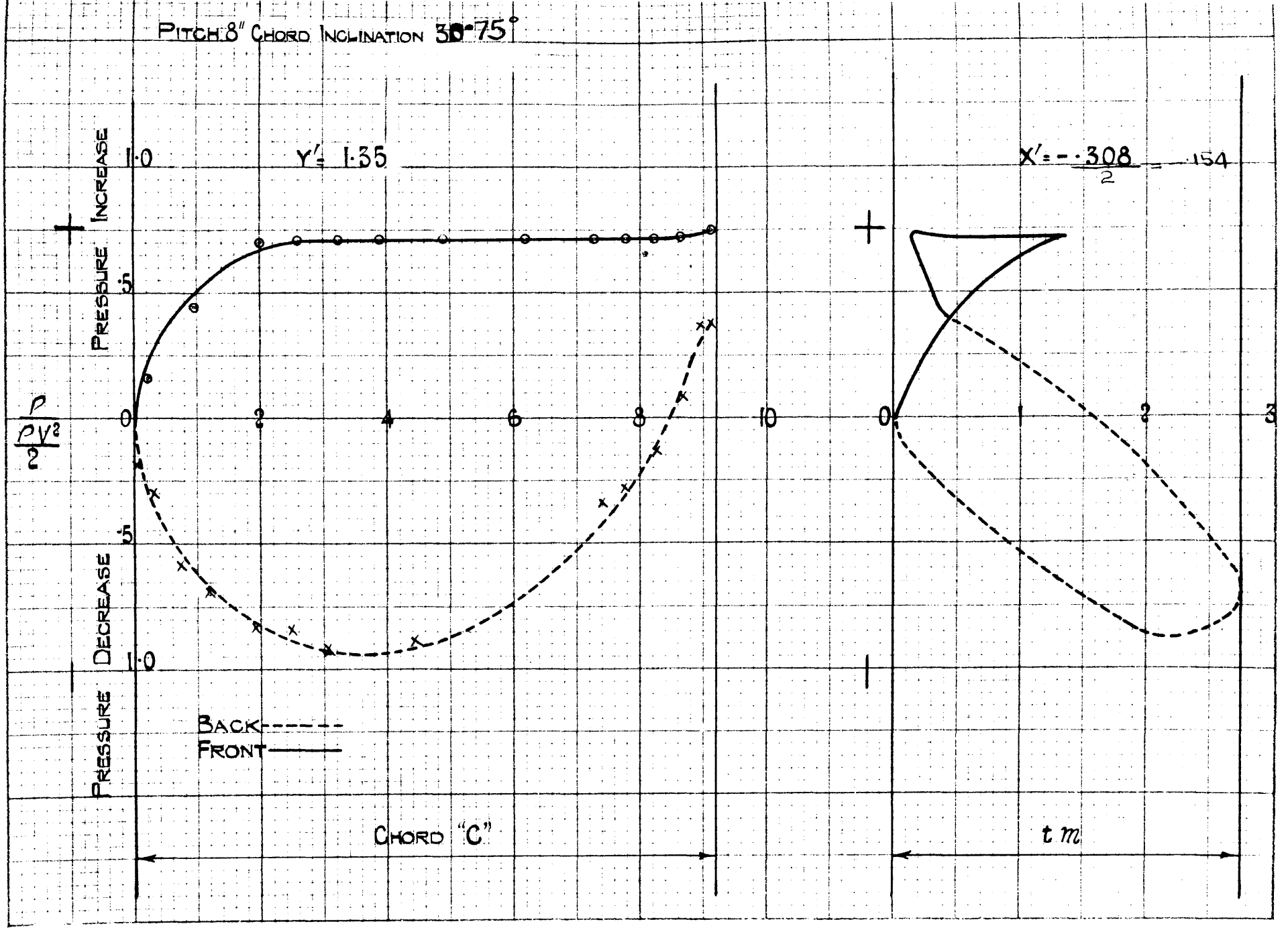
PITCH 8" CHORD INCLINATION 30°75'
Y' = 1.35
X' = -.308/2 = -.154
PRESSURE INCREASE
PRESSURE DECREASE
1.0
1.0
0
2
4
6
8
10
0
1
2
3
p/(ρV²/2)
BACK
FRONT
CHORD "C"
t m

FIG 26

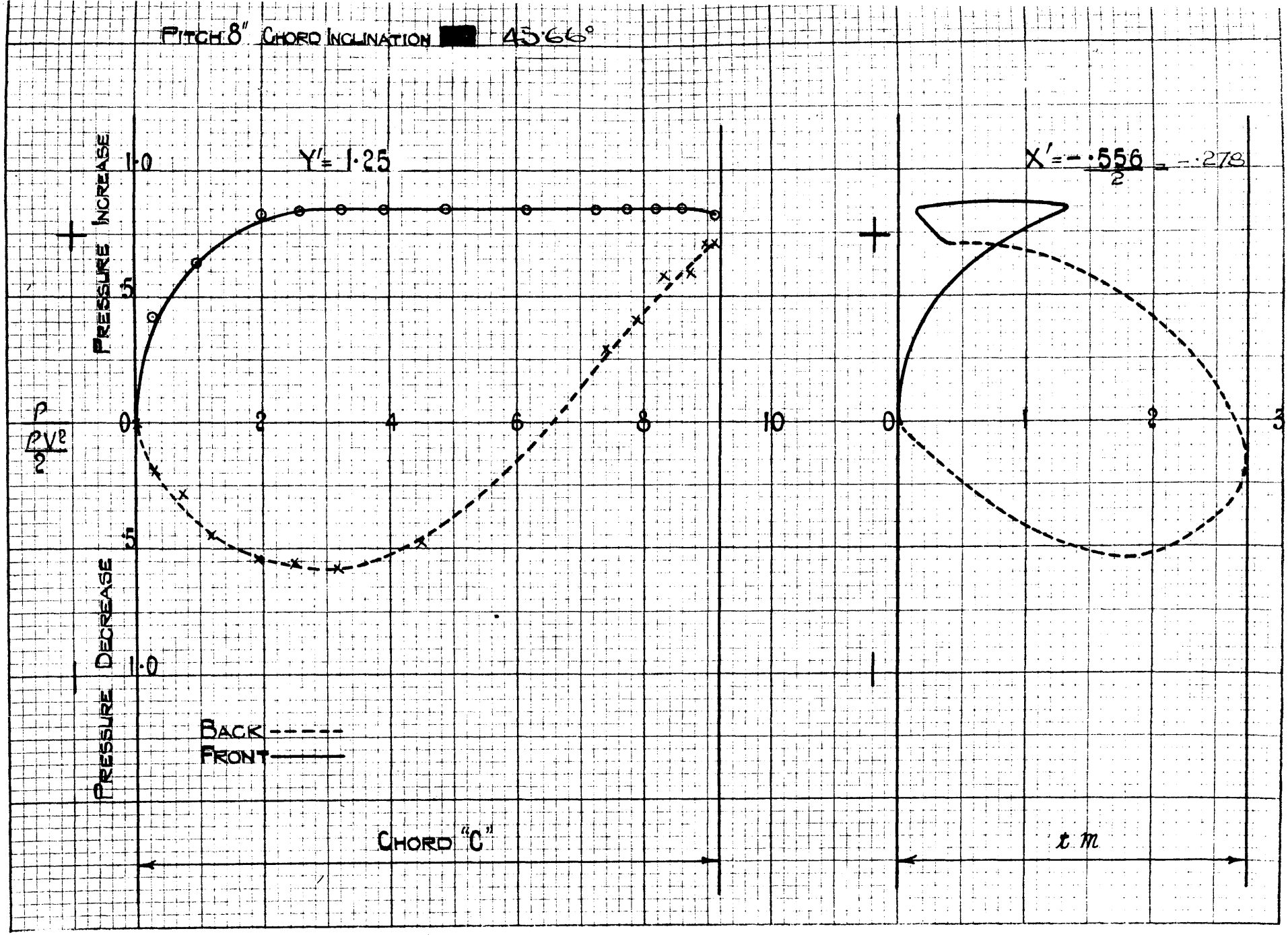
PITCH 8" CHORD INCLINATION [redacted] 45·66°
Y' = 1·25
X' = -·556/2 = -·278
PRESSURE INCREASE
PRESSURE DECREASE
1·0
·5
·5
1·0
P / ρV²/2
0
2
4
6
8
10
0
1
2
3
BACK
FRONT
CHORD "C"
t m

FIG 27

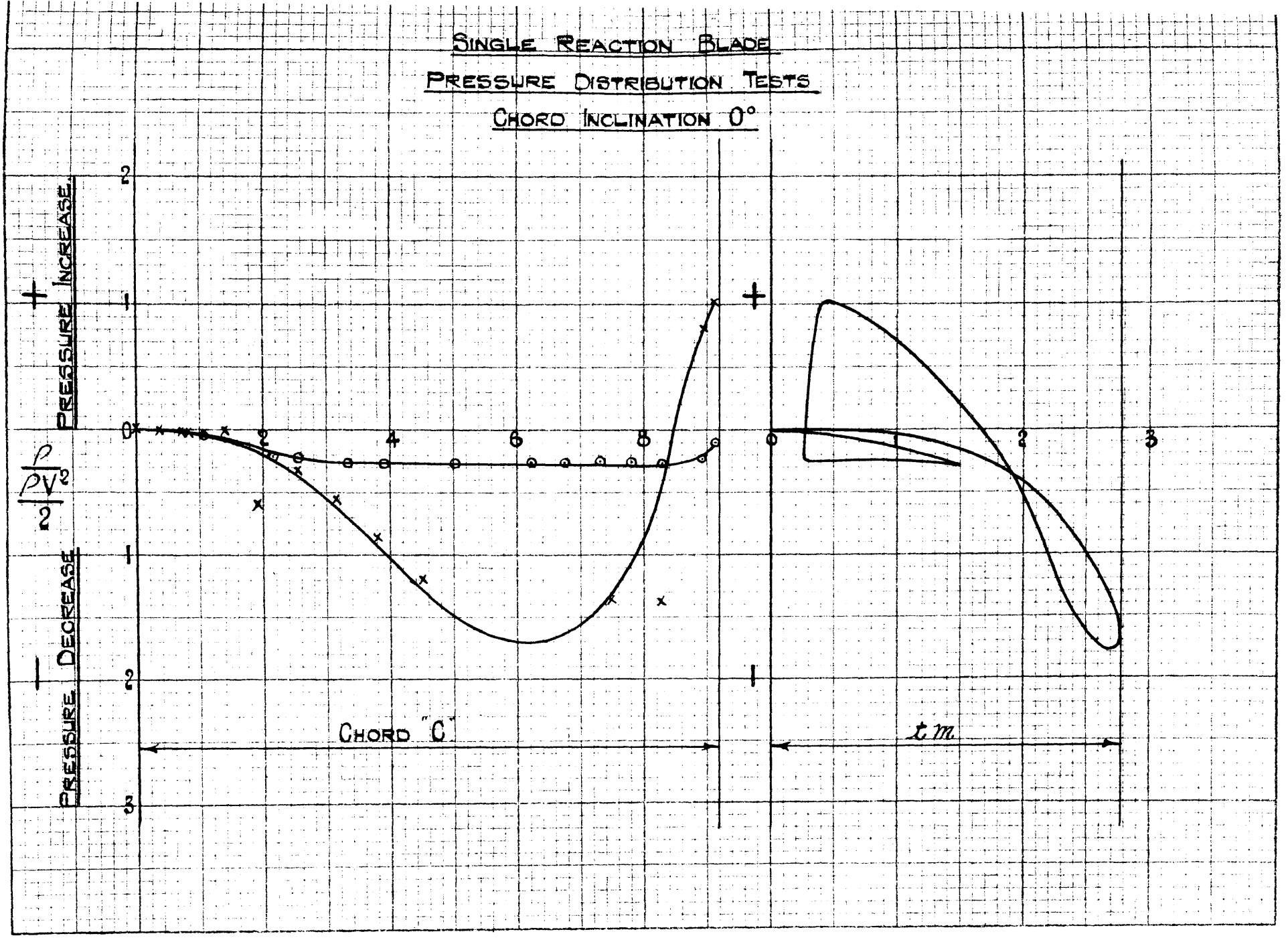
SINGLE REACTION BLADE
PRESSURE DISTRIBUTION TESTS
CHORD INCLINATION 0°
+ PRESSURE INCREASE
− PRESSURE DECREASE
p / (ρV²/2)
2
1
0
1
2
3
0
2
4
6
8
0
1
2
3
CHORD "C"
t m

FIG 28

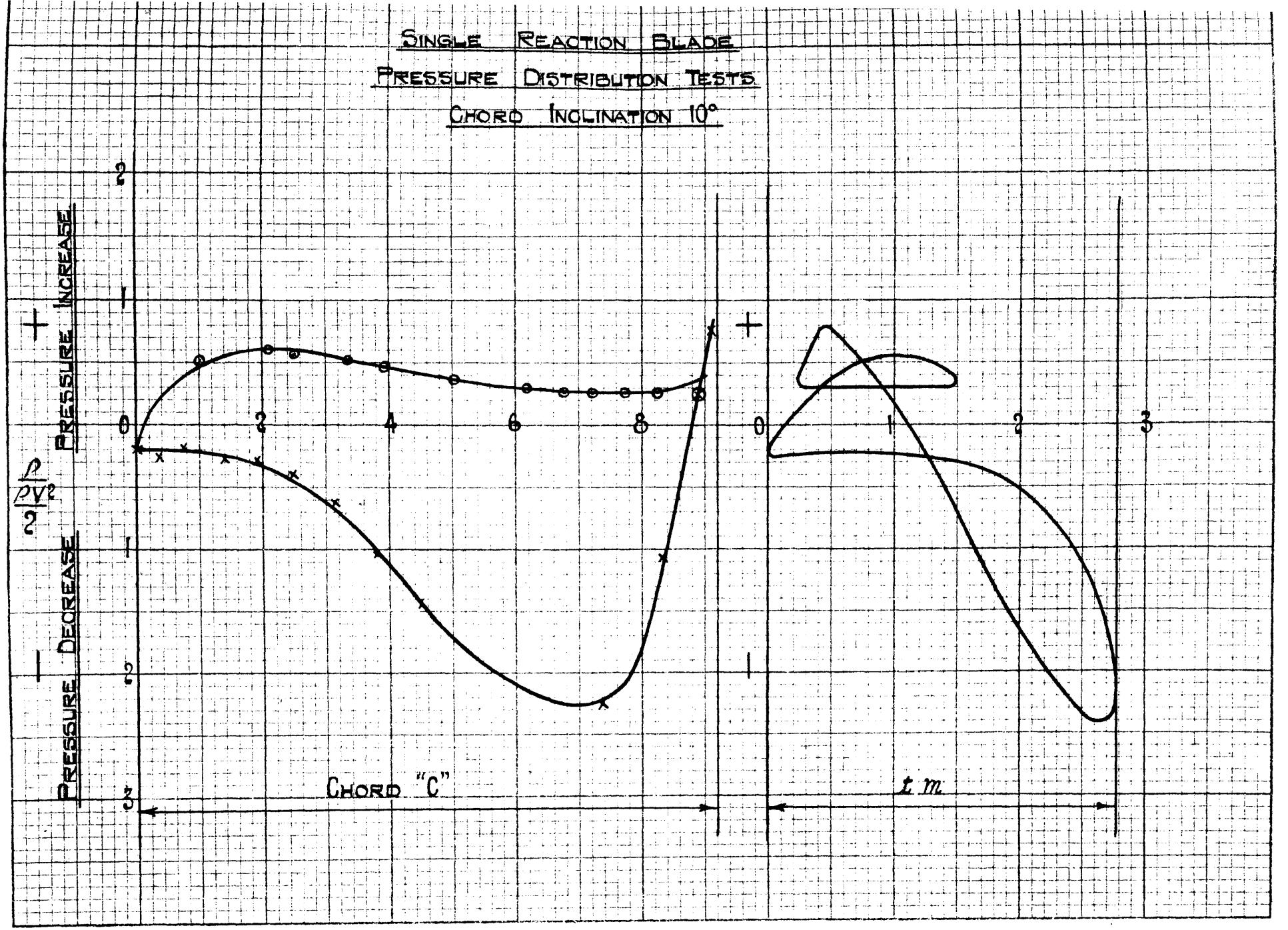
SINGLE REACTION BLADE
PRESSURE DISTRIBUTION TESTS
CHORD INCLINATION 10°
PRESSURE INCREASE
PRESSURE DECREASE
$\frac{p}{\frac{\rho V^2}{2}}$
+
—
2
1
0
1
2
3
0
2
4
6
8
0
1
2
3
CHORD "C"
t m

FIG 29

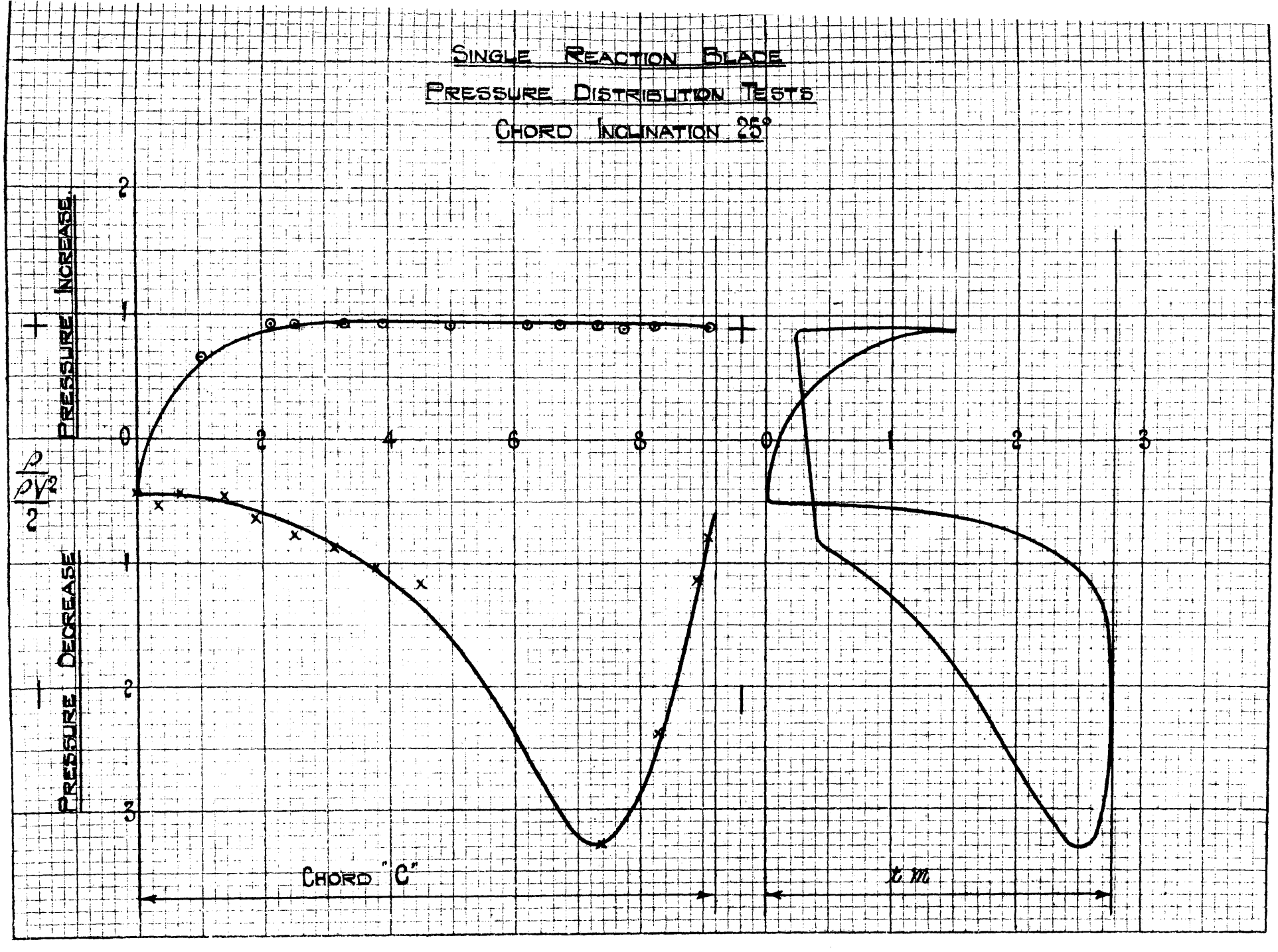
SINGLE REACTION BLADE
PRESSURE DISTRIBUTION TESTS
CHORD INCLINATION 25°
+ PRESSURE INCREASE
$\frac{p}{\rho V^2/2}$
− PRESSURE DECREASE
2
1
0
1
2
3
0
2
4
6
8
0
1
2
3
CHORD "C"
x m

FIG 30

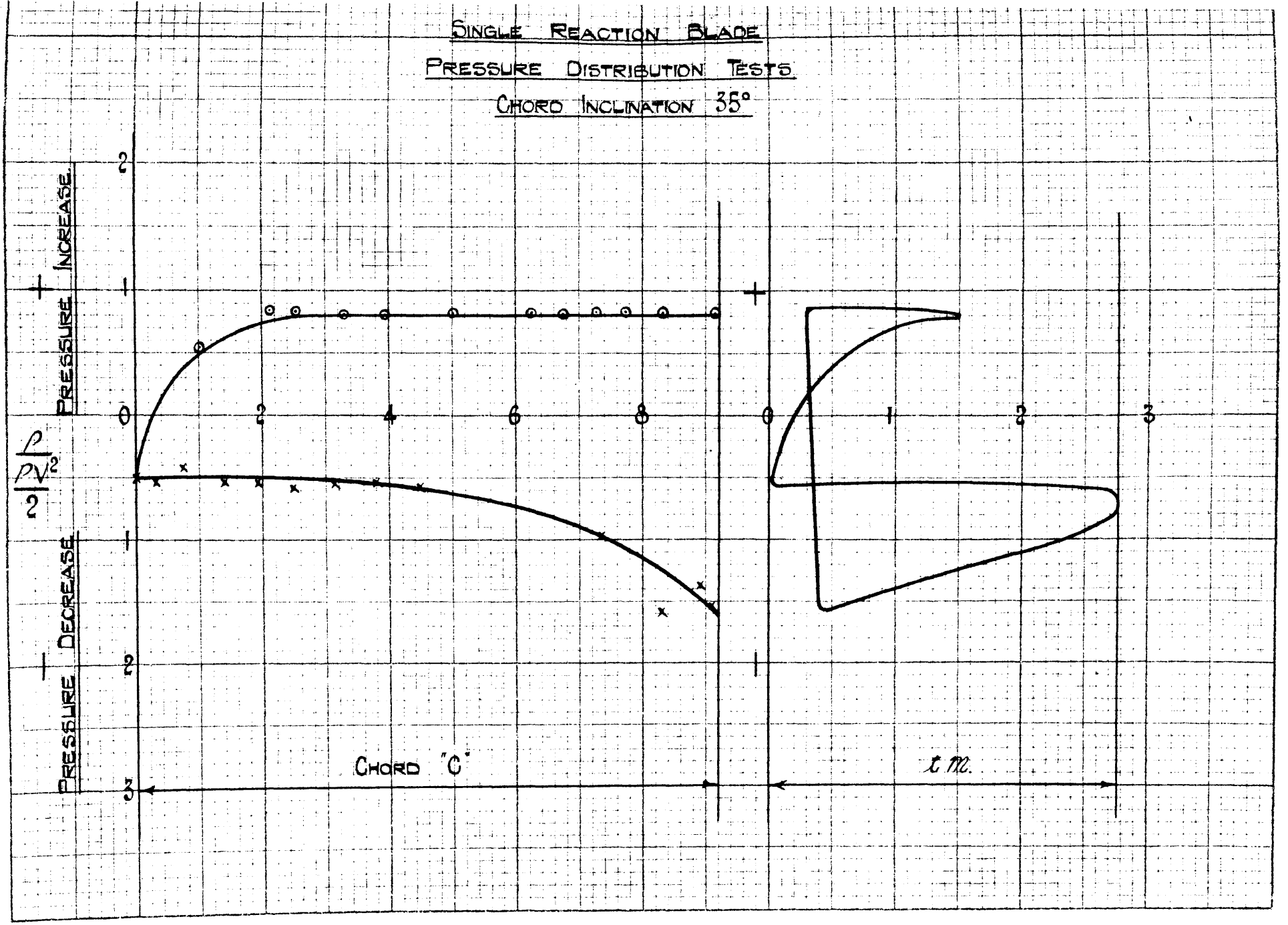
SINGLE REACTION BLADE
PRESSURE DISTRIBUTION TESTS
CHORD INCLINATION 35°
+ PRESSURE INCREASE
- PRESSURE DECREASE
p / (ρV²/2)
2
1
0
1
2
3
0
2
4
6
8
0
1
2
3
CHORD "C"
t m.

FIG 31

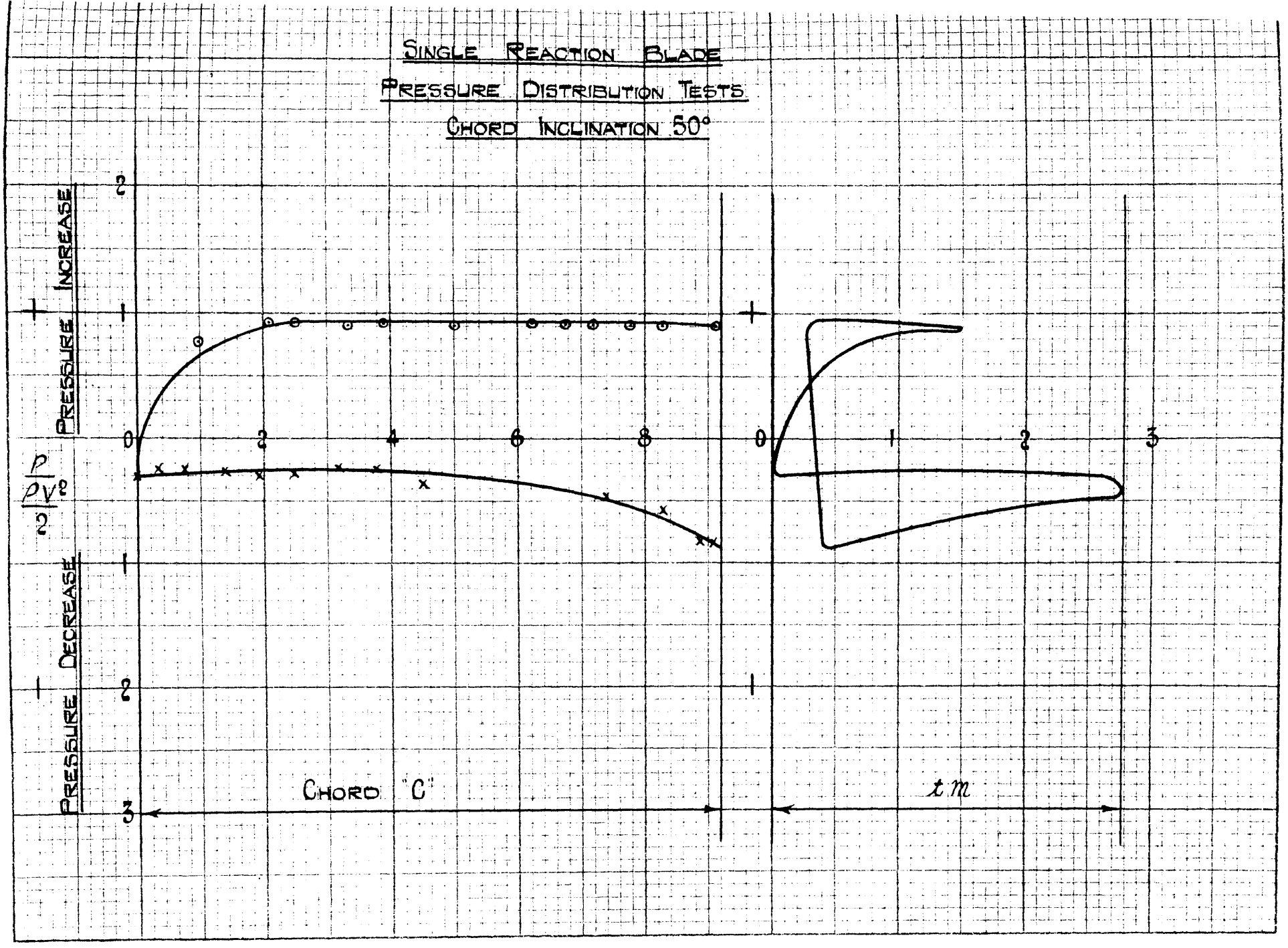
SINGLE REACTION BLADE
PRESSURE DISTRIBUTION TESTS
CHORD INCLINATION 50°
PRESSURE INCREASE
PRESSURE DECREASE
$\frac{P}{\frac{\rho}{2}V^2}$
2
1
0
2
4
6
8
0
1
2
3
CHORD "C"
t_m

FIG 32

As the incidences grow larger the pressure ratios tend to become more and more positive, the exception being at the back of the trailing edge of the blade which still maintains a negative pressure.

Figs. 28 - 32 give the pressure distribution curves for a solitary blade.

In comparing these curves of pressure distribution with those obtained from a blade placed in a series of identical blades, Figs. 8 - 27 , we can observe that the action of the blade in the series of identical blades is different and that the force is less than that given by an isolated blade.

Two points are particularly noticeable, especially in the lower incidences -

1. The decrease in pressure on the back surface of the blade is greater than the increase on the front surface of the blade.

2. The pressure is not by any means evenly distributed, both the decreased pressure on the back surface and the increased pressure on the front surface being most marked over the front portion of the blade.

CENTRE OF PRESSURE.

The second thing that we learn from the pressure distribution curves, namely that both the decreases and increases of pressure are greatest near the leading edge of the blade - will mean that if we were to replace all the distributed pressure by a single resultant force, this single force would act less than half way back along the chord.

The position on the chord at which this resultant force acts is called the Centre of Pressure.

The idea of a Centre of Pressure is very similar to that of the centre of gravity of a body whose weight is unevenly distributed.

The Centre of Pressures for the above tests were obtained by drawing down the forces X' and Y' in their correct positions and the line of action of the resultant, produced back to cut the chord, gives the Centre of Pressure.

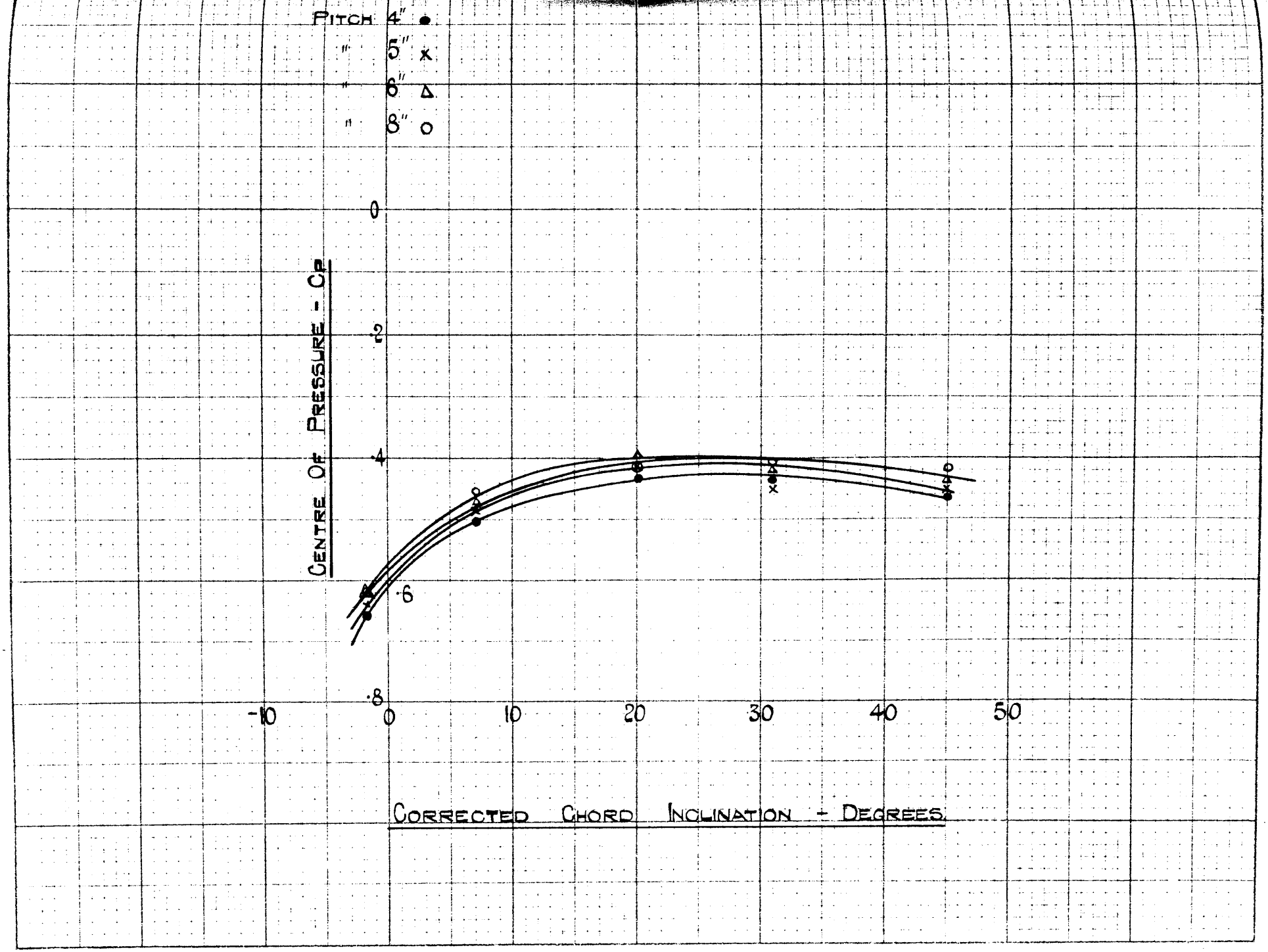
PITCH 4" ●
" 5" x
" 6" Δ
" 8" o
0
·2
·4
·6
·8
CENTRE OF PRESSURE - Cp
-10
0
10
20
30
40
50
CORRECTED CHORD INCLINATION - DEGREES.

Fig 42

The centre of pressure curves given in Fig. (42) show that there is almost a stable travel from about 16° upwards, whilst there is practically a stationary position of the centre of Pressure from about 20 to 30 degrees.

The total range of the moment of the Centre of Pressure in all cases is not, however, very great.

The Pressure Distribution tests show that as the angle of attack is altered the distribution of pressure over the blade changes considerably, and consequently there will be a movement of the Centre of Pressure.

The position of the Centre of Pressure is usually defined as being a certain portion of the chord back from the leading edge.

THE LIFT COEFFICIENT CURVES C_L

All the results were corrected to infinite aspect ratio, from the equations

$$\alpha_\infty = \alpha_e - 5.55\ C_L \qquad (1)$$

$$C_L = Y' \cos\alpha - X' \sin\alpha \qquad (2)$$

The lift coefficients C_L for the different Blade pitches and on a base of angles of incidences or chord inclinations is given by the full lines Figs., 33 - 36, for the pressure distribution tests.

In all the cases, when the angle of attack has reached zero there is already a definite lift coefficient and therefore a definite lift.

The angle of incidence at zero lift is approximatdy - 13 degrees.

BLADE PITCH 4"

FULL LINE REPRESENTS PRESSURE DISTRIBUTION TESTS.

DOTTED LINE REPRESENTS AERODYNAMIC BALANCE TESTS.

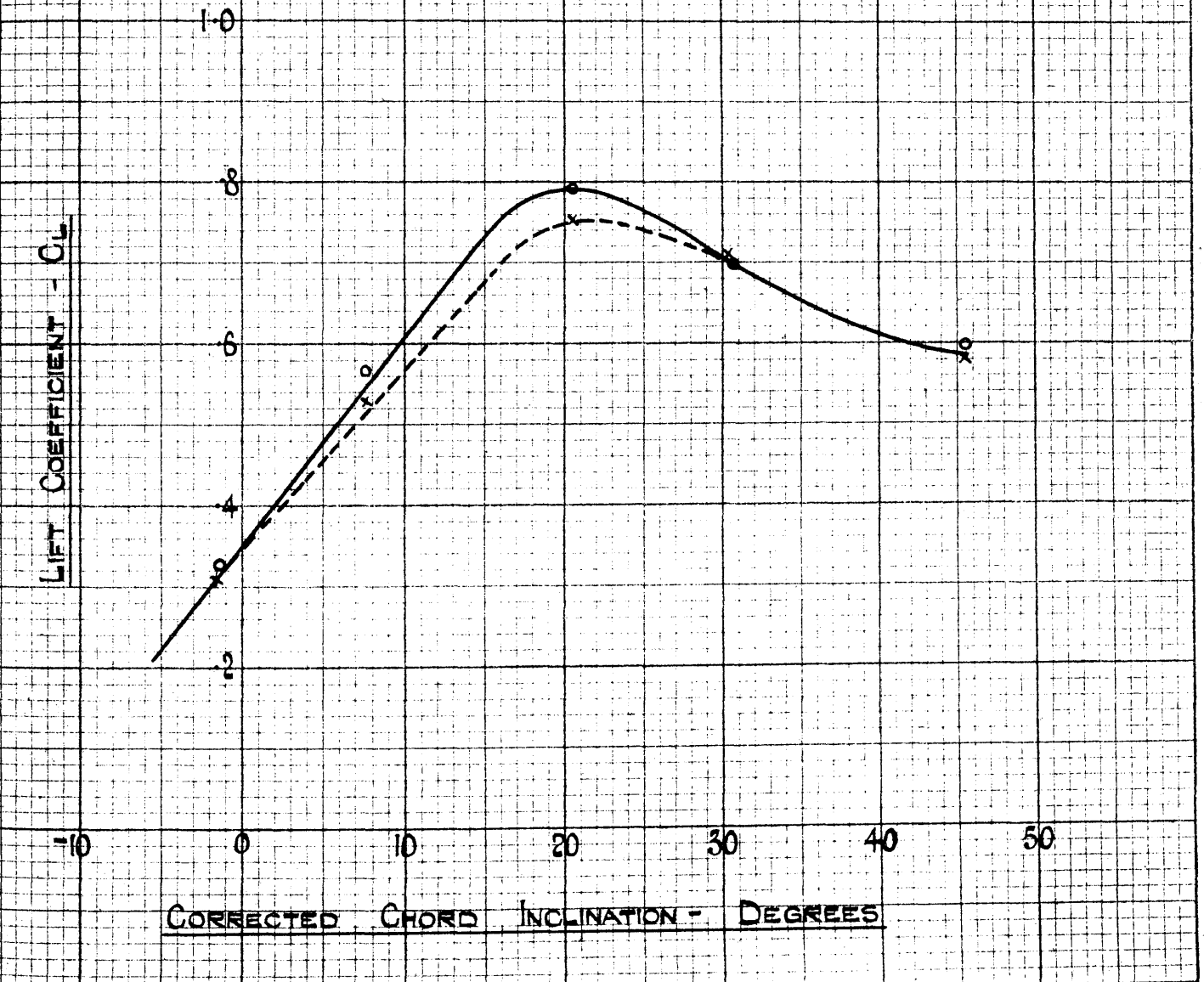

FIG 33

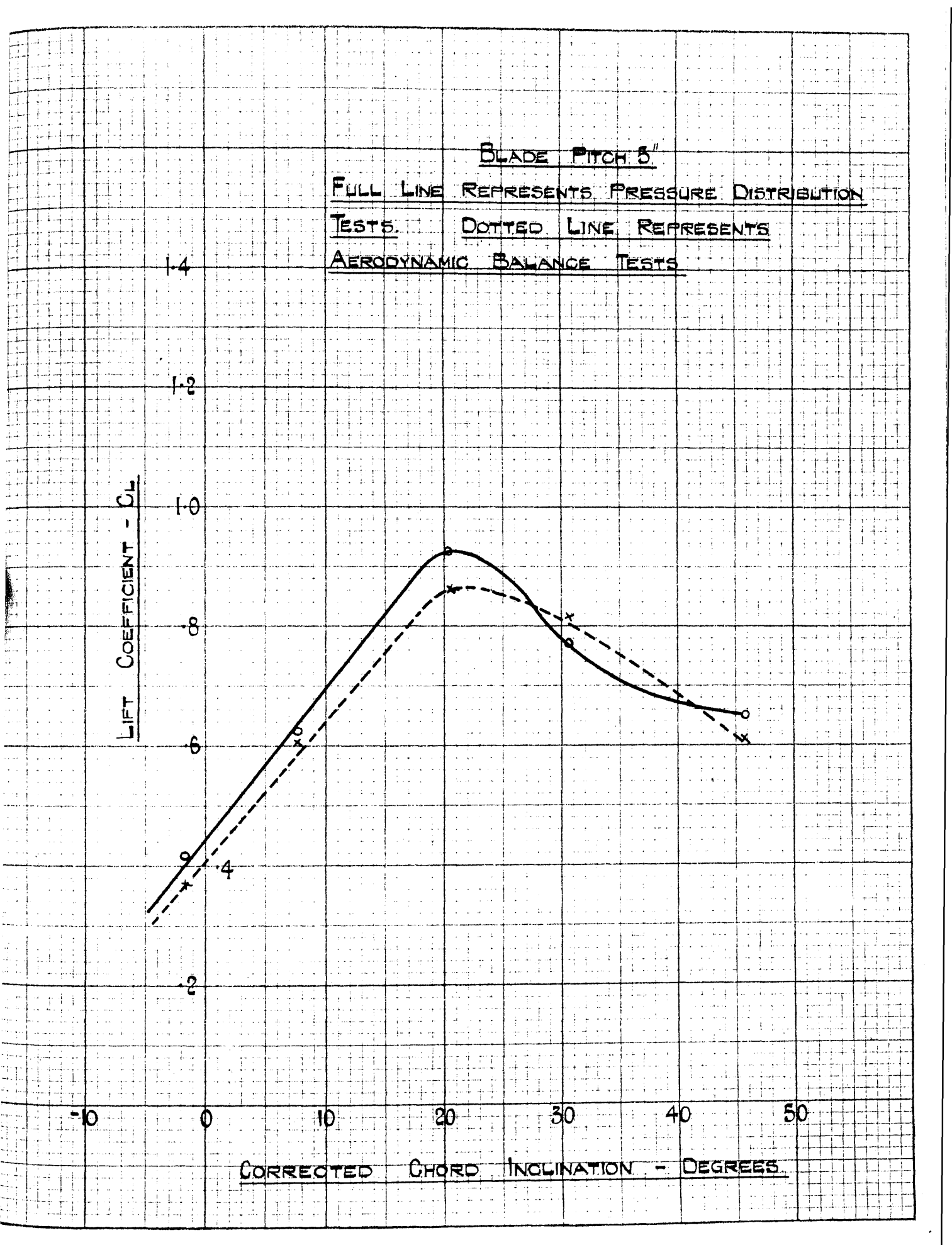
BLADE PITCH 5°
FULL LINE REPRESENTS PRESSURE DISTRIBUTION TESTS. DOTTED LINE REPRESENTS AERODYNAMIC BALANCE TESTS
LIFT COEFFICIENT - CL
1.4
1.2
1.0
.8
.6
.4
.2
-10
0
10
20
30
40
50
CORRECTED CHORD INCLINATION - DEGREES

FIG. 34

BLADE PITCH 6"

FULL LINE REPRESENTS PRESSURE DISTRIBUTION TESTS. DOTTED LINE REPRESENTS AERODYNAMIC BALANCE TESTS.

FIG 35

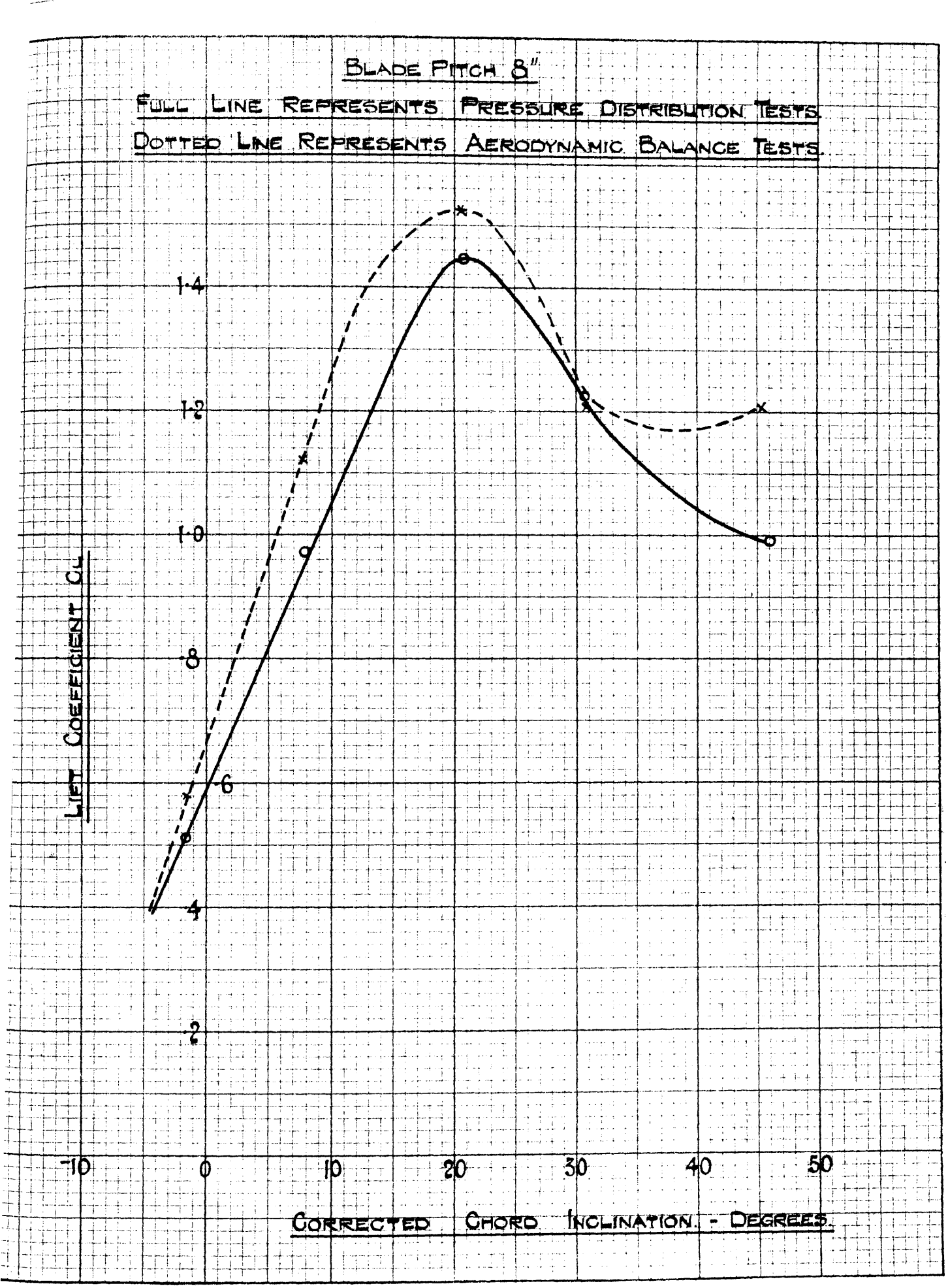
BLADE PITCH 8"
FULL LINE REPRESENTS PRESSURE DISTRIBUTION TESTS.
DOTTED LINE REPRESENTS AERODYNAMIC BALANCE TESTS.
LIFT COEFFICIENT C_L
1·4
1·2
1·0
·8
·6
·4
·2
-10
0
10
20
30
40
50
CORRECTED CHORD INCLINATION. - DEGREES.

FIG 36

The graph is of the nature of a straight line practically, to the angle of maximum lift which is about twenty degrees and which as already mentioned is correct designed angle of the blade.

This means that as the angle of attack increases there is a steady increase in the value of the lift, whereas at a few degrees before the angle of maximum lift is reached, the lift still increases for a few degrees, the increase is now comparatively small and the graph is curving to form a top of a maximum point.

When the blade is correctly inclined to face the stream at about twenty degrees a maximum lift is reached and above this angle the lift begins to decrease, the graph curving downwards.

(b) AERODYNAMIC BALANCE TESTS.

These tests were undertaken, as a check on the Pressure Distribution Tests for obtaining the different aerodynamic characteristics of the blade and especially for obtaining a true value of the drag force by weighing the different forces on the blade.

An illustration of the experimental layout is given in Fig. (37) and shows the position of the floating blade and of the balances.

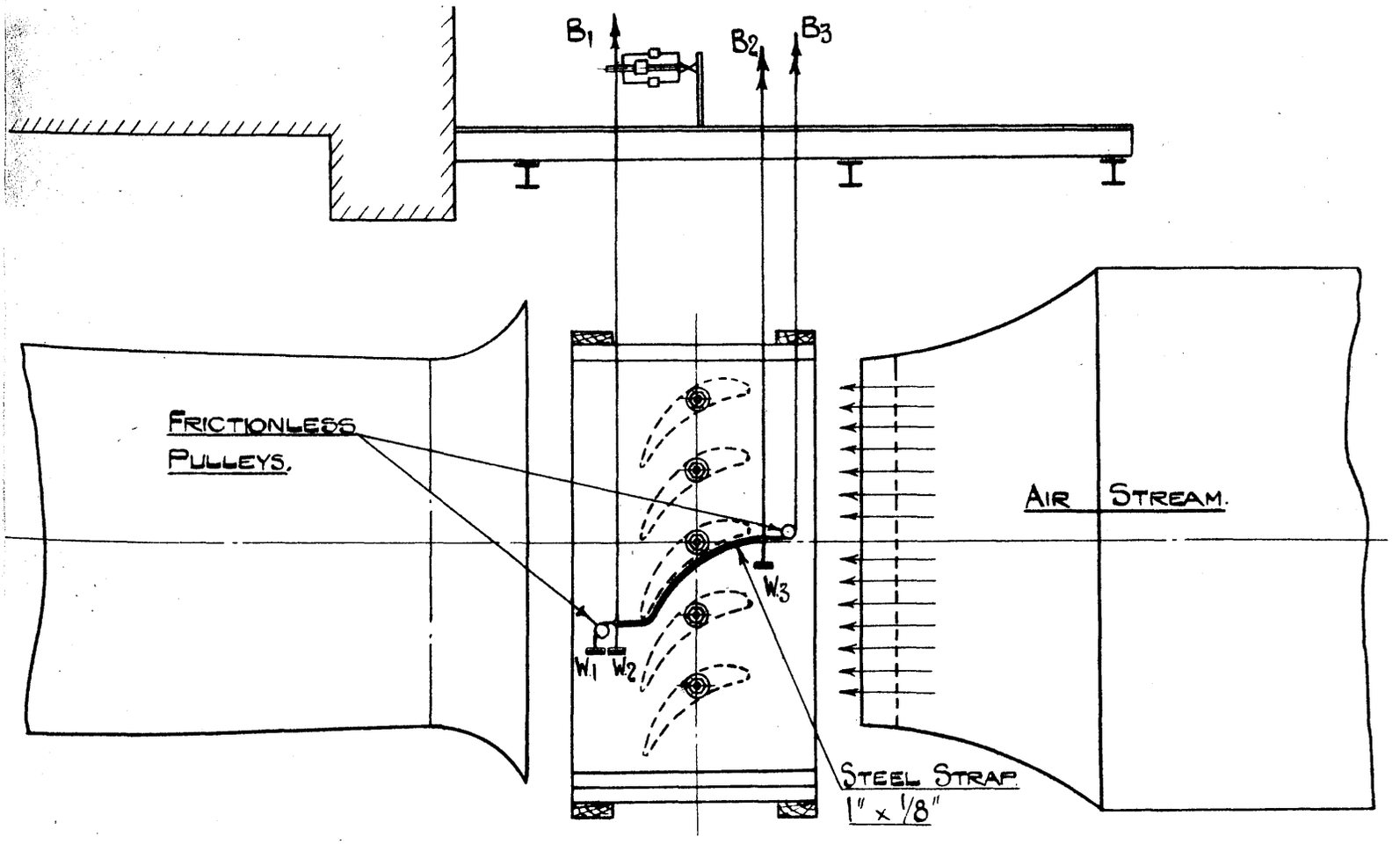

Fig.(37)
ARRANGEMENT OF FLOATING BLADE & BALANCES.

Fig. (38) gives the details of the floating blade.

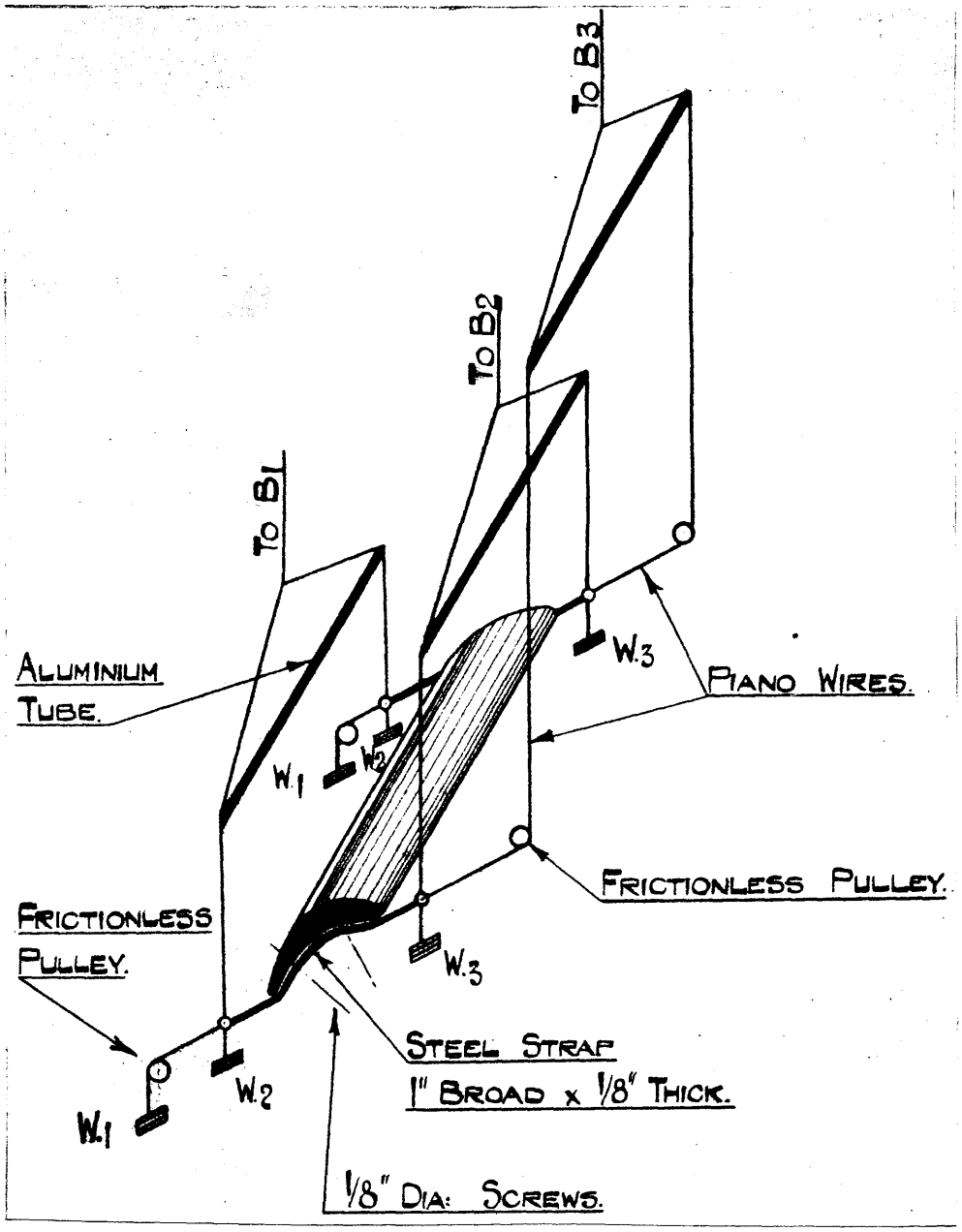

The forces exerted by the air on the blade model are measured by means of three very sensitive balances, B_1, B_2, and B_3, Fig. (37).

The Blade Model at the position C, Fig. (6) was suspended and kept floating by means of wires from three balances placed on the roof of the tunnel.

The blade models at the other positions, namely, A, B, D. & E, Fig. (6) and Fig. (37), were fixed at the two side planes in exactly the same way as for the Pressure Distribution tests.

The centre blade at the position C was made about $\frac{1}{8}$" shorter than the other blades and that allowed it to be free from both ends and suspended as in Fig. (38). Frictionless pulleys were used as in Fig. (38) to minimise the amount of friction to the least possible value.

The blade was perfectly free to move and the sensitive balances registered any pressure imposed on the blade by the air stream.

The blade was then brought back to its original position by adding loads on the weight carriers W_1, W_2, etc..

Examination of the blade under the same conditions as in the previous Pressure Distribution Tests was thus made possible, and at the different angles of incidences, by tilting the blade to the desired incidence by adding loads on the carriers until the required position is procured.

The same incidence for the other blades was got by measuring off the pitch at the back and front of the blades from the centre blade and then checking by means of the inclinometer.

The velocity of air was maintained at 90 ft. per sec. as for the Pressure Distribution Tests and the different forces acting on the blade were given by the balances.

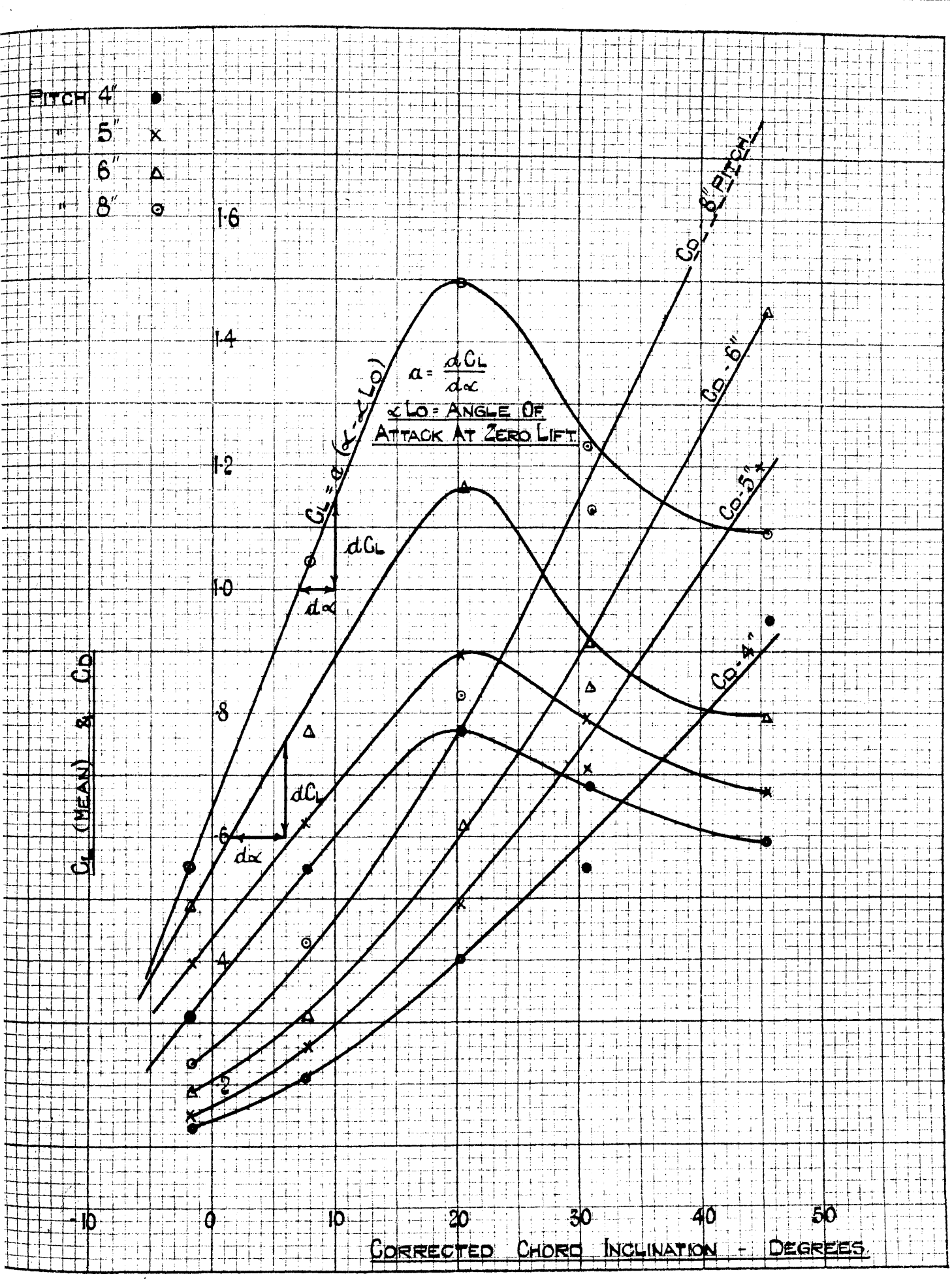
PITCH 4" ●
" 5" ×
" 6" △
" 8" ⊙
1·6
1·4
1·2
10
8
6
4
2
C_L (MEAN) & CD
$a = \frac{dC_L}{d\alpha}$
α_{LO} = ANGLE OF ATTACK AT ZERO LIFT.
$C_L = a(\alpha - \alpha_{LO})$
dC_L
$d\alpha$
CD-8" PITCH
CD-6"
CD-5"
CD-4"
-10
0
10
20
30
40
50
CORRECTED CHORD INCLINATION - DEGREES.

FIG 39

LIFT AND DRAG COEFFICIENTS.

In the general case of a body suspended in a Wind Tunnel the aerodynamic force is not a pure drag but is inclined often steeply to the direction of flow.

This inclination is not constant for a given shape and attitude of the body but is often a function of the Reynold's number.

When the flow has a single plane of symmetry for all angles of incidence of the body, the aerodynamic force can be resolved into two components in that plane, parallel and perpendicular to the relative wind - the Drag and the Lift respectively.

For any particular shape and incidence the Lift Coefficient

$$C_L = \frac{L}{\rho \frac{AV^2}{2}}$$

where L = lift in lbs. force

ρ = $\frac{w}{g}$ slugs per cu. ft.

A = Projected area of the blade in square ft.

V = Velocity in feet per sec.

and the Drag Coefficient

$$C_D = \frac{D}{\rho \frac{AV^2}{2}}$$

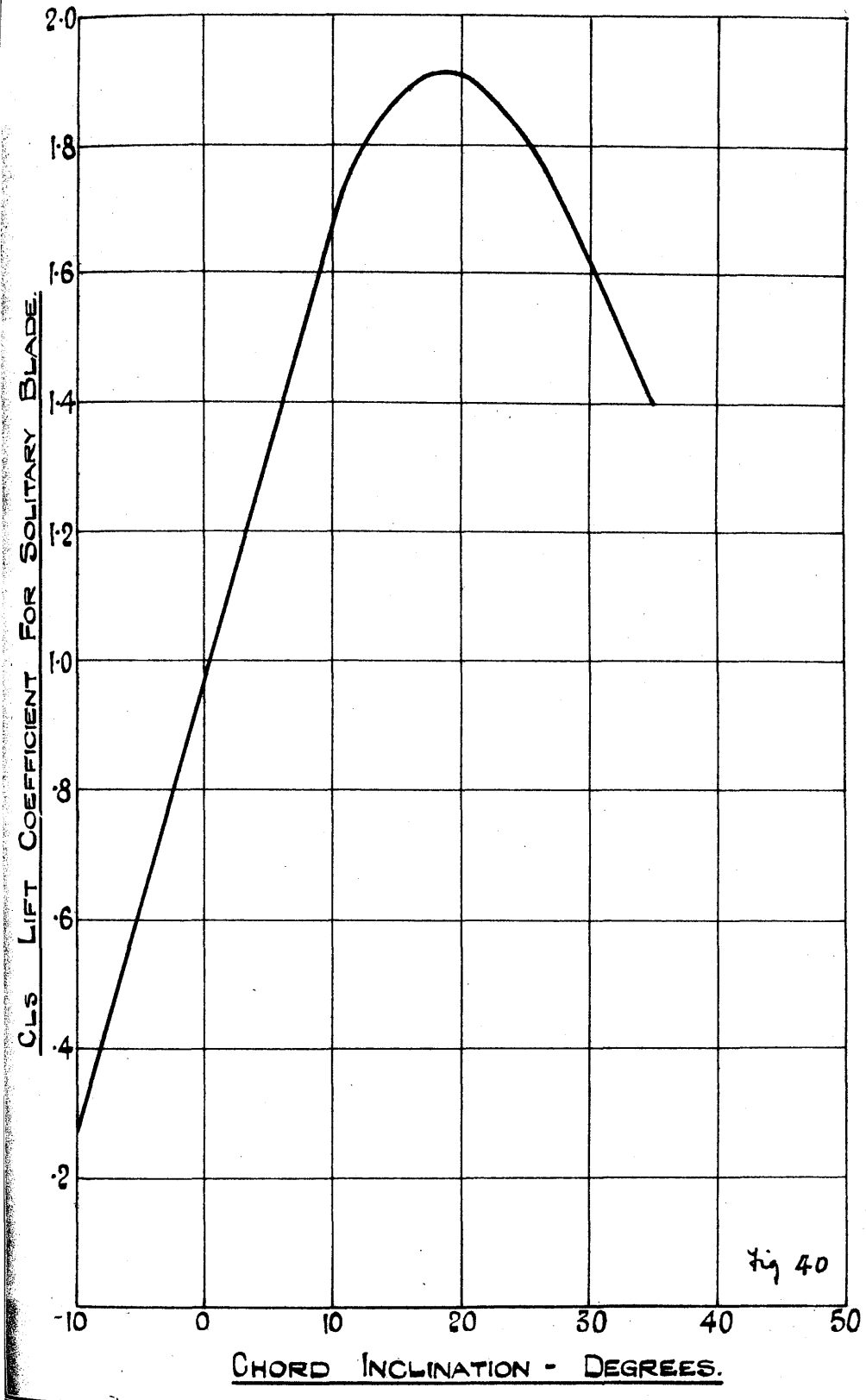
2·0
1·8
1·6
1·4
1·2
1·0
·8
·6
·4
·2
-10
0
10
20
30
40
50
CLs LIFT COEFFICIENT FOR SOLITARY BLADE.
CHORD INCLINATION - DEGREES.
Fig 40

The Lift and Drag Coefficients were determined for the Aerodynamic Balance Tests by measuring the forces on the Blade.

The Lift Coefficients derived from these tests are given in Figs. 33 to 36 and are represented by the dotted lines.

The mean values from the two tests were then plotted against a chord inclination base and are given in Fig. (39).

Zero lift occurs at a negative incidence at about -13 degrees.

The Lift Coefficient curves for a solitay blade derived from Pressure Distribution Tests is given in Fig. (40).

The maximum Lift is attained at an angle approximately 20 degrees, which is known as the Stalling or Critical Angle.

Minimum Drag occurs when the lift is very small.

The Drag and the chord inclination angle begin to increase rapidly at the critical angle.

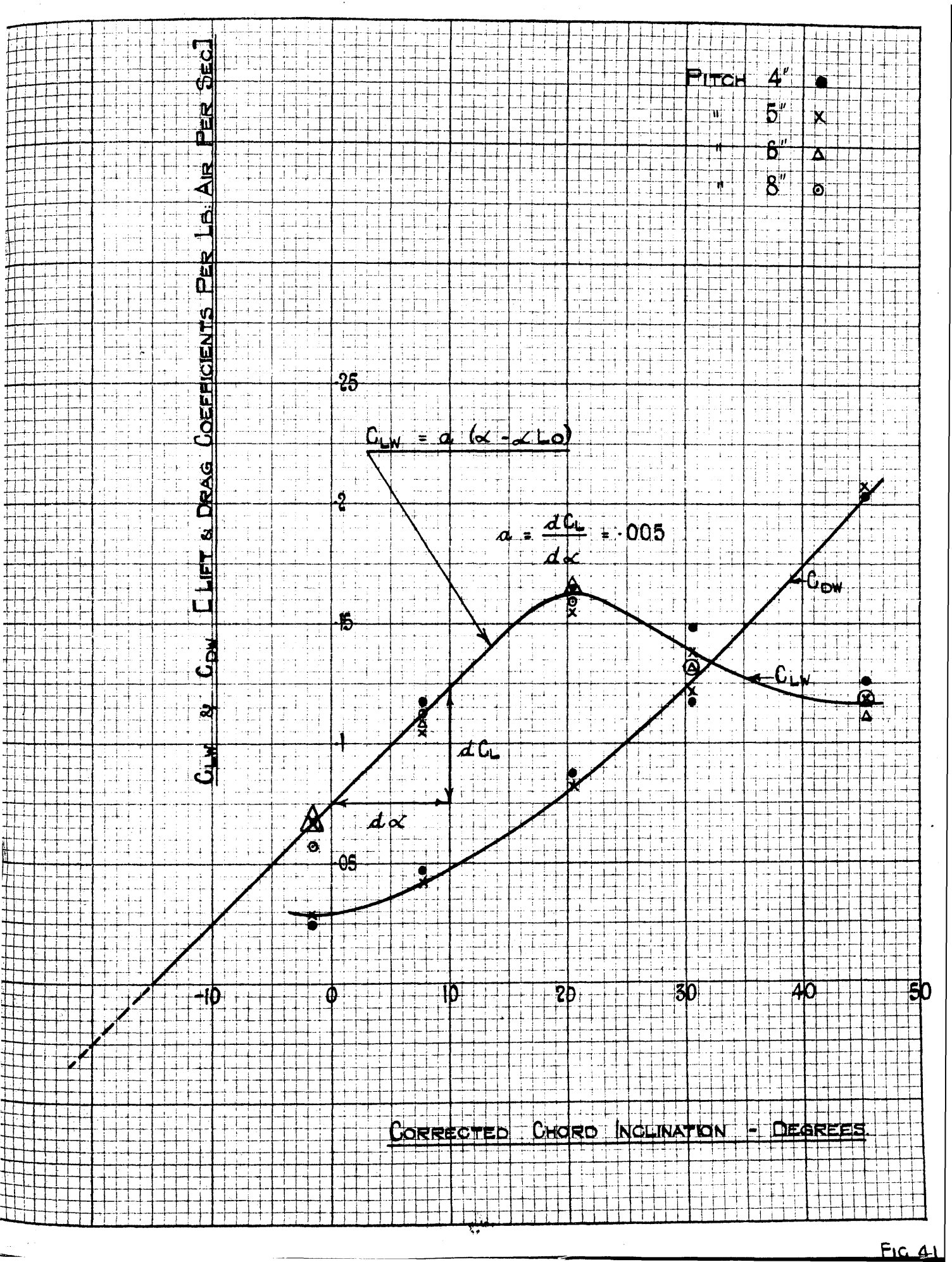
Pitch 4" ●
" 5" x
" 6" △
" 8" ⊙
C_{LW} & C_{DW} [Lift & Drag Coefficients Per Lb. Air Per Sec.]
.25
.2
.15
.1
.05
$C_{LW} = a\,(\alpha - \alpha_{L0})$
$a = \frac{dC_L}{d\alpha} = .005$
C_{DW}
C_{LW}
dC_L
$d\alpha$
-10
0
10
20
30
40
50
Corrected Chord Inclination - Degrees

Fig 41

C_{Lw} and C_{Dw} CURVES.

Fig. (41) gives the Lift and Drag Coefficients per lb. of air per second (Table of Results).

The characteristics of the Lift curve are the same as those in the Lift curves for the separate Blade Pitches.

The angle of zero lift is about -14.8° which compares very favourably with the angle previously obtained from the diagrams 33 to 36.

The graph follows a straight line law practically to the maximum lift angle which shows that there is a steady increase in the lift with the increase of incidence.

After the maximum lift is reached the graph falls and tends to become more steady at about the angle 45°.

The minimum drag occurs when the lift is quite small, and then the drag increases very rapidly with the increase of the angle of incidence.

CHORD INCLINATION -	1·8°	7·84°	20·28°	30·75°
BLADE PITCH 4"	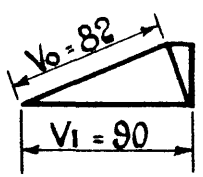	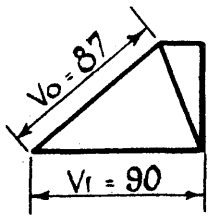	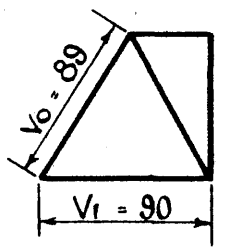	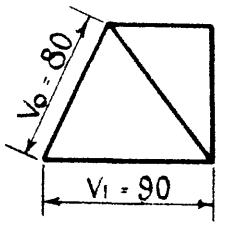
BLADE PITCH 5"	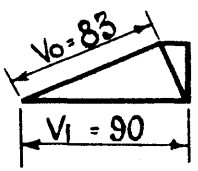	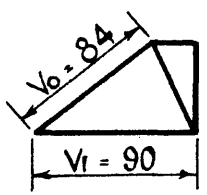	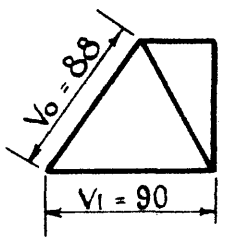	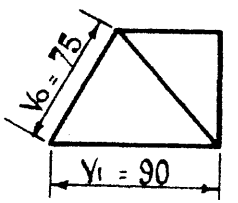
BLADE PITCH 6"	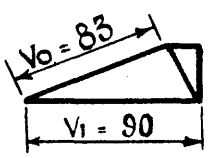	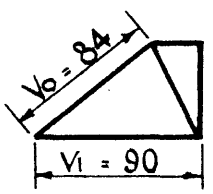	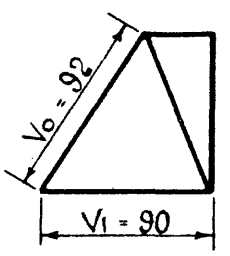	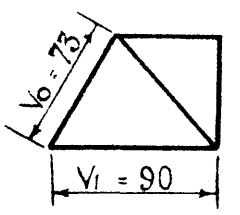
BLADE PITCH 8"	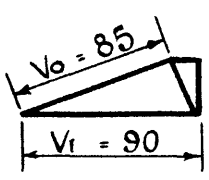	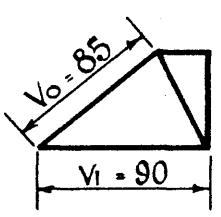	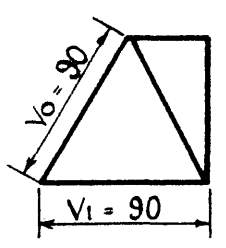	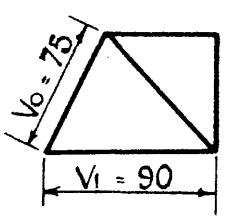

SCALE :- 1" = 100 FT. PER SEC.

Fig. 43

TOTAL REACTION ON THE BLADE.

Fig. (43) gives the velocity diagrams at the different inclinations, for a Blade Pitch of five inches.

The lift and drag are expressed in the same units as, V_i the velocity of air at the inlet to the blade, and V_o the velocity at outlet. The outlet velocity angle from the tests almost coincides with the actual Blade outlet angle at that particular inclination.

The drop in the value of the outlet velocity is due probably to friction losses.

PITOT TUBE EXPLORATIONS.

Explorations of the velocity head (with a small Pitot Tube (1) suitable for two dimensional flow. The head of this instrument was composed of two small tubes mounted in the same plane) at section Z Figs. (44), (45), (46), and (47) were made.

---

(1) Standard specification for the Testing of Mine Fans. Inst. of Mining Engineers 1934.

CHORD INCLINATION −1·8°

BLADE PITCH 5"

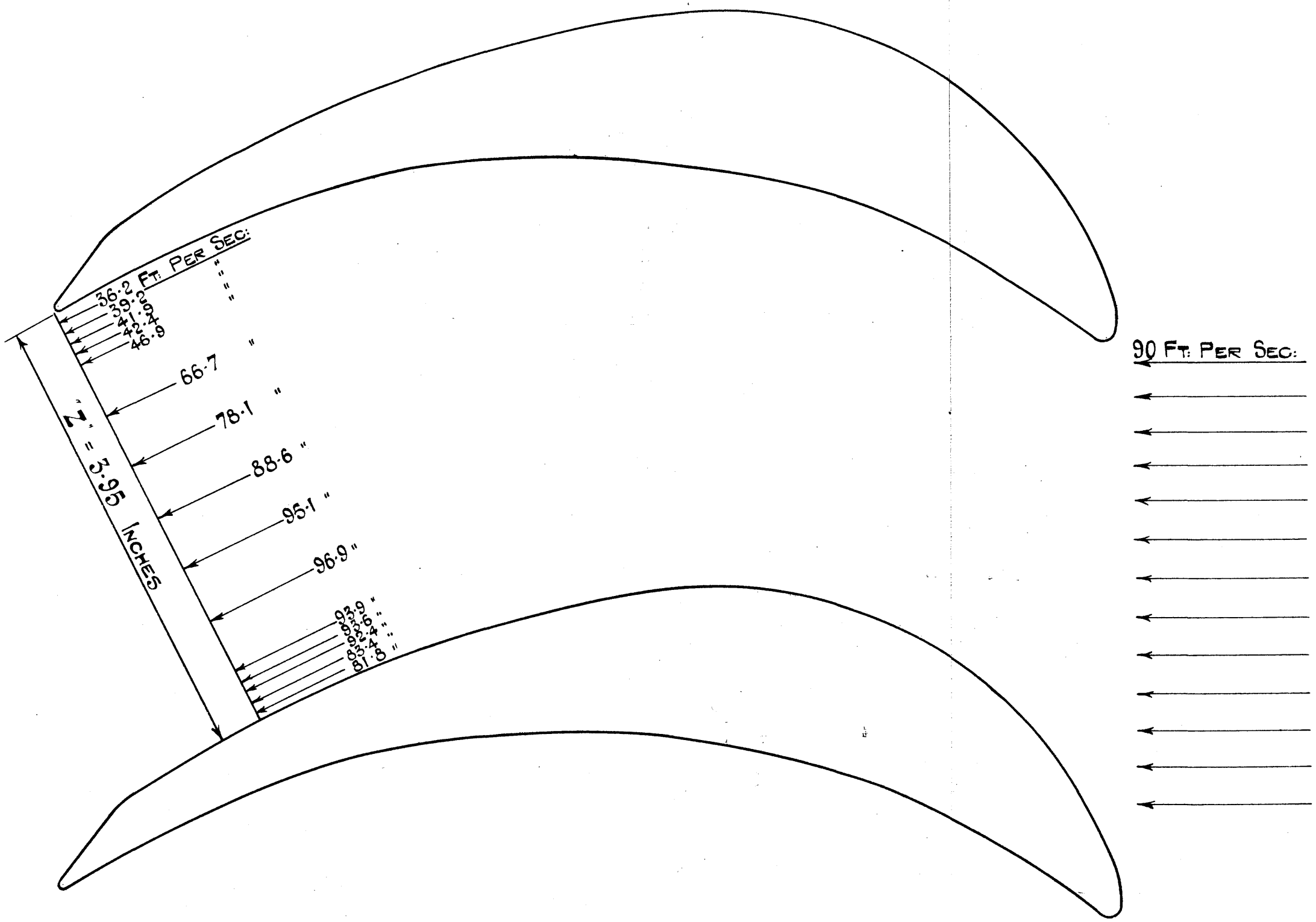

Fig 44

CHORD INCLINATION 7·84°

BLADE PITCH 5"

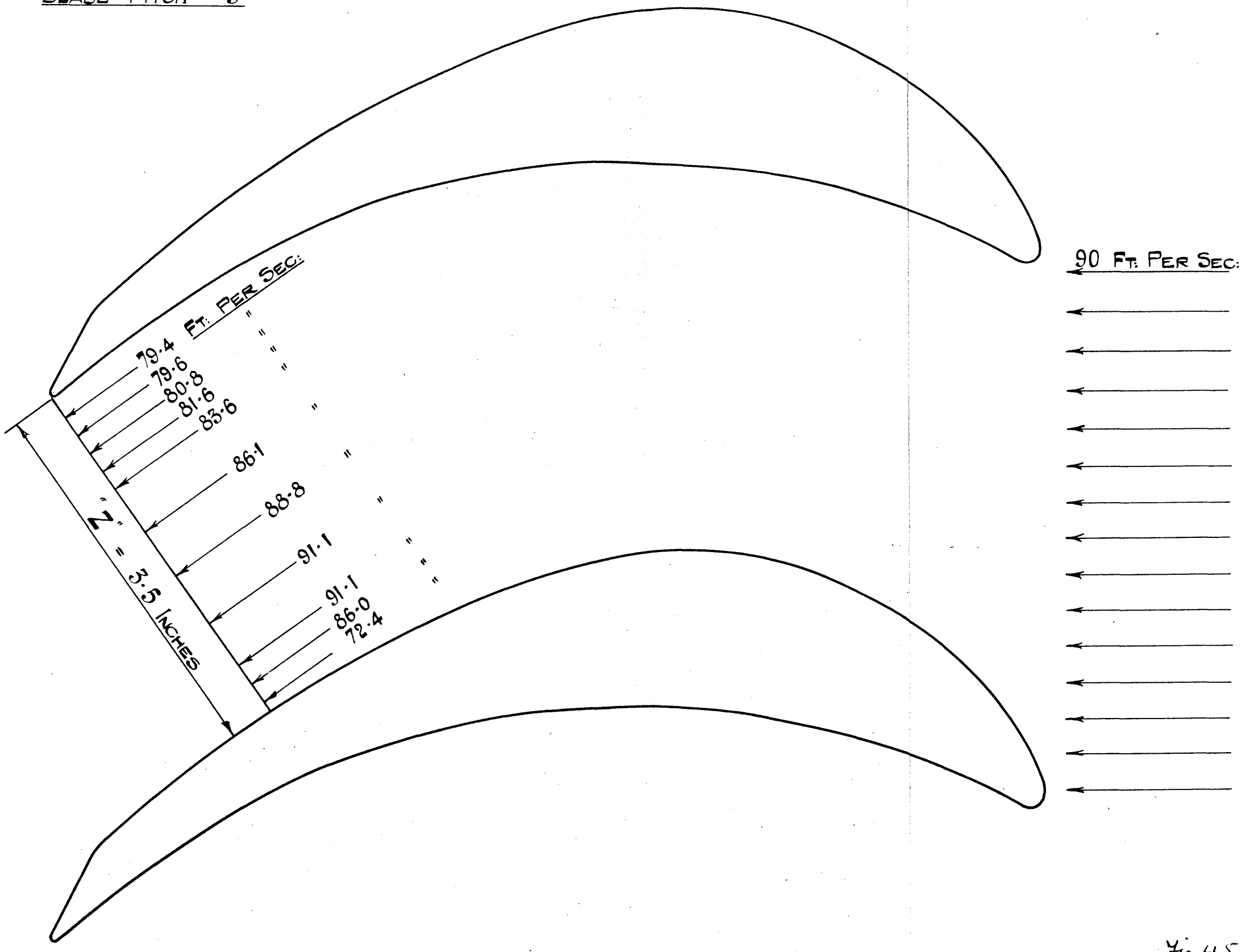

Fig 45

CHORD INCLINATION 20-24°

BLADE PITCH 5"

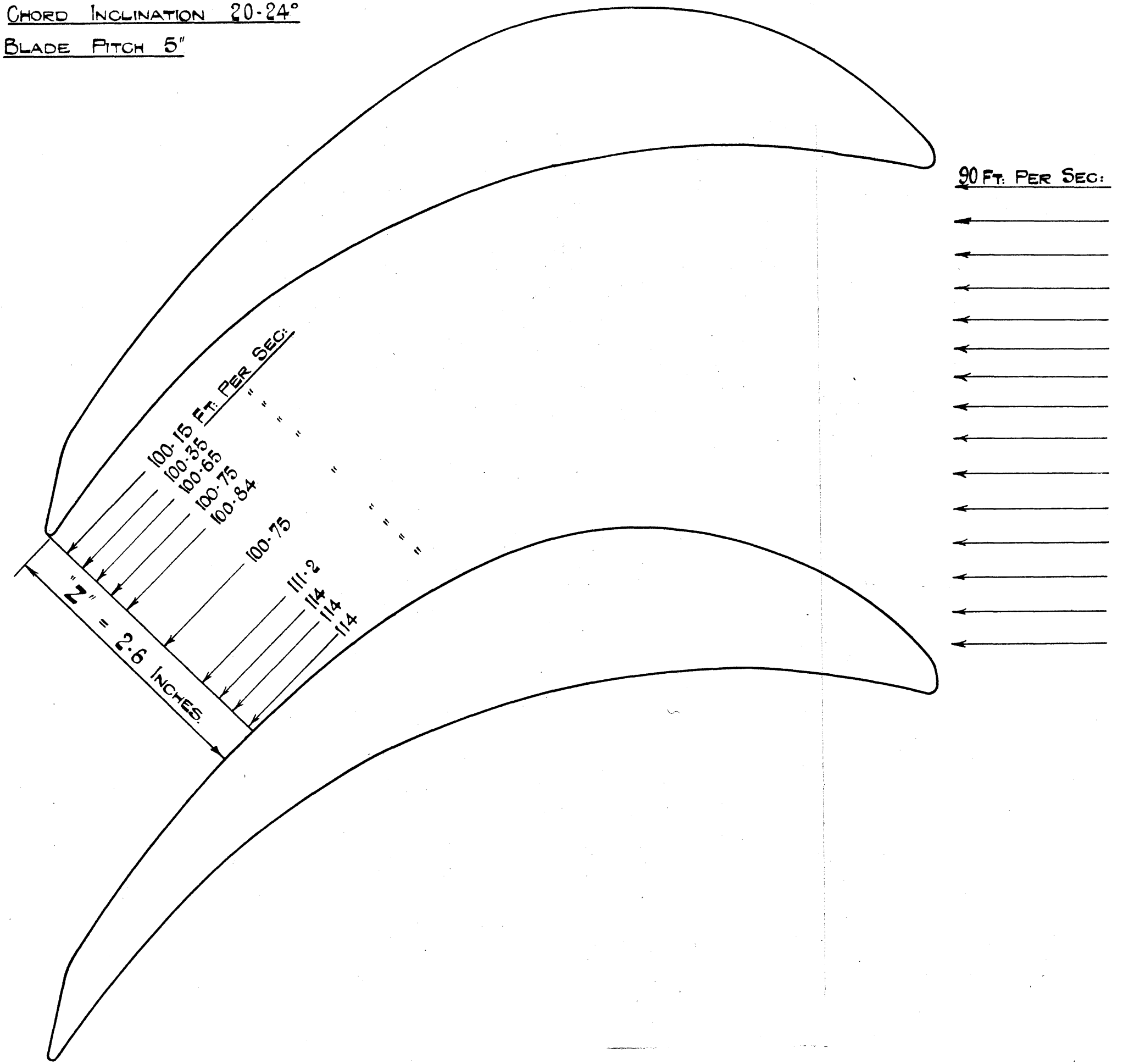

Fig 46

CHORD INCLINATION 30·75°

BLADE PITCH 5″

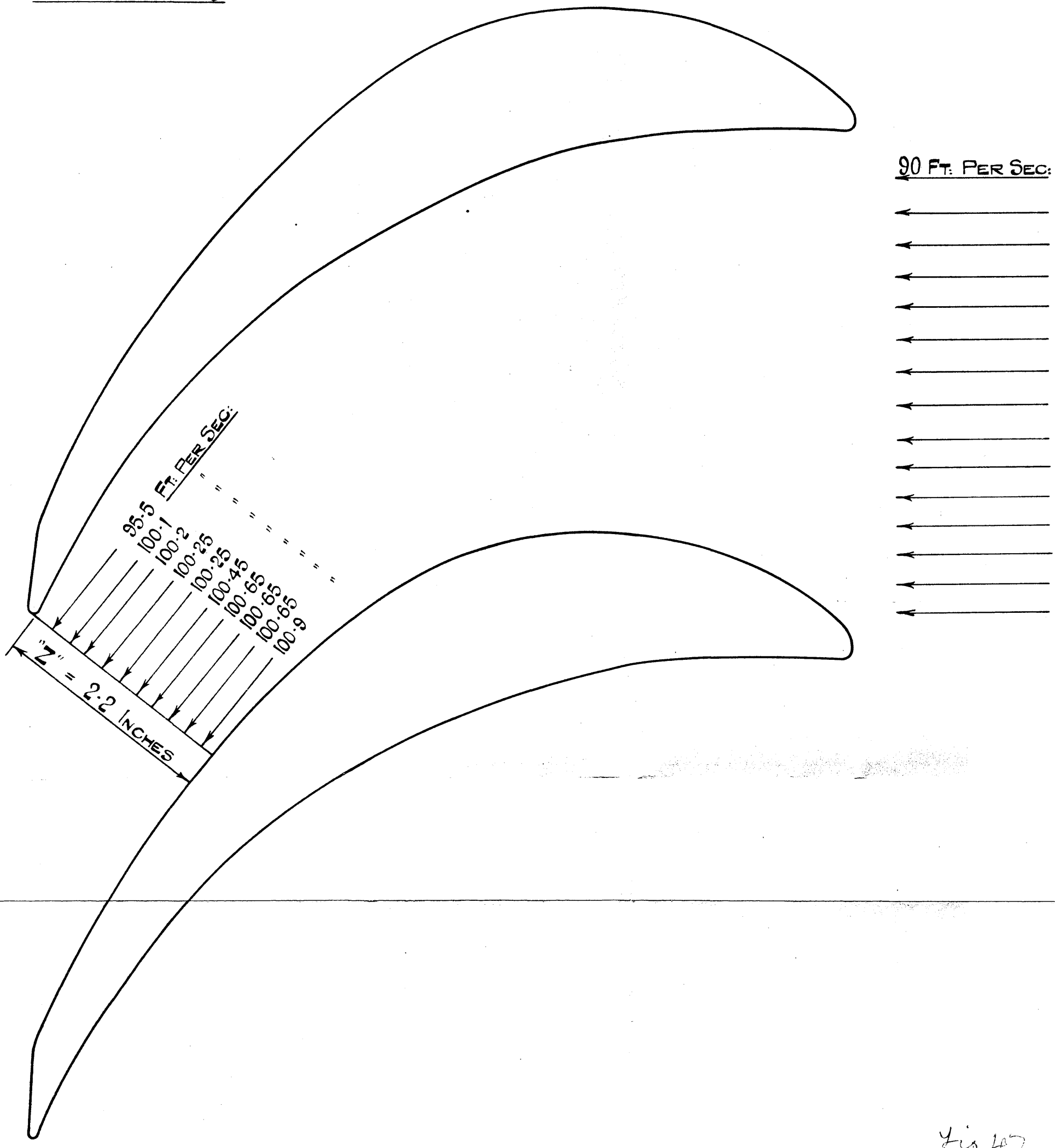

Fig 47

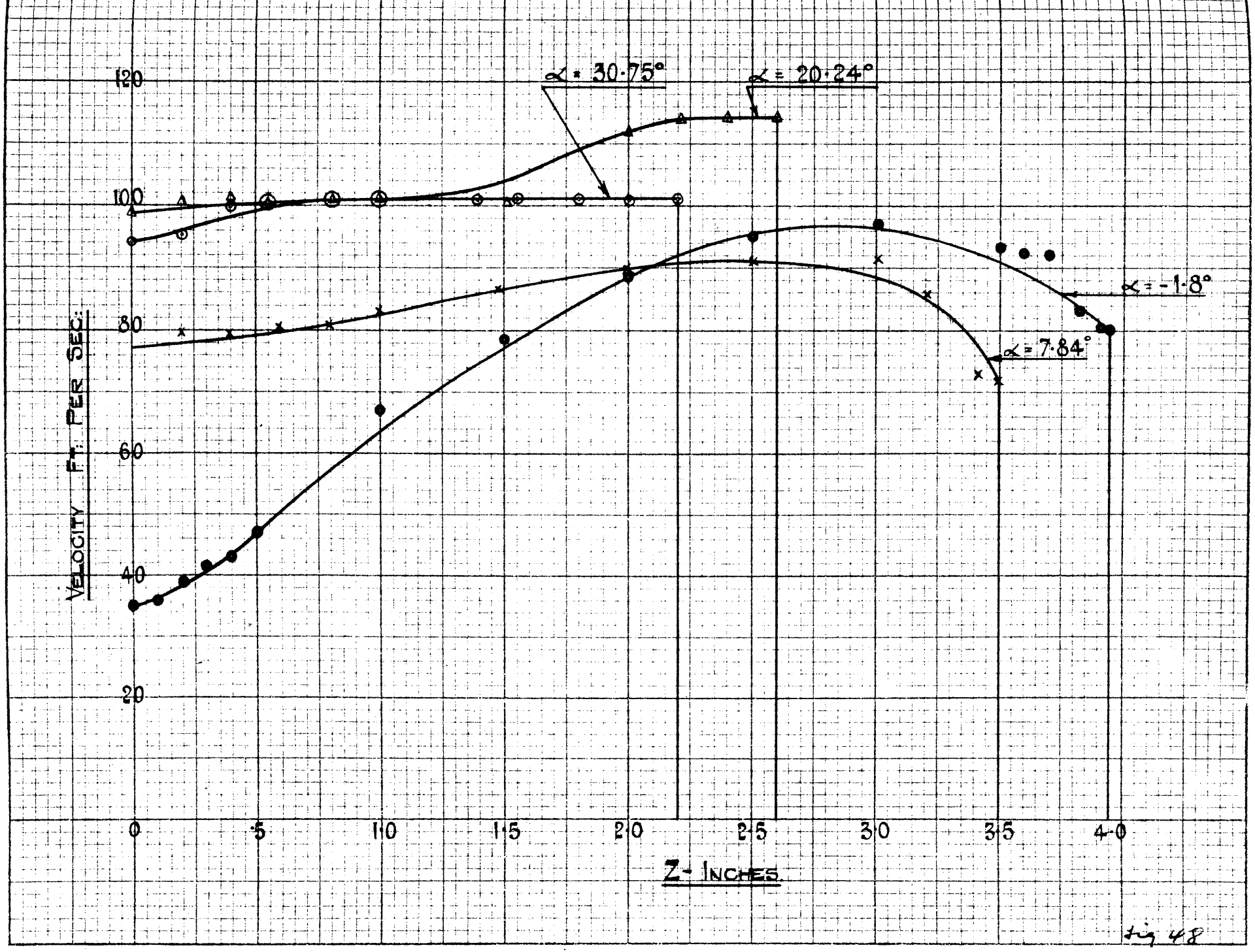
α = 30·75°
α = 20·24°
α = -1·8°
α = 7·84°
120
100
80
60
40
20
VELOCITY FT. PER SEC.
0
·5
1·0
1·5
2·0
2·5
3·0
3·5
4·0
Z - INCHES

Fig 48

These explorations were made at several points along Z and parallel to the line of flow in the passage between the blades.

The velocity was calculated from the head measured in inches and the velocity calculated from the expression,

$$V = 15.9\sqrt{\frac{h \times T}{B}}$$

where V = velocity in ft. per sec.

h = velocity head ins - H_2O.

T = °F + 460.

B = Barometer in ins - Hg.

Explorations of the head were made just behind the trailing edge of the blade and agreed very favourably with the results obtained from the velocity diagrams, Fig. (43).

These Figs. show the increase in velocity along the passage Z from the lower side of the blade as it approaches the upper side of the next blade. This of course, shows that there is a suction at that particular part of the upper blade and agrees with and confirms also the results obtained from the Pressure Distribution Tests.

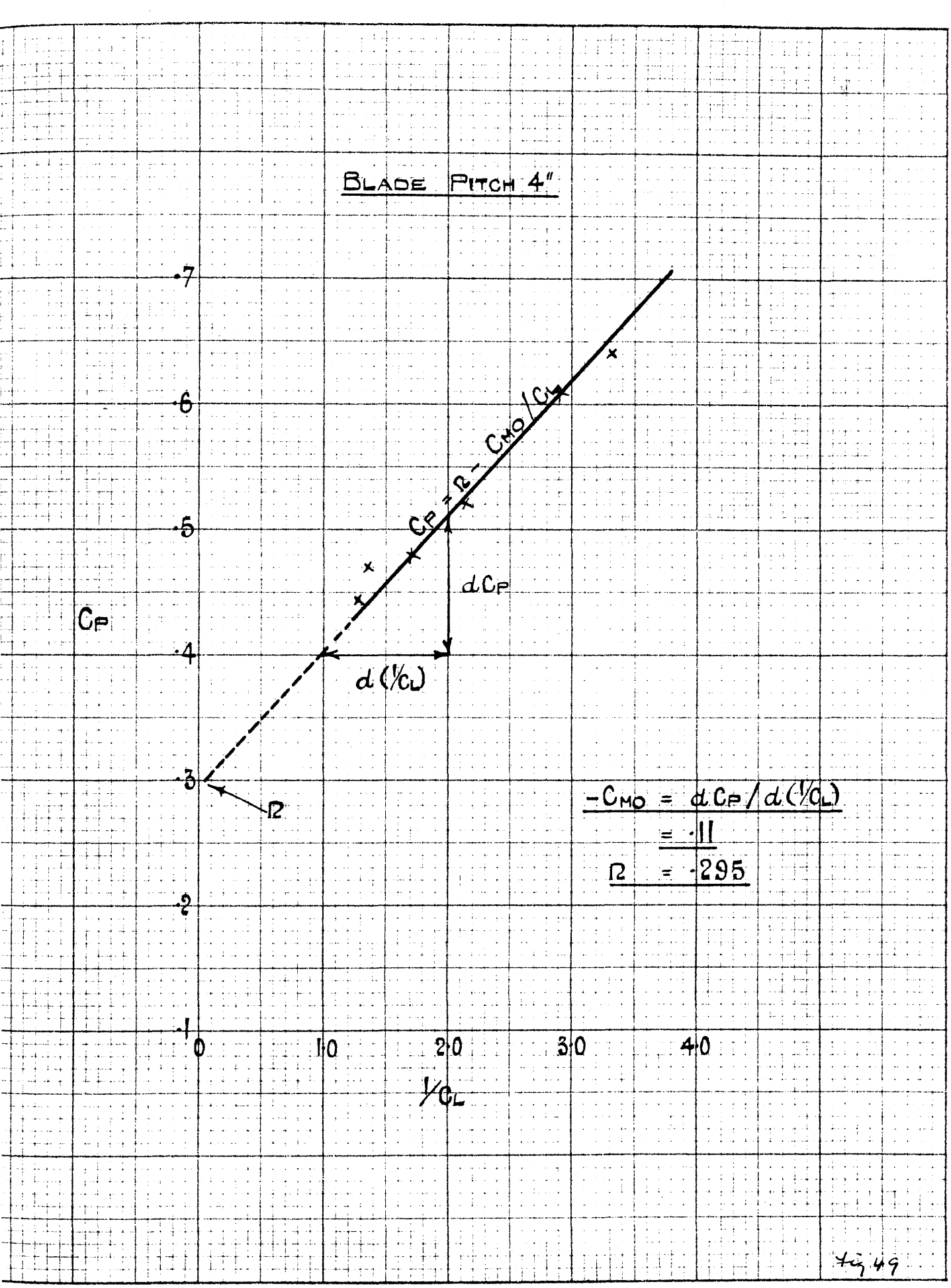
BLADE PITCH 4"
·7
·6
·5
·4
·3
·2
·1
C_P
$C_P = R - C_{MO}/C_M$
dC_P
$d(1/C_L)$
R
0
10
20
30
40
$1/C_L$
$-C_{MO} = dC_P / d(1/C_L)$
$= \cdot 11$
$R = \cdot 295$

Fig 49

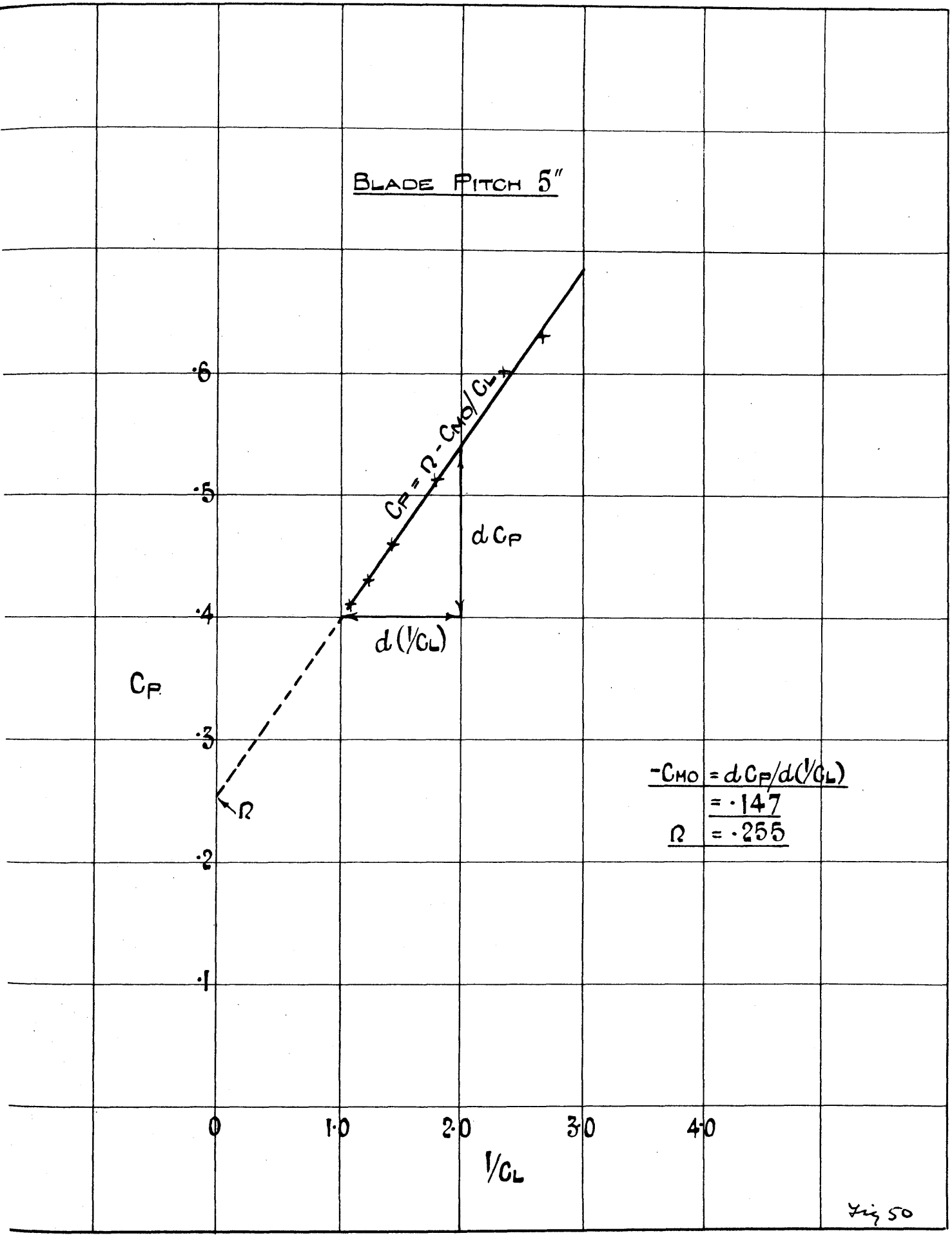
BLADE PITCH 5"
·6
·5
·4
·3
·2
·1
C_P
$C_P = \Omega - C_{MO}/C_L$
dC_P
$d(1/C_L)$
Ω
0
1·0
2·0
3·0
4·0
$1/C_L$
$-C_{MO} = dC_P/d(1/C_L)$
$= \cdot 147$
$\Omega = \cdot 255$

Fig 50

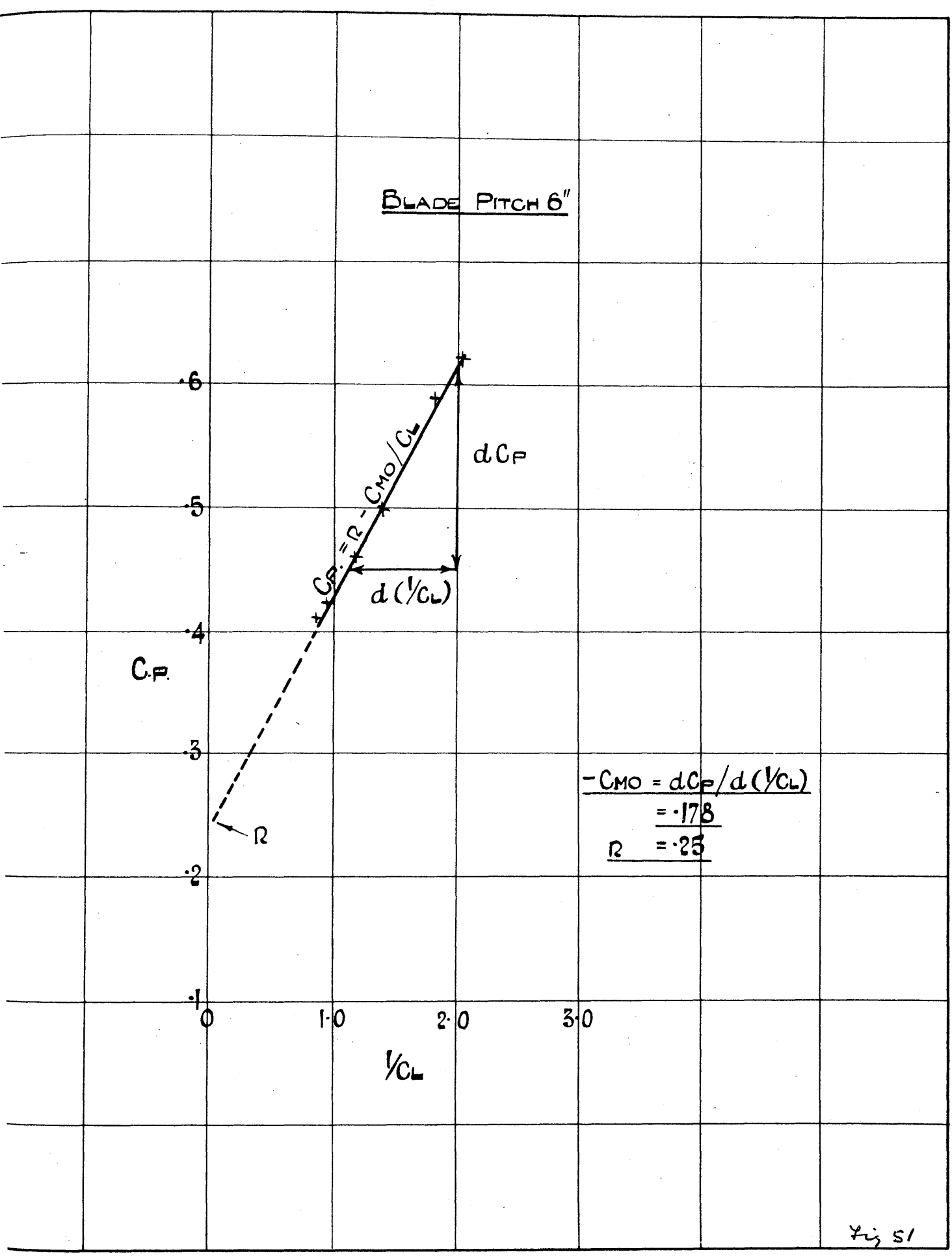
BLADE PITCH 6"
·6
·5
·4
·3
·2
·1
C.P.
0
1·0
2·0
3·0
1/CL
dCP
d(1/CL)
CP = R - CMO/CL
R
-CMO = dCP/d(1/CL)
= ·178
R = ·25
Fig 51

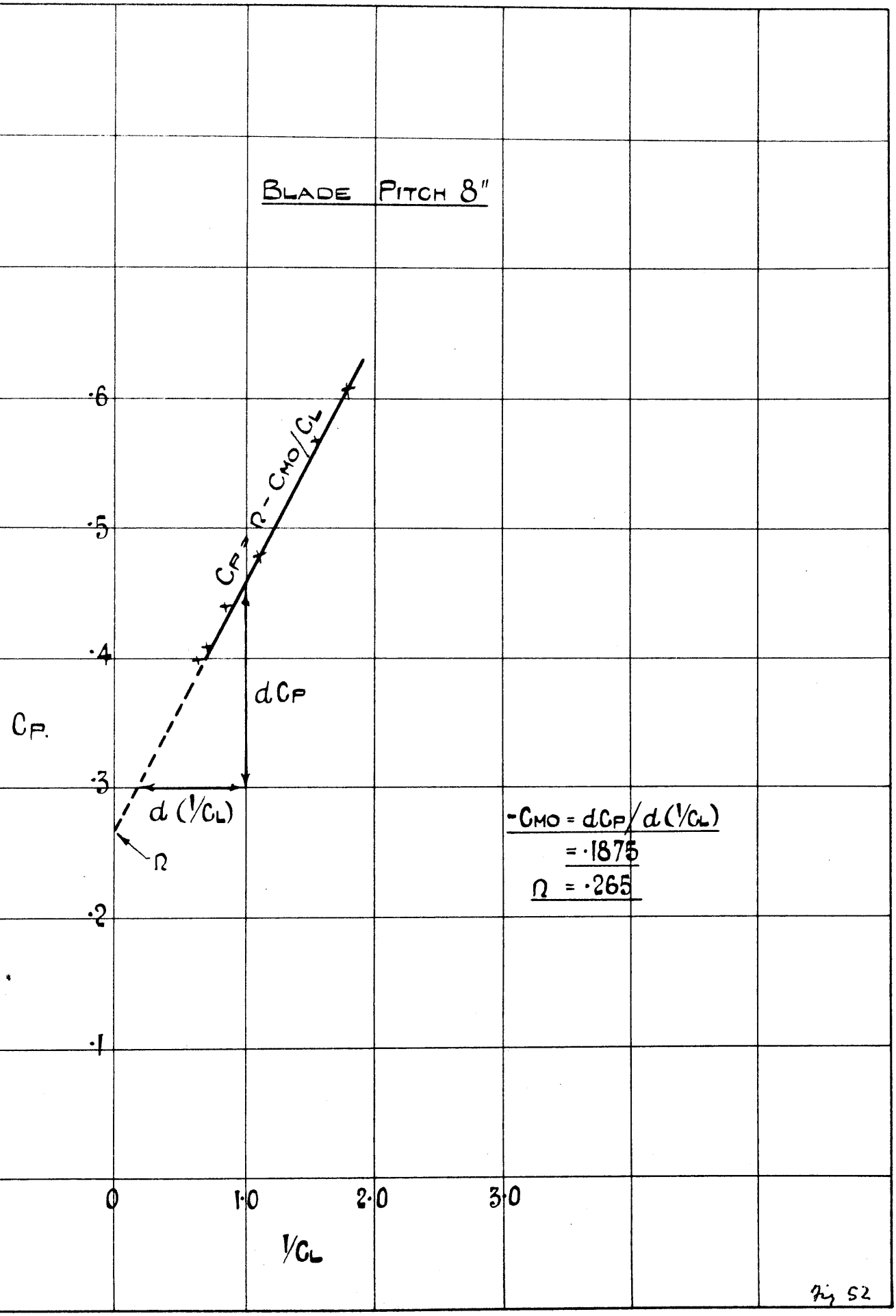
BLADE PITCH 8"
·6
·5
·4
·3
·2
·1
C_P
C_P
$-C_{MO}/C_L$
dC_P
$d(1/C_L)$
Ω
0
1·0
2·0
3·0
$1/C_L$
$-C_{MO} = dC_P / d(1/C_L)$
$= ·1875$
$\Omega = ·265$

Fig 52

STRAIGHT LINE PLOTTING OF CHARACTERISTICS.

Of the characteristic curves plotted in Fig. (39) only the coefficient of lift is a straight line up to the burble point where the flow breaks away from the upper surface.

The Drag Coefficient (C_D - chord Inclination) is seen by inspection to be approximately a parabola.

The Centre of Pressure curves Fig. (42) are seen also by inspection to be approximately a hyperbola.

Whether these relationships are exact or not is immaterial; it follows that if C.P is plotted against a base of $\frac{1}{\alpha}$ where α is the Chord Inclination in degrees or against $\frac{1}{C_L}$, the resulting plots will be more nearly fitted by straight lines than before.

The results have been plotted in this manner up to the maximum lift point and are given in Fig. 49 - 52 for the Centres of Pressure against $\frac{1}{C_L}$.

The Drag Coefficients were plotted against a base of $(C_L)^2$ and the resulting plots Figs. 53 - 56 represent a straight line at the

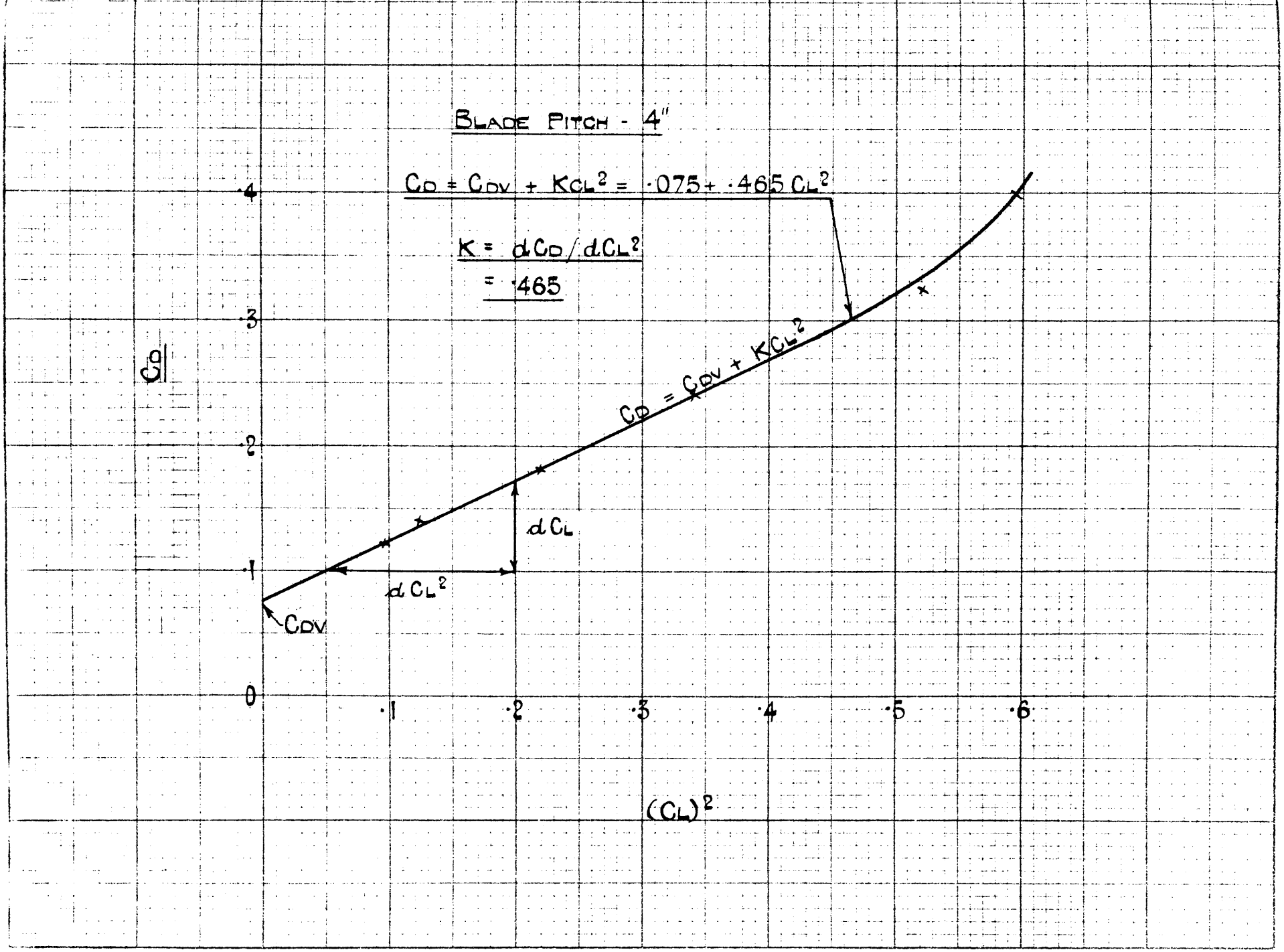
BLADE PITCH - 4"
$C_D = C_{DV} + KC_L^2 = .075 + .465\,C_L^2$
$K = dC_D/dC_L^2$
$= .465$
C_D
$C_D = C_{DV} + KC_L^2$
dC_L
dC_L^2
C_{DV}
0
.1
.2
.3
.4
.5
.6
1
2
3
4
$(C_L)^2$

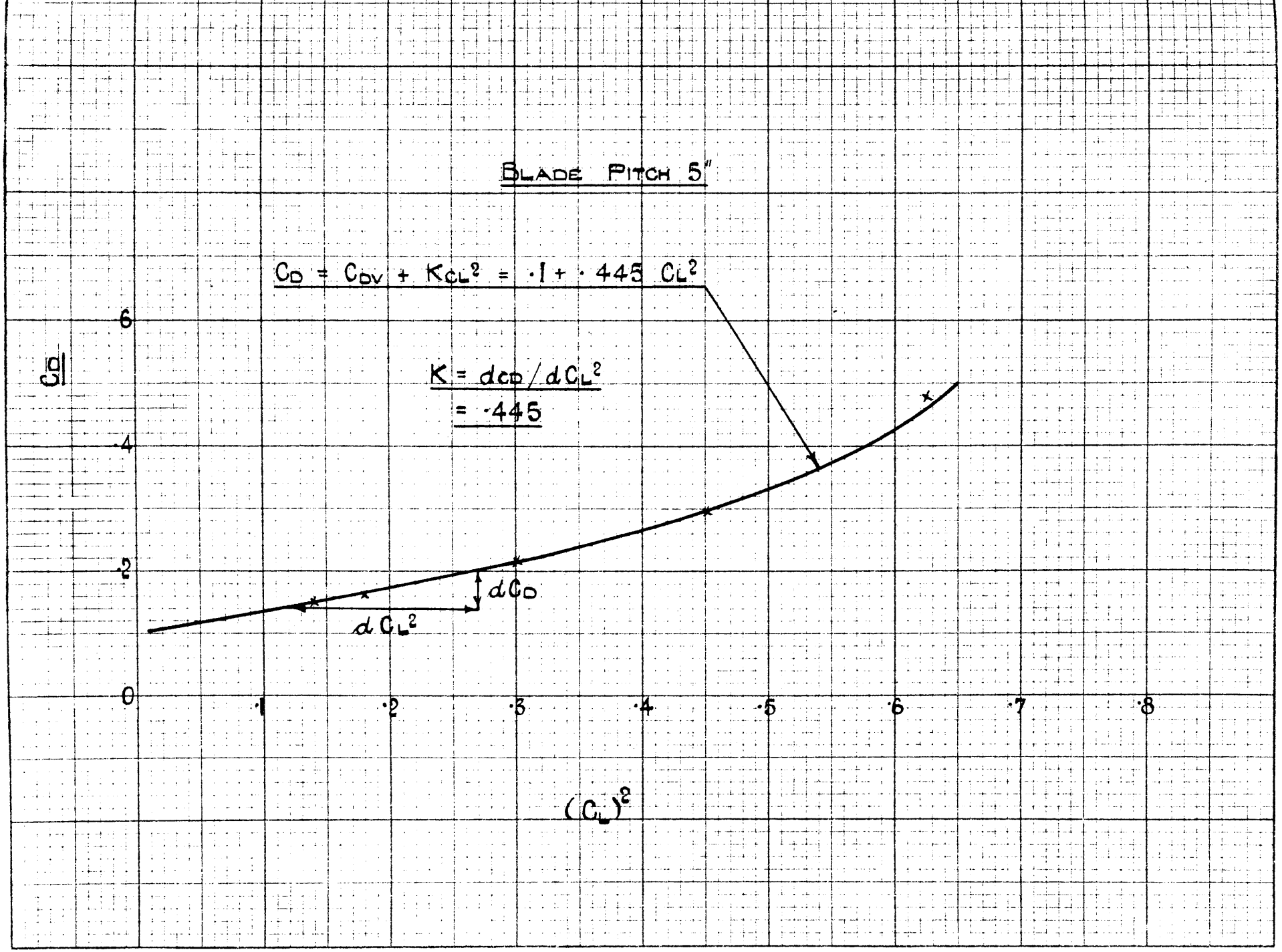
BLADE PITCH 5"
$C_D = C_{DV} + KC_L^2 = .1 + .445\ C_L^2$
$K = dC_D / dC_L^2$
$= .445$
C_D
6
4
2
0
.1
.2
.3
.4
.5
.6
.7
.8
dC_D
dC_L^2
$(C_L)^2$

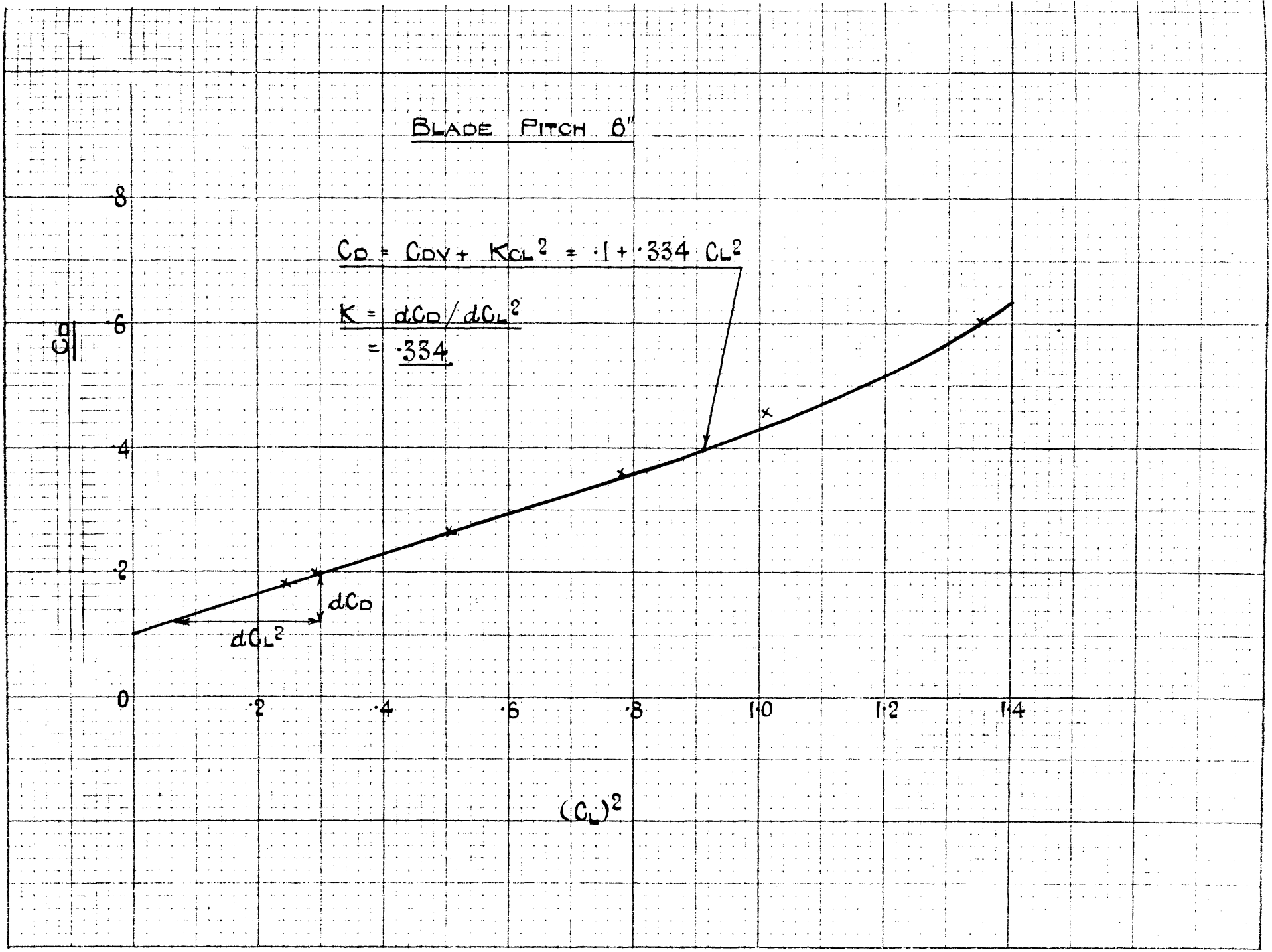
BLADE PITCH 6"
$C_D = C_{DV} + KC_L^2 = .1 + .334\ C_L^2$
$K = dC_D / dC_L^2$
$= .334$
C_D
8
6
4
2
0
.2
.4
.6
.8
1.0
1.2
1.4
dC_D
dC_L^2
$(C_L)^2$

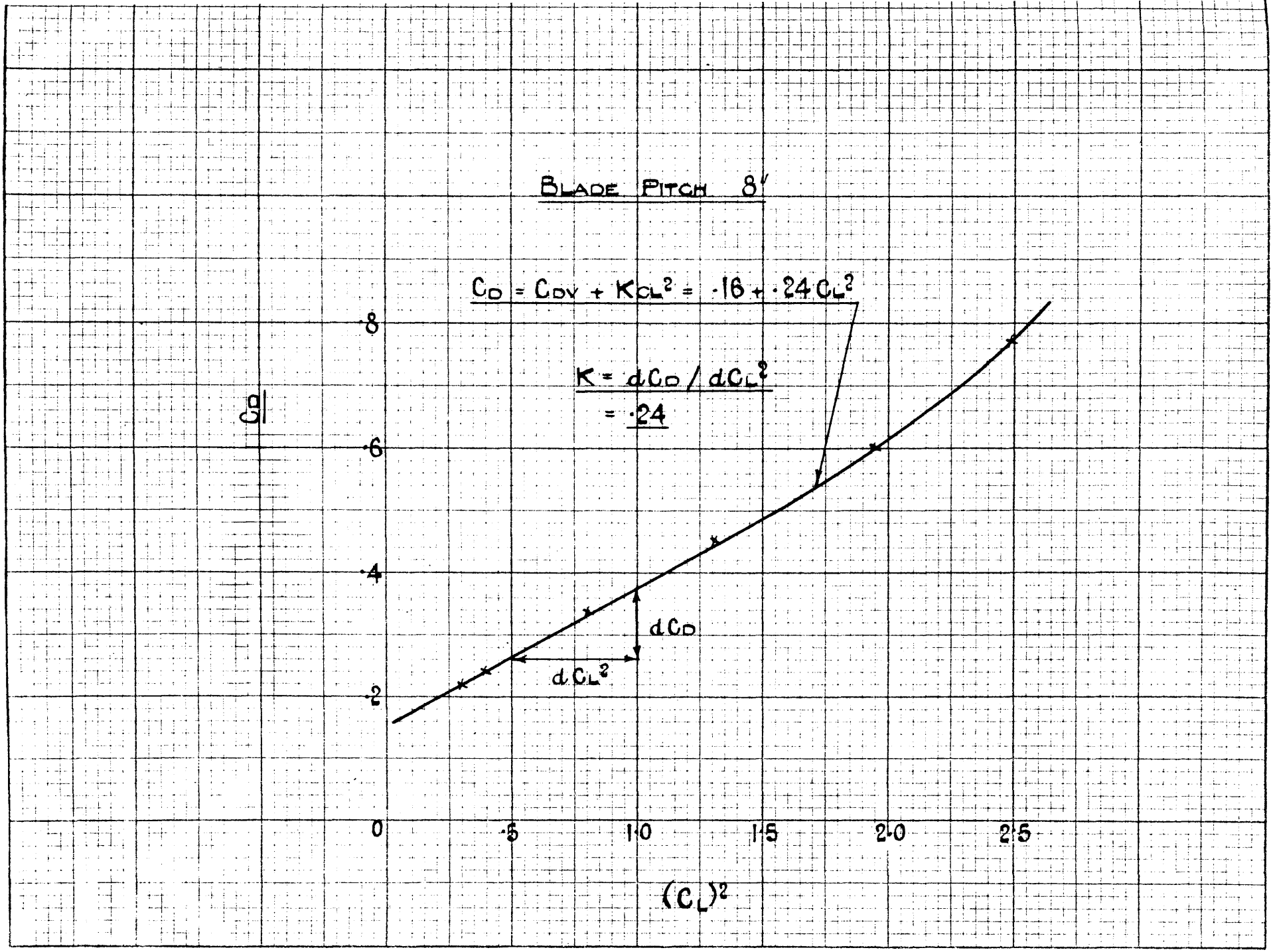
BLADE PITCH 8°
$C_D = C_{DV} + KC_L^2 = .16 + .24 C_L^2$
$K = dC_D / dC_L^2$
$= .24$
C_D
.8
.6
.4
.2
0
.5
1.0
1.5
2.0
2.5
$(C_L)^2$
dC_D
dC_L^2

Fig 56

$C_{DW} = C_{DV} + KC_{LW}^2 = .027 + 1.25\, C_{LW}^2$

C_{DW}

DRAG COEFF; PER LB AIR PER SEC:

$K = \frac{dC_{DW}}{dC_{LW}^2} = 1.25$

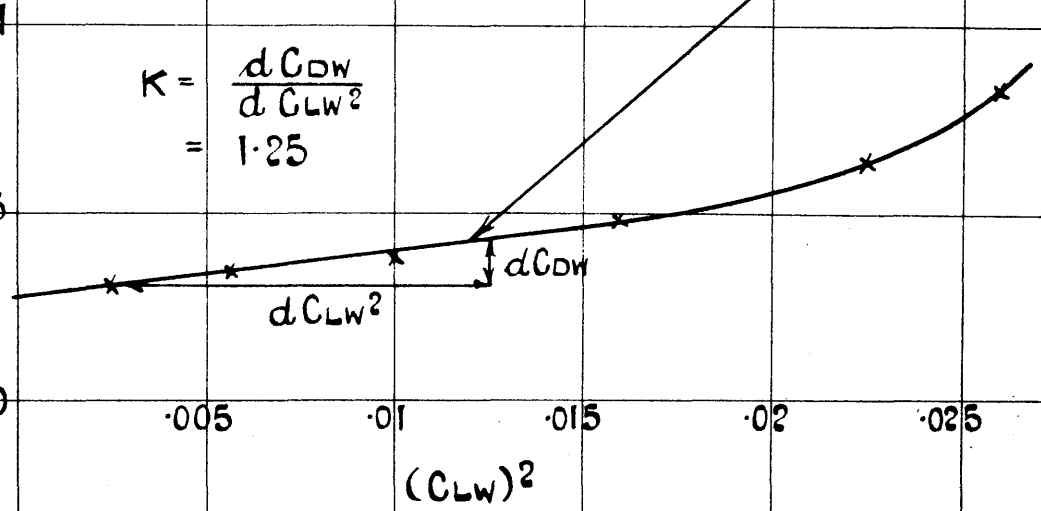

LIFT COEFFICIENT PER LB AIR PER SEC:

end of which the burbling point, where the flow starts to break away, is reached.

Each of the straight lines in these figures may be specified, by specifying a slope and an intercept.

Thus the constants (the slopes and the intercepts) specify the forces acting on the blade.

Values of these constants are given on the diagrams.

The equations of these straight lines may be written -

$$C_L = a(\alpha - \alpha_{L_o}) \qquad \text{----} \quad (1)$$

Figs. (39 & 41)

$$C_D = C_{D_V} + KC_L^2 \qquad \text{----} \quad (2)$$

Figs. (53 - 57)

$$C.P. = n - C_{M_o}/C_L \qquad \text{----} \quad (3)$$

Fig. (49 - 52)

In these equations -

$$a = \frac{dC_L}{d\alpha}$$

= slope of the Lift Curve.

and -

α_{Lo} = angle of attack at zero lift.

The term $(\alpha - \alpha_{Lo})$ is the aerodynamic angle of attack.

In equation (2)

C_{Dv} is the ideal drag coefficient at zero lift, the subscript V is used to imply viscous drag; viscosity is the major factor in determining the drag.

Equation (3) may be also written -

$$C_{M_o} = C_L (n - C_P)$$

where nC is a fraction of the chord C.

The MOMENT of the lift L about a point located nC from the leading edge is approximately -

$$M = - C_L \frac{\rho}{2} S V^2 (C_{P.C} - nC)$$

where nC is a fraction of the chord C.

The minus sign is in front of the right hand member of the equation, because nosing up moments are arbitrarily considered positive by the N.A.C.A..

Dividing the equation by

$$\frac{\rho}{2} S V^2 c$$

and defining C_M by the equation

$$C_M = \frac{M}{\frac{\rho}{2} S V^2 c}$$

The equation -

$$M = C_L \frac{\rho}{2} S V^2 (C_{pc} - nc)$$

becomes identical with the equation

$$C_{p.} = n - \frac{C_{Mo}}{C_L}$$

where C_M is called the moment coefficient.

Since n is a constant for this particular shape of blade, Fig. (49-52) and since the moment of the blade forces about that point is also a constant, n is called the AERODYNAMIC CENTRE.

The numerical value for the constants for these equations is given on the diagrams.

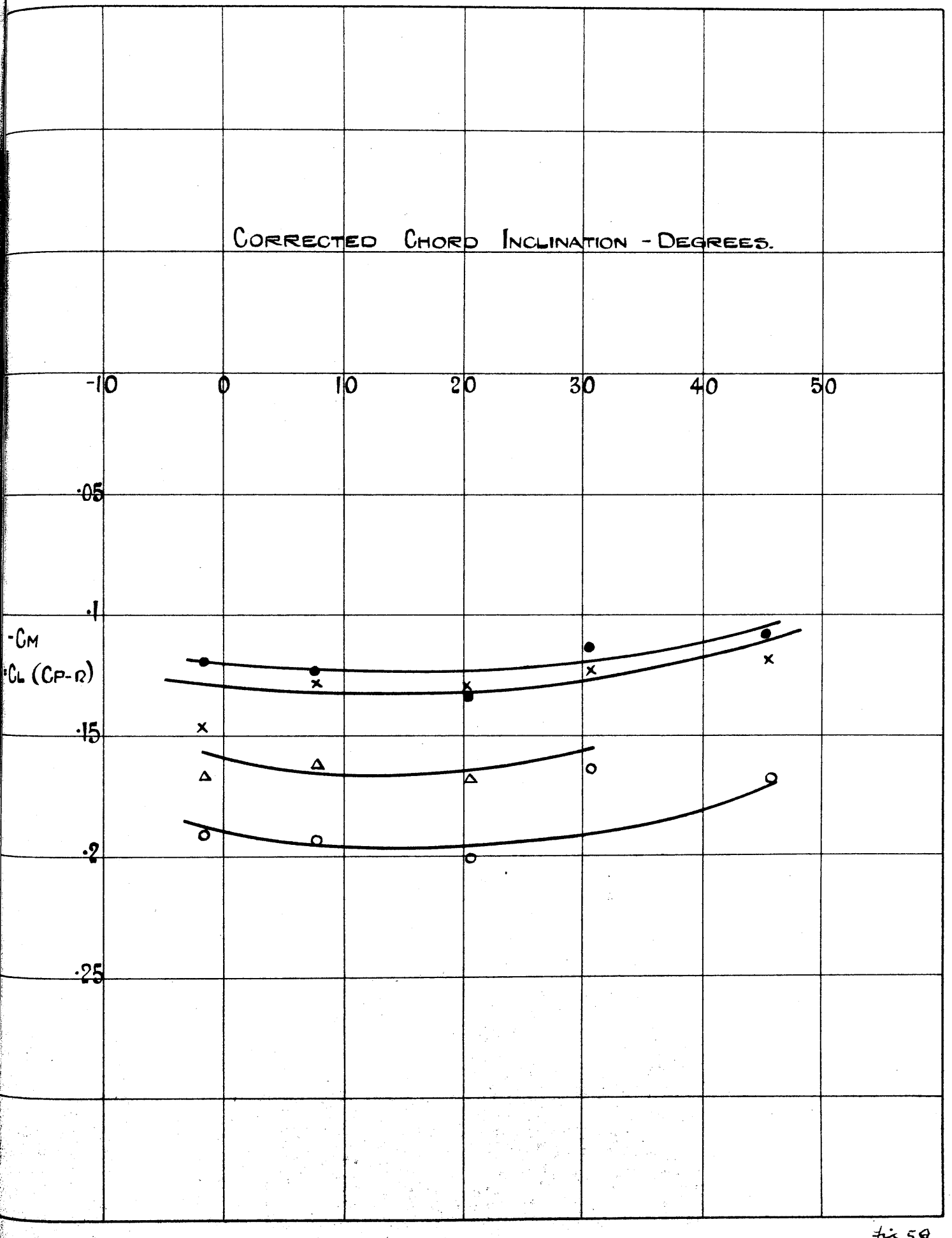
CORRECTED CHORD INCLINATION - DEGREES.
-10
0
10
20
30
40
50
·05
·1
·15
·2
·25
-CM
CL (CP-R)

fig 58

The intercept C_{Dv} (in the Drag Coefficient diagrams against the square of the lift, Figs. (53 - 57)) is approximately equal to the minimum Profile Drag, and this intercept is independent of the aspect ratio.

THE MOMENT COEFFICIENT.

Fig. (58) gives the diagrams for the Moment Coefficient.

The Moment Coefficient of an element depends upon the shape of the profile and the value of the effective angle of attack.

Since the lift coefficient is also governed by the effective angle of attack there exists a unique relation between the lift and the moment coefficient.

To understand why the location and inclination of the resultant force vector with respect to the element are determined by the value of the Lift Coefficient, one has but to remember that the streamline pattern near the surface of an aerofoil and, therefore the pressure distribution over it, are fixed by the effective angle of attack.

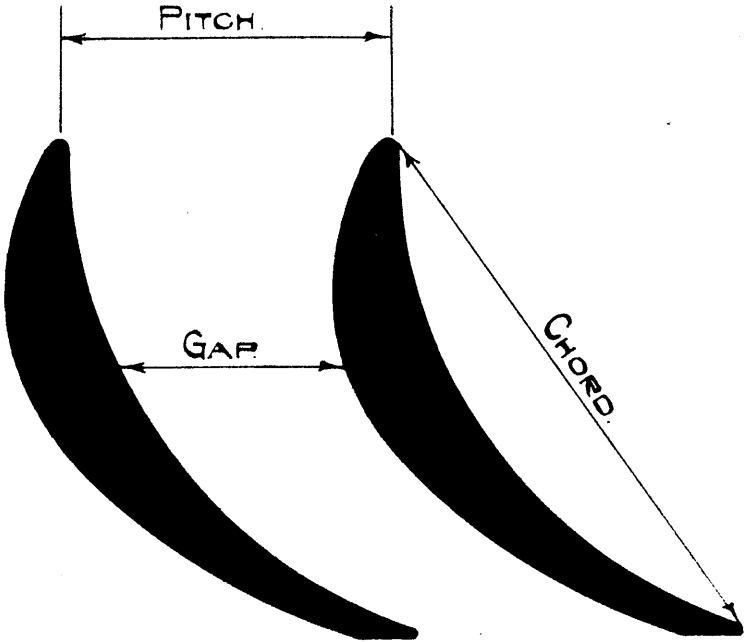

Fig 59

EFFECT OF VARYING THE BLADE PITCH.

Fig. (60) gives the maximum lift in lbs plotted against a base of gap/chord, Fig. (59).

It is found by experience that the lifting power of a biplane, and still more that of a triplane, is less per square foot of wing surface than that of a monoplane.

Additional planes interfere with the action of a single one by disturbing the flow of air past it, and thus prevent it from developing as great a pressure as it would do if alone.

This is quite true for any spacing of the planes that can be adopted in practice; and the question therefore arises as to how far the multiplicity of blades in a blade ring of a steam turbine is detrimental to the action of the blades considered as individual elements.

By analogy with the aeroplane, it would seem that the fewer the blades in the ring, the greater the torque that each would develop from a given steam flow.

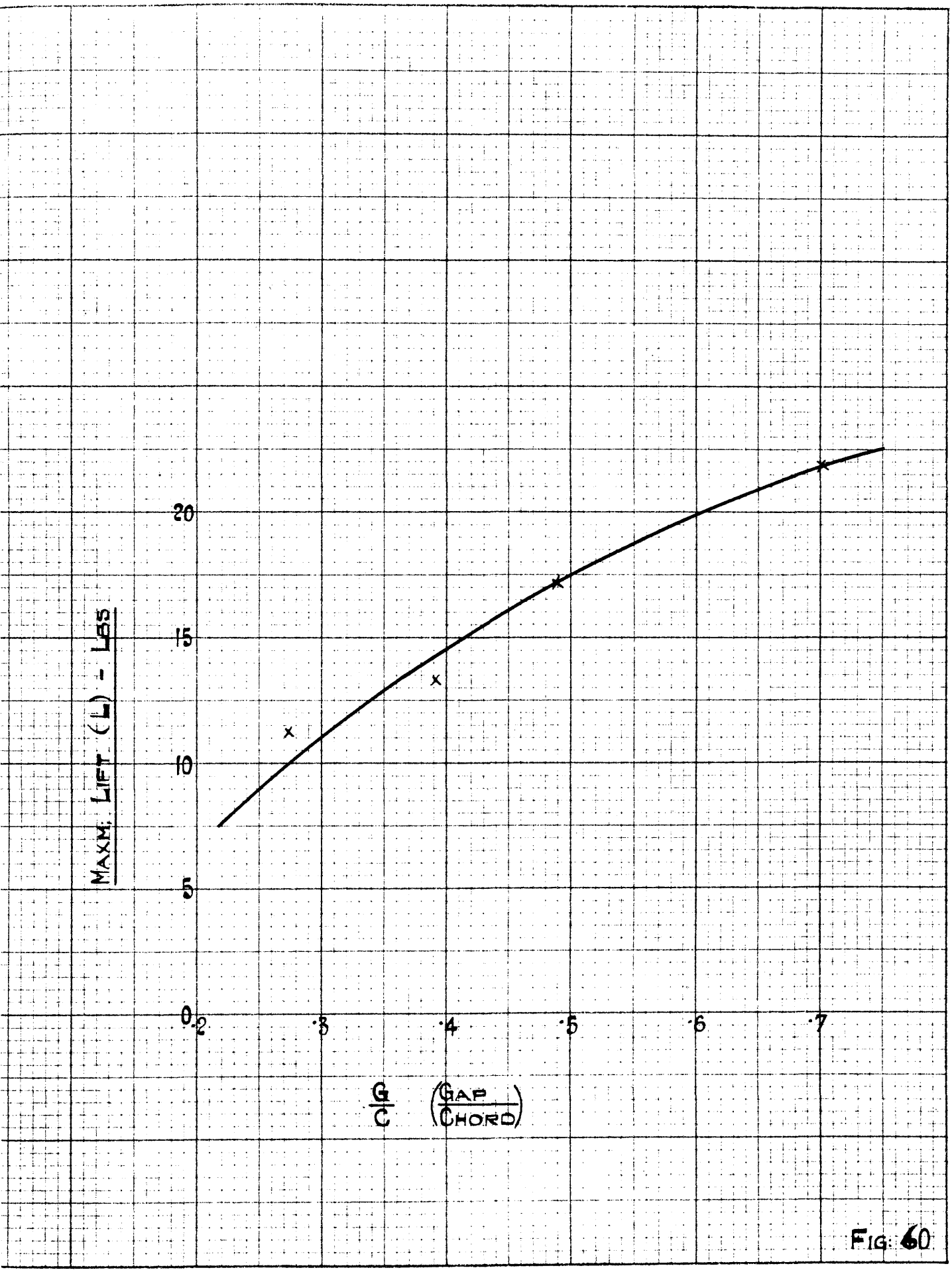

FIG. 60

On the other hand, with the blades too widely spaced, some part of the steam could evidently traverse the blade ring without sensible deflection and would therefore contribute nothing to the torque.

There must be clearly some optimum pitch for blades of a given width and form, but every turbine manufacturer must rely on experiments to find it, for it is not a matter that is very amenable to calculation.

A series of investigations were carried out to this end, at the works of Messrs. C. A. Parsons & Co. and were described by Mr. Robert Dowson at a meeting of the Inst. of Mechanical Engineers in March 1938.

A small turbine designed specially for experimental work was fitted with seven rows of fixed reaction blading acting as nozzles, which remained unchanged throughout the investigation.

Several rotors, each having blades of different pitch, were tested in this machine, the torque and the total steam consumption obtained with each being determined over a large range of speed.

The pitch of the moving blades at their roots varied from .191 ins. to .382 ins. in the course of experiments, and it was found that the turning force per blade increased continually as the pitch was increased, the maximum of the curve not being reached at the widest pitch that was tried.

Fig. (60) gives the curve of maximum lift against a $\frac{c}{C}$ base and is very consistent with the results obtained by Messrs. Parsons.

The total torque on a turbine rotor is, however, equal to the torque per blade multiplied by the number of blades, so that the gain due to an increase of pitch will soon be lost by the reduction of the number of blades in action.

The practical question raised is, whether any better results would be obtained by spacing the moving blades of a steam turbine much more widely than is now customary.

Against such a proposal must be set the long experience of turbine builders and the apparent confirmation by the present tests which show that every increase in the pitch beyond a certain maximum results in a lower efficiency ratio for the turbine.

We have also to remember how small is the margin now existing for any appreciable improvement in the turbine blading.

On the other hand, if we could reduce the number of moving blades without thereby incurring increased losses, it would be all to the good.

But since the fixed and moving blades of a Reaction Turbine are similar in their functions, any argument for increasing the pitch of the one would apply with equal force to the other.

The illogicality of making any discrimination between them will be evident on considering turbines of the Ljungstrom type, in which both sets are moving.

If, however, in defiance of logic, we give the moving blades of an ordinary turbine a greater pitch than the guide blades, one result will be to diminish the reactive effect of the steam in the moving blades, owing to the altered proportions of the channel.

For a given heat drop across any pair of rows, the velocity of the steam entering the moving blades will be increased, while the drop in pressure through them will be diminished, until ultimately all advantages of the principle will be lost.

It seems evident therefore that if any increase in the pitch is desirable, it should be given equally to both the fixed and moving blades.

The conclusion of the whole matter seems to be that, although the performance of each individual blade may be improved by keeping it so far from its neighbours, on either side that they cannot disturb the flow round it, this desirable state of affairs cannot be attained without allowing a considerable proportion of the steam to pass through the blading without yielding up its energy.

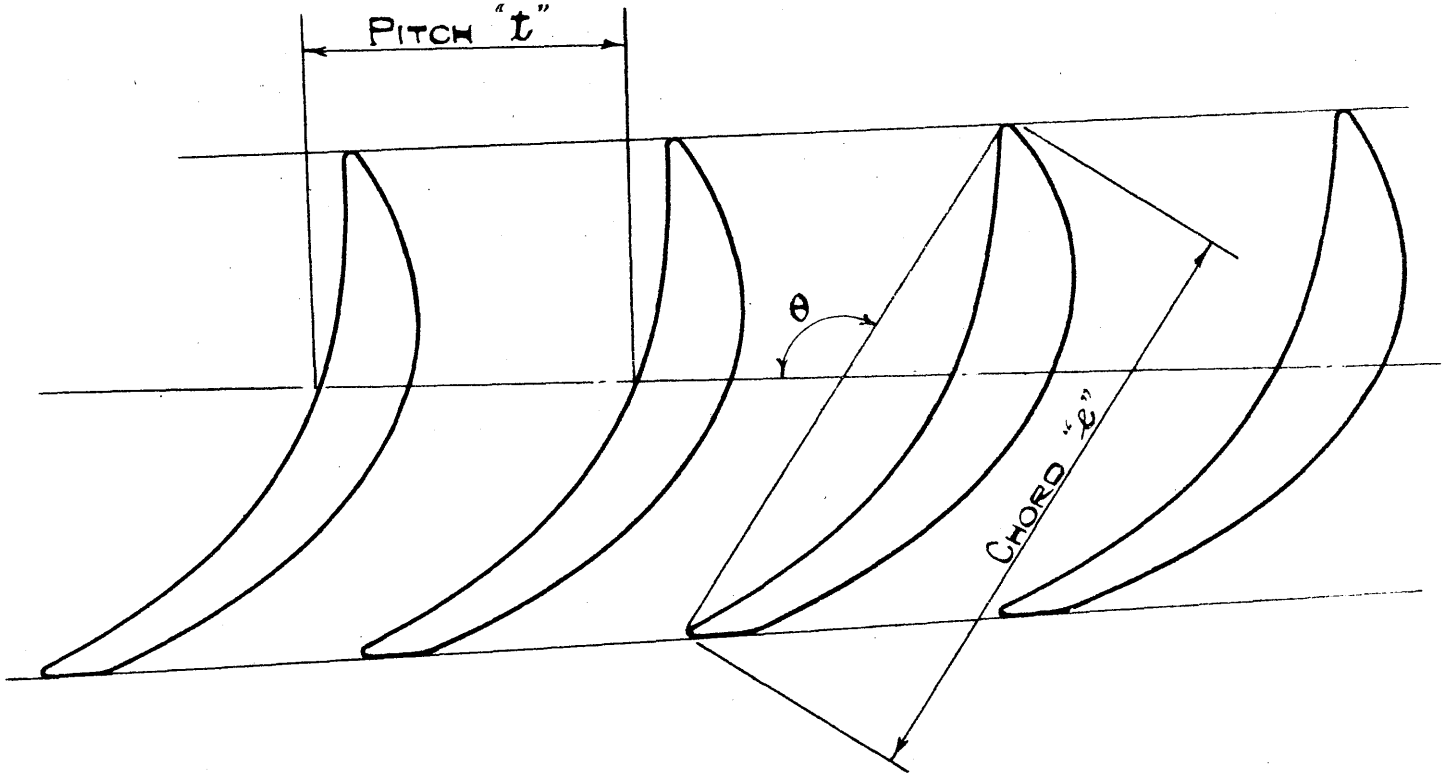

FIG; a

EFFECTS OF BLADE INTERFERENCE. IN A REACTION TURBINE.

If the surface of a blade drum is unrolled we have an endless series of blade sections as shown in Fig. (a), each of which may be regarded as an aerofoil profile.

Thus when identical aerofoils ane arranged in an infinite series, it is to be expected that the action of each aerofoil will be different from what it is when it is isolated, due to the effects of mutual interference.

The Theoretical treatment described here is an attempt to examine the interference effects upon the lift or the lift coefficient, by the ratio of lift coefficients, expected for a blade or aerofoil arranged in a series, to that of an isolated one, in terms of the chord "l", the blade angle θ, and the pitch "t", and ix this theory is deduced for the Reaction Blade from the Works of -

(1) Numachi, World Engineering Congress, Tokyo, 1929; also Technology Reports of the Tohoku Imperial University, Japan.

(2) Keller, "Axialgebläse von Standpunkt der Tragflügeltheorie." (A.C. Gebr. Leemann and Company, Zurich.)

(3) Bauersfeld, Z.V.D.I., 1922, vol. 66, pp. 461,514.

(4) Pfleiderer, "Die Kreiselpumpen", (Julius Springer, Berlin), p.224.

(5) Ackeret, Schweizerische Bauzeitung, 1934, vol. 104, pp. 259, 275, and 292.

(6) Eck, Engineering, 1926, vol. 121, pp. 98, 125.

and others on the design of Axial Flow Turbines, Propeller Turbines, and Pumps, by using

The Lift Force or Lift Coefficient is deduced from the results of the Wind Tunnel experiments both for the blade in series and for a solitary blade.

With respect to the literature concerning the above problem, mention should be made to Kuttas paper (Uber ebene zirkulationsstromung flugtechnichen abwendungen - Munchen, 1911), which was adopted by Bauersfeld as a basis for his theory on Screw Propellers.

The Kuttas Theory was limited to the case when

θ - 90 degrees. Fig. (b).

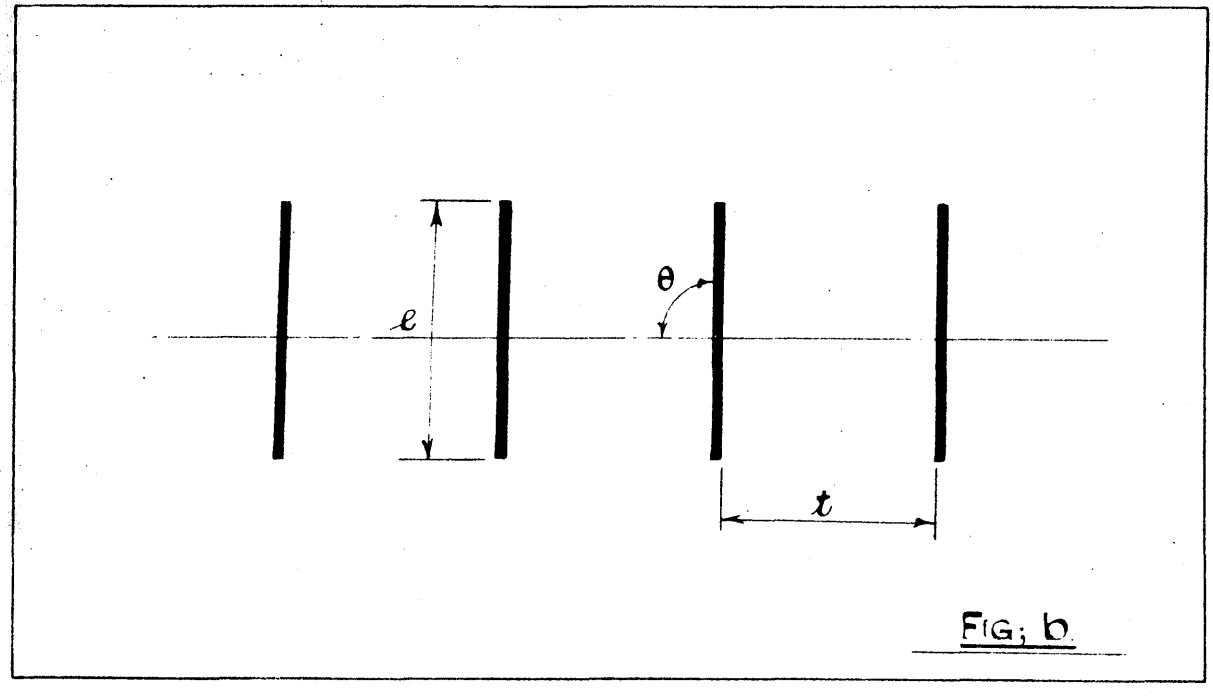

FIG; b

Grammel has made a treatment not only of the problem for the cases when $\theta = 90$ and $\theta = 0$ Figs. (b. & c).

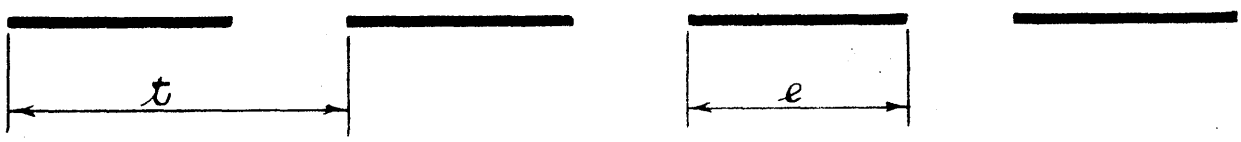

FIG. C

but also of the general study of the potential flow through the infinite multiplane with an arbitrary angle of stagger.

VARIATION OF LIFT DUE TO MUTUAL INTERFERENCE.

According to Grammel (Die Hydrodynamische Grundlagen des Fluges. S.93,96), when identical very thin aerofoils of chord length 2b Fig. (d) are arranged infinitely and parallel to each other along a grate axis MM, the distance of the centres of the adjacent aerofoils on the axis M being $|a_1 + ia_2|$ apart; then the conjugate complex

of the velocity $\omega(v_x + i v_y)$ at the point $Z(x+iy)$ is expressed, referring to the cartesian co-ordinates as follows;-

The conjugated complex of $\omega = v_x + i v_y$

$$v = v_x - i v_y$$

$$= B_0 + (B_1 + iB_2)\sqrt{\frac{\sin \frac{\pi(b-z)}{a_1 + i a_2}}{\sin \frac{\pi(b+z)}{a_1 + i a_2}}} \qquad (1)$$

where

$$B_0 = v_{x(-\infty)} + v_{y(-\infty)} \frac{S(a_2 C - a_1 S) - a_1 Sh(Sh + Ch)}{S(a_1 C + a_2 S) + a_2 Sh(Sh + Ch)}$$

$$B_1 = -v_{y(-\infty)} \frac{a_1 S Ch + a_2 C Sh}{S(a_1 C + a_2 S) + a_2 Sh(Sh + Ch)} \qquad (2)$$

$$B_2 = -v_{y(-\infty)} \frac{a_1 C Sh - a_2 S Ch}{S(a_1 C + a_2 S) + a_2 Sh(Sh + Ch)}$$

and

$$S = \sin \frac{\pi a_1 b}{a_1^2 + a_2^2}$$

$$C = \cos \frac{\pi a_1 b}{a_1^2 + a_2^2}$$

$$Sh = \sinh \frac{\pi a_2 b}{a_1^2 + a_2^2} \qquad (3)$$

$$Ch = \cosh \frac{\pi a_2 b}{a_1^2 + a_2^2}$$

Let the velocities at the plus and minus infinities, the co-ordinates of which are in relation of $\frac{y}{x} = -\frac{a_1}{a_2}$, be $v_{+\infty}$ and $v_{-\infty}$ respectively, then from equation (1) we have -

$$\left.\begin{aligned} v_{+\infty} &= B_0 + i\,(B_1 + iB_2)(C\lambda + iS\lambda) + (B_1 + iB_2)(S\lambda - iC\lambda) \\ v_{-\infty} &= B_0 + i\,(B_1 + iB_2)(C\lambda + iS\lambda) - (B_1 + iB_2)(S\lambda - iC\lambda) \end{aligned}\right\} \quad (4)$$

and

$v_{x(-\infty)}$ and $v_{y(-\infty)}$ in equation (2) are the x and y components respectively of the velocity $v_{-\infty}$ in equation (4).

The velocities at these infinities are resolved into the translational component and the circulational component due to the vortice of the aerofoils, and if the former be denoted by putting a dash and the latter by putting two dashes to the sign of the resultant, we have -

$$\left.\begin{aligned} v_{+\infty} &= v_\infty' + v_{+\infty}'' = v_\infty' - v_{-\infty}'' \\ v_{-\infty} &= v_\infty' + v_{-\infty}'' = v_\infty' - v_{+\infty}'' \end{aligned}\right\} \quad (5)$$

From equations (4) and (5)

we have ;

Translational Component.

$$V_\infty' = B_0 + (iB_1 - B_2)(CC_A + iSS_A)$$

Circulational Component.

$$V_{\pm\infty}'' = \pm (B_1 \pm iB_2)(SC_A - iCS_A) \qquad (6)$$

Further, the circulation around any one of the aerofoils is -

$$\Gamma = 2\sqrt{a_1^2 + a_2^2}\,|V_{-\infty}''|$$

$$= 2V_{y(-\infty)} \frac{(a_1^2 + a_2^2)(C_A^2 - C^2)}{S(a_1C + a_2S) + a_2S_A(S_A \pm C_A)} \qquad (7)$$

All the above is due to Grammel.

By Kutta - Joukowsky's theorem, the lift L_g (The suffix "g" is added to distinguish the quantity referring to an aerofoil in an aerofoil grate from that referring to an isolated one) of an aerofoil grate is expressed

$$L_g = \rho |V_\infty'| \Gamma \qquad (8)$$

where ρ is the density.

Hence by equation (7) we get -

$$L_g = 2\rho \left| U_\infty' \right| v_{y(-\infty)} \frac{(a_1^2 + a_2^2)(C_h^2 - C^2)}{S(a_1 C + a_2 S) + a_2 S_h (S_h + C_h)} \qquad (9)$$

The lift obtained above is now to be expressed by referring to the translational component which corresponds to the geometrical mean of $U_{-\infty}$ and $U_{+\infty}$

Since by equation (5)

$$U_\infty' = U_{-\infty} + U_{+\infty}''$$

or by equation (6)

$$U_{x\infty}' - i v_{y\infty}' = U_{x(-\infty)} - i v_{y(-\infty)} + (B_1 + i B_2)(S C_h - i C S_h)$$

we have

$$\left.\begin{aligned} U_{x\infty}' &= U_{x(-\infty)} + B_1 S C_h + B_2 C S_h \\ v_{y\infty}' &= v_{y(-\infty)} - B_2 S C_h + B_1 C S_h \end{aligned}\right\} \qquad (10)$$

Substituting the value of B_1 and B_2 of equation (2) in the above we have -

$$v_{y\infty}' = \frac{a_1 S C + a_2 S_h C_h}{S(a_1 C + a_2 S) + a_2 S_h (S_h + C_h)} v_{y(-\infty)}$$

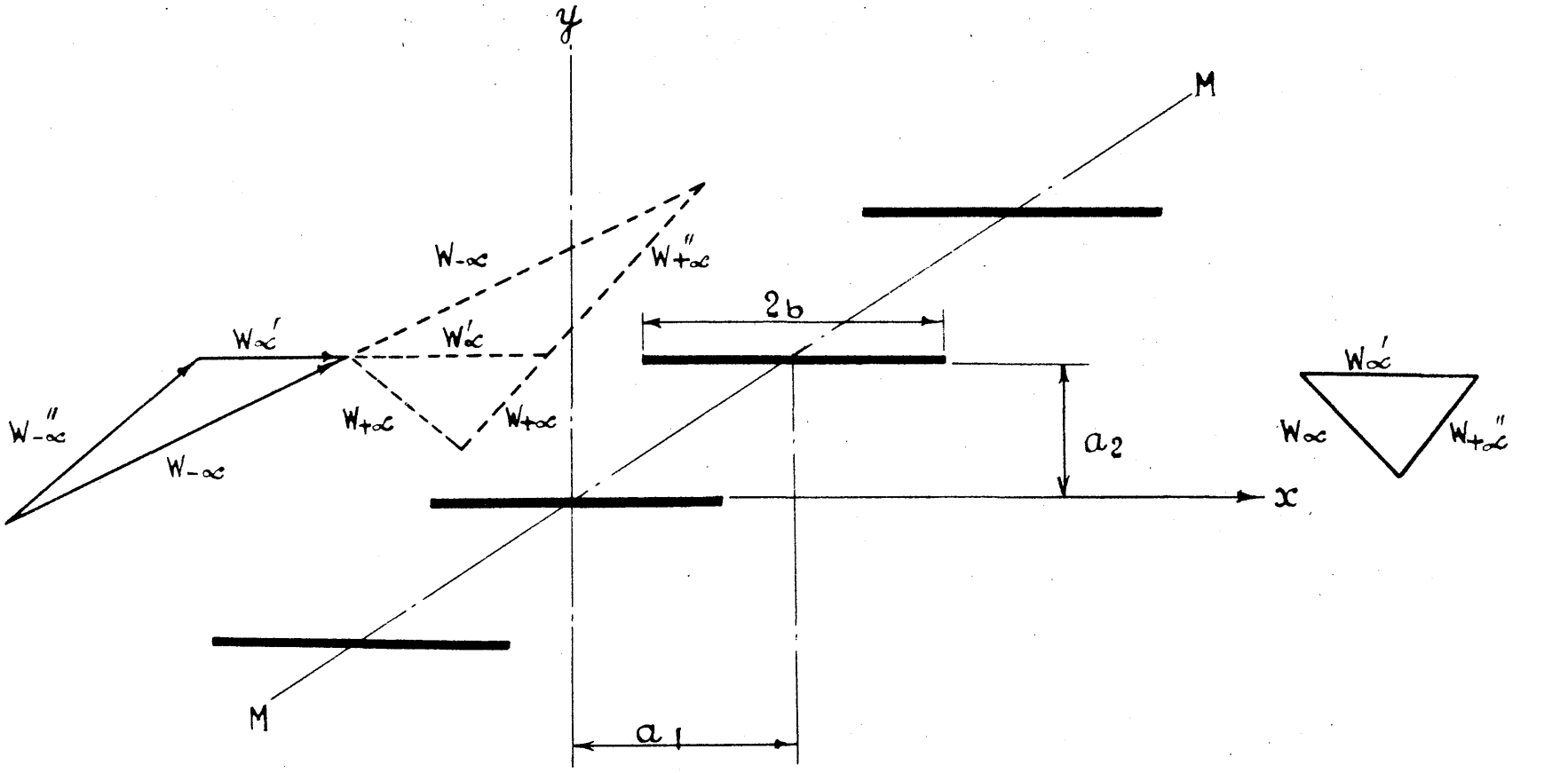

FIG; d

Since by equation (3)

$$S^2 + C^2 = 1$$

$$C_h^2 - S_h^2 = 1$$

or

$$v_{y(-\infty)} = \frac{S(a_1 C + a_2 S) + a_2 S_h (S_h + C_h)}{a_1 SC + a_2 S_h C_h} v_{y(\infty)}' \quad (11)$$

similarly we have

$$v_{x(-\infty)} = v_{x\infty}' \left[1 + \tan a' \frac{a_1 (C_h^2 - C^2)}{a_1 SC + a_2 S_h C_h} \right] \quad (12)$$

where $\tan a' = \frac{v_{y\infty}'}{v_{x\infty}'}$

Inserting the value of $v_{y(-\infty)}$ of equation (11) in equation (9),

we have

$$L_g = 2\rho |v_\infty'|^2 \sin a' \frac{(a_1^2 + a_2^2)(C_h^2 - C^2)}{a_1 SC + a_2 S_h C_h} \quad (13)$$

Now introducing t, θ and l

where

t - the pitch of the blade elements,

θ - the blade chord angle in degrees

l - the chord length of the blade section,

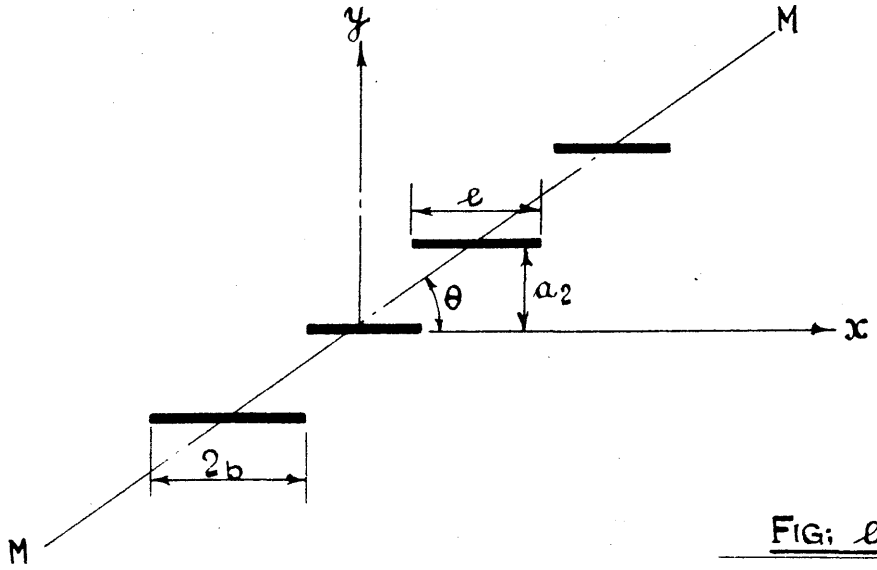

FIG; e.

instead of a_1, a_2, and b as shown in Fig. (e).

Then since $a_1 = t \cos\theta$

$a_2 = t \sin\theta$

$a_1^2 + a_2^2 = t^2$

and $l = 2b$

We have from equation (3)

$$\left.\begin{aligned} S &= \text{Sin}\ \left(\frac{\pi l}{2t}\cos\theta\right) \\ C &= \text{Cos}\ \left(\frac{\pi l}{2t}\cos\theta\right) \\ Sh &= \text{Sinh}\ \left(\frac{\pi l}{2t}\sin\theta\right) \\ Ch &= \text{Cosh}\ \left(\frac{\pi l}{2t}\sin\theta\right) \end{aligned}\right\} \qquad (14)$$

Therefore

$$L_1 = 2\rho\left|V_\infty'\right|^2 \sin a' \quad \frac{t\left[\cosh^2\left(\frac{\pi l}{2t}\sin\theta\right)\right.}{\cos\theta \sin\left(\frac{\pi l}{2t}\cos\theta\right)\cos\left(\frac{\pi l}{2t}\cos\theta\right)}$$

$$\frac{\left. - \cos^2\left(\frac{\pi l}{2t}\cos\theta\right)\right]}{+ \sin\theta \sinh\left(\frac{\pi l}{2t}\sin\theta\right)\cosh\left(\frac{\pi l}{2t}\sin\theta\right)} \qquad (15)$$

The amount of the lift L of the aerofoil in the isolated state for the same angle of incidence a' will be obtained if we put

$$t = \infty$$

in equation (5), supposing θ, and l to be constant.

Since $t = \infty$

we have,

$$S = 0$$

$$C = 1$$

$$Sh = 0$$

and $$Ch = 1$$

and accordingly

$$L_g\big|_{t=\infty} = L = 2\rho V_\infty'^{2} \sin a' \, I$$

where

I is an indeterminate form which is evaluated as follows;-

Rewriting it as

$$I = \left| \frac{\left[\cosh^2\left(\frac{\pi l}{2t}\sin\theta\right) - \cos^2\left(\frac{\pi l}{2t}\cos\theta\right)\right]}{\frac{1}{t}\left[\cos\theta \sin\left(\frac{\pi l}{2t}\cos\theta\right)\cos\left(\frac{\pi l}{2t}\cos\theta\right) + \sin\theta \sinh\left(\frac{\pi l}{2t}\sin\theta\right)\cosh\left(\frac{\pi l}{2t}\sin\theta\right)\right.} \right|_{t=\infty}$$

and differentiating twice the numerator and the denominator respectively with respect to t, we have ,

$$I = \left| \frac{2\left[\left(Ch^2 + Sh^2\right)\sin^2\theta + \left(C^2 - S^2\right)\cos^2\theta\right]}{\frac{4}{t}\left[\cos^3\theta \cdot SC + \sin^3\theta \, ShCh\right] + \frac{4}{\pi l}\left[\cos^2\theta\left(C^2 - S^2\right) + \sin^2\theta\left(Sh^2 + Ch^2\right)\right]} \right|_{t=\infty}$$

$$= \frac{\pi l}{2t}$$

Therefore

$$L = \rho \left| V_\infty' \right|^2 \sin a' \, \pi l \qquad (16)$$

Similarly evaluating some indeterminate forms equation (2) becomes, for $t = \infty$

$$B_0 = \left| \begin{array}{cc} v_{x(-\infty)} + v_{y(-\infty)} & \dfrac{S(\cos\theta \cdot C - \sin\theta \cdot S)}{S(\cos\theta \cdot C + \sin\theta \cdot S)} \\ & \dfrac{-\cos\theta \cdot Sh(Sh + Ch)}{+\sin\theta \cdot Ch(Sh + Ch)} \end{array} \right|_{t=\infty} = v_{x-\infty}$$

$$B_1 = \left| - v_{y(-\infty)} \quad \frac{\cos\theta \cdot SCh + \sin\theta\, C\, Sh}{S(\cos\theta \cdot C + \sin\theta \cdot S) + \sin\theta \cdot Ch(Sh + Ch)} \right|_{t=\infty} \quad (17)$$

$$= -v_{y(-\infty)}$$

$$B_2 = \left| - v_{y(-\infty)} \quad \frac{\cos\theta \cdot CSh - \sin\theta \cdot SCh}{S(\cos\theta \cdot C + \sin\theta \cdot S) + \sin\theta \cdot Ch(Sh + Ch)} \right|_{t=\infty} = 0$$

Substituting the above in equation (6) we have -

$$\left.\begin{array}{l} v_{\infty}' = v_{-\infty} \\ v_{\pm\infty}'' = 0 \end{array}\right\} \quad (6a)$$

and accordingly, by equation (5)

$$v_{+\infty} = v_{-\infty} = v_{\infty}' \quad (5a)$$

Hence from equation (16)

$$L = \rho \left| v_{\infty} \right|^2 \sin a\, \pi l \quad (18)$$

Where

$$a = \tan^{-1} \frac{v_{y\infty}}{v_{x\infty}}$$

= The angle of incidence.

The empirical formula for the lift is usually in the form

$$A = \tfrac{1}{2}\rho \left|V_\infty\right|^2 F C_L \qquad (19)$$

where F - chord x span

- chord l in this case.

C_L = The Lift Coefficient.

Therefore equation (18) may be written as -

$$\left.\begin{aligned} L &= \tfrac{1}{2}\rho \left|V_\infty\right|^2 l\,(2\pi \sin a) \\ C_L &= 2\pi \sin a \end{aligned}\right\} \qquad (18a)$$

In the same way equation (15) may be interpreted as ,

$$\left.\begin{aligned} L_q &= \tfrac{1}{2}\rho \left|V_\infty'\right|^2 l \left[\frac{4 \sin a'}{l} \cdot \frac{t(C_1^2 - C^2)}{\cos\theta \cdot SC + \sin\theta\, S_1 C_1}\right] \\ C_{Lq} &= \frac{4 \sin a'}{l} \cdot \frac{t(C_1^2 - C^2)}{\cos\theta \cdot SC + \sin\theta\, S_1 C_1} \end{aligned}\right\} \qquad (15a)$$

Where

C_{Lq} = Lift Coefficient for an aerofoil in the aerofoil grate, the velocity being referred to the translational component.

The ratio

$$K_a = \frac{L_g}{L} = \frac{C_{Lg}}{C_L}$$

Therefore

$$K_a = \frac{2t}{\pi l} \cdot \frac{C_h^2 - C^2}{\sqrt{C}\cos\theta + \sqrt{h}\,C_h \sin\theta}$$

or

$$K_a = \frac{2t}{\pi l} \cdot \frac{\cosh^2\left(\frac{\pi l}{2t}\sin\theta\right) - \cos^2\left(\frac{\pi l}{2t}\cos\theta\right)}{\cos\theta \sin\left(\frac{\pi l}{2t}\cos\theta\right)\cos\left(\frac{\pi l}{2t}\cos\theta\right) + \sin\theta \sinh\left(\frac{\pi l}{2t}\sin\theta\right)\cosh\left(\frac{\pi l}{2t}\sin\theta\right)} \quad (20)$$

As a special case, when $\theta = 90$ as shown in Fig. (b) we get -

$$K_a = \frac{2t}{\pi l} \tanh \frac{\pi l}{2t} \quad (20a)$$

which coincides with Kutta's and Grammel's results and when

$$\theta = 0$$

as shown in Fig. (c)

$$K_a = \frac{2t}{\pi l} \tan \frac{\pi l}{2t}$$

which coincides with Grammel's results.

Thus the lift for one of the aerofoils arranged in a series will be expressed by

$$L_g = \frac{1}{2} \rho F \omega^2 C_L K_a$$

Where C_L = the lift coefficient reduced to the infinite span which is obtained from experiments in the wind tunnel for an isolated aerofoil.

The configuration of the aerofoil assumed here is very thin and straight, but for a thick aerofoil with a curvature like the blade under examination in the present tests mentioned at the beginning of this work, it is better to measure the blade angle with reference not to the chord but to line known as the Second Profile Axis of the Joukowsky's Profile.

AEROFOIL THEORY OF A RE-ACTION TURBINE.

Consider a runner wheel of radius r and blade length "dr" which could be produced by cutting the wheel with two adjacent cylindrical surfaces co -axial with the turbine shaft. If this cylindrical section be unrolled on a plane we shall have a series of identical blade profiles as shown in Fig. (f).

Let the absolute velocity of the flow before the aerofoil grate be c_1 which becomes c_2 behind the grate due to the circulation exerted by the aerofoils.

Let the circumferential velocity of the rotation of the runner be u and let the relative velocities of the flow be w_1 and w_2 before and behind the grate respectively.

Then the velocity diagram will be as shown in Fig. (f)

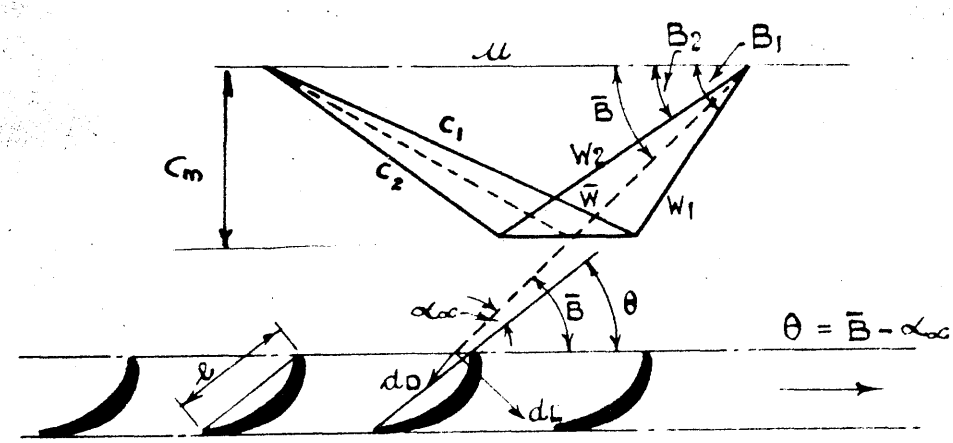

FIG; f

It should be known here that the suffixes (1) and (2) do not mean the entrance and exit points which is the usual case in turbine practice, but they do mean respectively, such places before and behind the grid as the action of the blade does not react to.

According to the aerofoil theory such places are at infinite distances from the grid but in actual aerofoils the places will be recognised to be very near to the grate, the positions of which, however, do not materially affect the present theory.

Referring to Fig. (f) the forces acting on the blade element are the Lift dL and the Drag dD, the former being perpendicular to the direction of the translational velocity $\overline{w}$, which is the geometrical mean of the velocities w_1 and w_2, the latter being in the direction of $\overline{w}$

Therefore the effective power dP and the axial force dF when the number of blades is "Z" will be expressed as follows -

$$dP = uz(dL \sin \overline{B} - dD \cos \overline{B})$$

$$= uz\, dL(\sin \overline{B} - e \cos \overline{B})$$

and

$$dF = z(dL \cos \overline{B} + dD \sin \overline{B})$$

$$= z dL\, (\cos \overline{B} + e \sin \overline{B})$$

Where e - the ratio of Drag to Lift.
The values for the Drag and Lift are obtained from the Wind Tunnel measurements made on an aerofoil of infinite span which is a member of the corresponding grid system. The forces on an aerofoil in a grid differ from those on an isolated aerofoil because of the interference of the other aerofoils. This effect depends on the chord length, the incidence, and the spacing of the aerofoils as shown by expression (20).

In the writer's opinion it is not desirable in the design of Re-action Turbine Blades, to attempt to work out an exact result by applying immediately to the aerofoil (Blade Model) in steam, the values from the Wind Tunnel experiments, since they are functions of the Reynold's Number.

In order to obtain the accurate values for the coefficients for steam, it is necessary to establish the functions given in terms of the Reynold's Number, unless they are obtained directly by experiments in steam.

BIBLIOGRAPHY.

1. A. Fage. "Aerodynamical Research and Hydraulic Practice".

2. Numachi. World Engineering Congress, Tokyo, 1929.

3. Keller. "Axialgeblase von Standpunkt der Tragflugeltheorie".

4. Bauersfeld. Z. V. D. I., 1922, vol. 66. pp. 461 - 514.

5. Pfleiderer. "Die Kreisel Pumpen" (Julius Springer, Berlin, p. 244).

6. Ackeret. Schweizerische Bauzeitung 1934, vol. 104. pp. 259, 275, and 292.

7. Eck. Engineering 1926, vol. 121, pp. 98, 125.

8. Robert Dowson. (The Effect of Circumferential Pitching of Steam Turbine Blades on Torque as compared with "Biplane" Effect "on the "Lift" of Aerofoils).

9. Henry Lewis Guy. "Some Researches on Steam Turbine Nozzle Efficiency" (The Institution of Civil Engineers) 1939.

.....

Pressure Distribution Tests.							Aerodynamic Balance Tests.								
Pitch - Inches.	Corrected Chord Inclination	Y′	X′	C_L $Y'\cos\alpha - X'\sin\alpha$	$W = \frac{PV}{RT}$ Lbs. Air / Sec.	C_{Lw} Lift Coefficient Per Lb. Air / Sec.	Total Lift Lbs	$C_L = L/\frac{\rho A V^2}{2}$	Total Drag Lbs	$C_D = D/\frac{\rho A V^2}{2}$	C_{Lw}	C_{Dw}	C_L (Mean)	C_{Lw} (Mean)	Total Lift Lbs
4"	-1·8	·327	·195	·321	4·65	·069	4·6	·313	1·8	·1225	·0674	·0264	·317	·068	4·67
	7·84	·565	-·046	·566		·1215	7·8	·530	3·1	·211	·114	·0454	·548	·118	8·06
	20·28	·771	-·173	·784		·1685	11·0	·749	6·0	·408	·161	·0878	·766	·165	11·35
	30·75	·695	-·173	·683		·1465	10·2	·695	8·2	·557	·149	·119	·689	·148	10·2
	45·66	·602	-·228	·584		·125	8·5	·579	14·0	·954	·1245	·205	·581	·125	8·55
5"	-1·8	·413	·223	·417	5·85	·0714	5·4	·367	2·28	·155	·0627	·0265	·392	·067	5·76
	7·84	·625	-·0507	·627		·108	8·9	·607	3·82	·26	·1035	·044	·613	·105	9·02
	20·28	·945	-·152	·938		·162	12·6	·855	7·2	·49	·146	·0839	·896	·153	13·2
	30·75	·790	-·184	·772		·132	12·0	·815	10·4	·707	·139	·1206	·795	·137	11·65
	45·66	·679	-·238	·645		·110	9·0	·612	17·7	1·201	·1045	·206	·678	·116	9·98
6"	-1·8	·450	·228	·453	7·03	·0645	7·4	·514	2·75	·1875	·073	·0267	·485	·0687	7·09
	7·84	·750	-·064	·753		·108	11·5	·781	4·7	·319	·111	·045	·767	·109	11·3
	20·28	1·235	-·131	1·205		·1715	16·6	1·130	9·1	·62	·161	·0881	1·167	·166	17·15
	30·75	·920	-·157	·868		·124	13·9	·954	12·35	·84	·1355	·1195	·911	·131	13·4
	45·66	·940	-·260	·838		·116	11·2	·759	21·3	1·45	·108	·206	·798	·1137	11·7
8"	-1·8	·540	·250	·518	9·30	·056	8·6	·585	3·5	·238	·0629	·0256	·555	·0598	8·16
	7·84	·972	-·081	·975		·106	16·5	1·12	6·3	·428	·1205	·046	1·047	·1125	15·4
	20·28	1·5	-·130	1·453		·158	22·5	1·53	12·1	·824	·1647	·0886	1·491	·161	21·9
	30·75	1·35	-·154	1·238		·133	18·0	1·225	16·4	1·115	·132	·121	1·231	132	18·1
	45·66	1·25	-·278	·993		1075	17·7	1·2	28·2	1·915	129	·206	1·096	113	15·1